ACOUSTIC SCATTERING BY DISCONTINUITIES IN WAVEGUIDES

by

Rahul Sen

Dissertation submitted to the Faculty of the
Virginia Polytechnic Institute and State University
in partial fulfillment of the requirements for the degree of

Doctor of Philosophy
in
Engineering Mechanics

APPROVED:

Charles Thompson, chairman

M.S. Cramer, co-chairman

J.W. Grant

C.W. Smith

C.L. Prather

January, 1988

Blacksburg, Virginia

ACOUSTIC SCATTERING BY DISCONTINUITIES IN WAVEGUIDES

by

Rahul Sen

Committee Chairman: Charles Thompson

Engineering Science and Mechanics

(ABSTRACT)

The scattering of acoustic waves by boundary discontinuities in waveguides is analyzed using the Method of Matched Asymptotic Expansions (MAE). Existing theories are accurate only for very low frequencies. In contrast, the theory developed in this thesis is valid over the entire range of frequencies up to the first cutoff frequency. The key to this improvement lies in recognizing the important physical role of the cutoff cross-modes of the waveguide, which are usually overlooked. Although these modes are evanescent, they contain information about the interaction between the local field near the discontinuity and the far-field. This interaction has a profound effect on the far-field amplitudes and becomes increasingly important with frequency. The cutoff modes also present novel mathematical problems in that current asymptotic techniques do not offer a rational means of incorporating them into a mathematical description. This difficulty arises from the non-Poincaré form of the cross-modes, and its resolution constitutes the second new result of this thesis. We develop a matching scheme based on block matching intermediate expansions in a

transform domain. The new technique permits the matching of expansions of a more general nature than previously possible, and may well have useful applications in other physical situations where evanescent terms are important. We show that the resulting theory leads to significant improvements with just a few cross-mode terms included, and also that there is an intimate connection with classical integral methods. Finally, the theory is extended to waveguides with slowly varying shape. We show that the usual regular perturbation analysis of the wave regions must be completely abandoned. This is due to the evanescent nature of the cross-modes, which must be described by a WKB approximation. The pressure field we so obtain includes older results. The new terms account for the cutoff cross-modes of the variable waveguide, which play a central role in extending the dynamic range of the theory.

ACKNOWLEDGMENTS

My foremost debt of gratitude is to my advisor, Dr. Charles Thompson, for his guidance, support and friendship, and for making the last three years a period of intellectual stimulation and academic growth. I have benefited enormously from my association with him, professionally as well as personally. I am also grateful for the encouragement and help of Dr. Mark Cramer, who helped me acquire a taste for things nonlinear. I thank my friends in the ESM computer laboratory; I have truly enjoyed the exchange of ideas and the camaraderie. I am especially grateful for the help of Charlotte Hawley and Nasrin Lotfi for facilitating the computer work. And finally, I would like to thank my wife Megan for her patience and grace through all the late nights and working weekends.

Table of contents

List of figures

CHAPTER 1 : INTRODUCTION

Problems involving wave propagation in waveguides have long been of interest to acousticians and researchers in other fields such as applied electromagnetism. Waveguides are devices that transport wave energy in a directed fashion. Generally speaking, any mode of transmitting wave energy that is not entirely through free space may be said to be guided. Thus from a practical point of view, interest in guided wave propagation is rooted in numerous applications both in industry and in everyday life.

Theoretical analysis of waveguide problems is equally rich in variety. The reason behind this is that only a handful of simple problems admit an exact solution of the wave equation. Most problems of interest usually defy an exact mathematical description. In such cases, the most fruitful recourse is a phenomenological approach that is based on identifying and modeling the principal underlying physical mechanisms. The resulting theory is typically an approximate one, and is restricted to a certain range of physical parameters. This is still far more preferable than a numerical solution, however, since numerical methods for the wave equation are prone to resolution problems in regions of rapid wave variation and in geometries with reentrant corners. They also fail to provide much physical insight. Besides, when based on rational approximation techniques like perturbation methods (Lesser and Crighton, 1972), a phenomenological theory is capable, in principle, of yielding results that are as accurate as one may desire from a practical point of view. We mention that in certain problems, formally exact methods are applicable. Complex-variable methods such as the

Wiener-Hopf and the mode-matching techniques (Noble,1958; Mittra and Lee,1971) fall into this category. These methods, however, are restricted to special geometries. In the present study, we develop a general theory of low-frequency wave propagation in waveguides with boundary discontinuities. The analysis is based on singular perturbation theory, and is consequently applicable to a wide class of geometries. Furthermore, in contrast to existing studies based on perturbation methods, the theory presented here may be applied over a wide range of frequencies.

The behaviour of guided waves depends largely on the wavelength of the impressed excitation. When the wavelength is much larger than the characteristic axial dimension of the waveguide, much of the wave character of the guided field may be ignored, and the waveguide may be approximately modeled as a combination of lumped circuit elements. On the other hand, when the source wavelength is comparable to or less than the characteristic axial dimension, wave phenomena play an important role. Thus there are two main divisions from an analytical standpoint - high and low frequency problems. Our interest is in the low-frequency end, in which the source wavelength is much larger than the width of the waveguide and the axial extent of the boundary discontinuity. In this regime, lumped-parameter models are usually employed to obtain engineering estimates. These, however, assume that the relevant parameters are linear functions of frequency; this is equivalent to considering a one-term Taylor expansion about a zero-frequency base state. A deeper analysis of the scattering process is necessary if the theory is to be extended to intermediate frequencies. In this study,we use the method of Matched Asymptotic Expansions (MAE).

The motivation for this study is that available asymptotic theories for this class of problems are currently restricted to very low frequencies. We show that certain aspects of the interaction between the far-field and the local field near the discontinuity contain the key ingredients for a theory with an improved dynamic range. These interactions occur through evanescent local modes, and become increasingly important at intermediate frequencies. Since evanescent modes are usually viewed as essentially local features of a scattering problem, their contribution to traveling mode amplitudes was ignored by previous investigators (Lesser and Lewis,1972; Thompson, 1984a,b). This resulted in theories that are valid only for very low frequencies. In this thesis, the effects of the local modes are explained and incorporated into the theory using the method of Matched Asymptotic Expansions. We show that there are some fundamental mathematical problems associated with including the evanescent modes, and develop a new matching technique to circumvent these difficulties. The technique is formally capable of handling asymptotic expansions of a more general nature than currently possible, and may well have applications in other physical problems where evanescent terms are important.

Several investigators have studied the problem of acoustic scattering by boundary discontinuities in waveguides. Most early studies were primarily concerned with overall estimates of scattering such as the impedance Z of the discontinuity and the reflection and transmission coefficients R, T. These parameters were then used as lumped circuit elements in a transmission line model of the waveguide (Morse and Ingard, p.467; Slater). Miles (1946a,b) and Schwinger and Saxon (1968) used variational methods to estimate the junction

impedance of planar discontinuities. These methods are based on expressing the impedance in terms of a symmetric quadratic form involving the field on the junction plane. Since such forms are relatively insensitive to the choice of trial functions for the actual field (Morse and Ingard, pp.155-157; Appendix A, this thesis), the impedance obtained by this method is extremely accurate. Variational methods, however, are suitable only for special geometries, since the quadratic forms are usually derived from Green's functions of regular regions. In addition, they are better suited for obtaining overall parameters such as R, T and Z rather than the scattered field itself. It is possible to obtain accurate field information only if the local field can be estimated accurately; in some problems, this may serve as a limitation. Nevertheless, these studies provide important benchmark estimates for more comprehensive theories. Besides, there are certain aspects of them that are of direct relevance to the present work. These have to do with the approximate determination of the field on the junction plane. Morse and Ingard (pp.480-488), for example, approximate the local field near a discontinuity as static, or incompressible. This idea is attributable to Rayleigh (1897), and is based on the fact that the axial extent of the discontinuity is much smaller than the incident wavelength. This is formally exploited in the present singular perturbation analysis. Of particular interest in the present context is Schwinger's solution of the local field by the Method of Static Equivalence (MSE) (Schwinger and Saxon, 1968; Appendix A, this thesis). Schwinger improves the incompressible approximation by adding dynamic (wave) corrections to the local field. Used in conjunction with a variational principle, this gives a remarkably accurate estimate of impedance valid all the way up to the

first cutoff frequency of the waveguide. Schwinger's approach contains the key ingredient necessary for a theory to be applicable over a wide range of frequencies - the inclusion of dynamic effects in the local field. Since Schwinger's main goal was to obtain a trial field for the variational method, the significance of these effects is not pointed out in his study. Instead, the focus is on MSE, in which the wave problem is formally recast as a solution of Laplace's equation with boundary conditions at infinity. This procedure bears a very strong resemblance to the asymptotic method, and it is only when one views Schwinger's method in an MAE perspective that the role of the local field becomes apparent. Unfortunately, MSE itself is restricted to planar junction discontinuities of zero axial extent - the formalism depends heavily on the inherent geometric simplicity. As mentioned earlier, this is characteristic of methods that seek to formally solve the wave equation in the entire waveguide. It is possible, however, to incorporate the important physical interactions - implicit in Schwinger's method - into a comprehensive asymptotic theory. We show that the crucial interaction between the local field and the wave field far away from the discontinuity takes place through the cutoff cross-modes induced by the discontinuity. Although these modes decay rapidly away from the discontinuity, they contribute not only to the local fine structure, but more importantly, have a profound influence on overall scattering parameters as well. This can be attributed to their source-like nature in the local field equations, the effect of which is to modify the amplitudes of the propagating waves. Thus the most important aspect of extending the frequency range of the theory is the proper description of this effect, which in turn depends on the determination of the cross-mode source amplitudes.

Schwinger achieves this by formulating an equivalent static (incompressible) problem and by requiring its solution to match the dynamic solution on the junction plane. In MAE, the analog of this is asymptotic matching, which merges the local and wave fields into each other in some overlap region. Lesser and Lewis (1972) and Thompson (1984a, 1984b) used the MAE technique to study the present problem. Their analyses, however, do not include the cutoff cross-modes, which play an important role at intermediate frequencies. This results in a limitation of the theory to very low frequencies. The absence of cross-modes in these studies may be attributed to the use of a regular perturbation expansion for the wave field. The cross-modes, however, are associated with rapid phase variations, which arise from the singular nature (Bender and Orszag, p.484) of the scaled wave equation. For uniform sections, the cross-modes may be obtained directly from an eigenfunction expansion of the wave equation. For slowly varying wave sections, however, a WKB method - rather than a regular perturbation expansion - must be used to generate the cross-modes. We will show that the results obtained in this manner contain the expansions of Lesser and Lewis and of Thompson as a special case. The important difference is that our description contains the cutoff modes. These, as we mentioned, are responsible for the important interaction between the local and wave regions.

Including the cutoff modes, however, is complicated by a mathematical difficulty. The cutoff modes are in non-separated exponential form, and when subjected to the usual techniques of asymptotic matching, lead to a paradox. We find that the cross-modes of the wave region cannot be matched to corresponding local modes if we use the MAE technique as it stands. Because of the

orthogonality relations that exist between the transverse eigenfunctions, however, this is absolutely impermissible. To resolve this, we show that it is necessary to examine some fundamental aspects of asymptotic matching theory. This provides the basis for some new ideas on the subject. We use these ideas to develop an extended version of MAE that is capable of handling asymptotic expansions of a more general nature than the technique presently permits.

The layout of this thesis is as follows. In Chapter 2, we present the governing equations, introduce natural length scales, and derive scaled equations. A brief review of the MAE technique is also provided, with particular emphasis on aspects that are relevant to the present study. We expand on these in Chapter 3, where the new matching technique is developed. This is done in the context of scattering by an arbitrary discontinuity between two uniform sections of a waveguide. The low-frequency theory is developed in general detail in this chapter. In Chapter 4, we apply the theory to the special case of a square stepped duct. This is a benchmark problem in that explicit results are available from previous investigations. We shall solve this problem in full detail, with most of the emphasis falling on the solution of the local problem near the junction. We use conformal mapping and a static version of MSE to construct this solution. Explicit formulae are obtained for overall scattering parameters, and results are compared to those of Lesser and Lewis. We show that our theory is capable of accurate predictions over a wide frequency range. In Chapter 5, the theory is extended to slowly varying waveguides. The main focus is on the solution in the wave region. Due to reasons mentioned above, our analysis departs significantly from those of previous investigators. Lastly, in Appendix A, we

present a brief review of variational methods and outline Schwinger's MSE technique. The latter is of direct relevance to this thesis, and is therefore presented in some detail.

CHAPTER 2 : PROBLEM STATEMENT AND METHOD OF ANALYSIS

The problem considered in this thesis is that of low-frequency acoustic wave propagation in a waveguide of slowly varying shape and containing a height discontinuity. In this chapter, we shall define the problem precisely, and introduce the nomenclature used throughout the thesis. We also present the governing equations and briefly describe the method of analysis. It is appropriate to make a few remarks on our choice of method at this point. Let us consider the simplest problem in the above category - that of scattering by a height discontinuity joining two uniform waveguides (fig. 1).

Even for this simple geometry, it is not possible to obtain an exact solution in closed form. This is so because the wave equation does not lend itself to a separation-of-variables solution. The best one may achieve through exact methods is to reduce the problem down to an infinite algebraic system. This results if we apply a formally exact extension of the Wiener-Hopf method, for example, or the mode-matching technique (Noble, 1958; Mittra and Lee, 1971). Similar results are also obtained by applying the Method of Static Equivalence (Schwinger and Saxon; Appendix A). This method is less-known compared to other classical techniques, but is of direct relevance to the present work. There are several drawbacks to these approaches, however, a serious one being the inherent limitation to special geometries. A second difficulty lies in the solution of the infinite system. For practical reasons, the system must be truncated at some point. It is difficult to estimate the error caused by truncation unless the

approximate solution so obtained is used in conjunction with a variational method. Perhaps the most persuasive argument against most classical methods is the fact that they do not shed any light on or take advantage of the important physical processes and the natural scales present in a problem. This, together with the limitation to special geometries, precludes these methods from being applicable to the entire range of physical problems of interest. If one views the present problem as a special case of a more general situation in which various phenomena like nonlinearity and viscosity also play important roles, it becomes obvious that these methods have to be completely abandoned.

The same remarks apply to a purely numerical solution of the problem. In addition, numerical methods for the wave equation are often inaccurate due to insufficient spatial resolution. This is the case in regions where field quantities vary rapidly, for example near a boundary discontinuity in a waveguide, or in the vicinity of a reentrant corner. If we traverse an axial cut such as AA' in the duct of fig. 1, for example, the pressure field will typically exhibit slow variations on the fundamental wavelength scale in the uniform sections (fig. 2), and undergo rapid variations in the vicinity of the junction plane. The fast variation is strictly a local feature, and it might appear that a lack of spatial resolution in this region would do no more than smear out the fine structure of the local field. We will show, however, that some of the most important information about the scattered field is contained in the local structure, except when the frequency of the incident wave is very small. Thus at most frequencies of interest, even overall estimates of scattering are critically dependent on accurate local information.

The resolution of this difficulty lies in recognizing that the local field has a fundamentally different behaviour from the wave field in the uniform sections. In fact, the leading-order behaviour of the local field is incompressible, and is described by the Laplace equation rather than the wave equation. A purely numerical method, however, does not take advantage of such physical information. Seeking the local field as a solution of the wave equation runs contrary to the physics of the problem, and numerical inaccuracy results as a consequence. On the other hand, if one were to solve the correct local problem separately and then match the solution with that in the smooth sections, much better results could be obtained. The vehicle for an approach of this kind is the Method of Matched Asymptotic Expansions (MAE), which is the method used in this thesis. For discontinuities of arbitrary geometry, a numerical solution is still necessary for the local fields. It is much easier to solve the Laplace equation in arbitrary regions, however, than it is to solve the wave equation. Thus in problems where different physical behaviours dominate in different regions of space or time, MAE is often the most effective means of integrating numerical and analytical information into a comprehensive theory.

A further advantage of the MAE technique is that it yields a globally valid description of the field. This is in contrast to variational methods (Miles, 1946a,b; Morse & Ingard, 1968; Schwinger and Saxon, 1968), which provide extremely accurate overall estimates such as junction impedance, but do not accurately predict the scattered field everywhere. Variational methods are based on using an approximate local field in a variational expression for the quantity of interest, such as the junction impedance. The variational expression is

typically of the Rayleigh-Ritz type, and is therefore relatively insensitive to small errors in the local field. Thus a physically motivated approximation of the local field - the incompressible approximation, for example - usually leads to excellent results for the impedance. The incompressible approximation is good for low frequencies. As the frequency is increased, the compressibility of the local field becomes important. Schwinger (Appendix A) accounts for this by the Method of Static Equivalence (MSE), in which compressibility in the local field is simulated by sources in the local equations. The method, however, can only be applied to special geometries and besides, is tailored for determining the junction impedance. The main contribution of this thesis is that we will develop a theory that is applicable to arbitrary geometries, and at the same time, accurate over a wide range of frequencies by properly accounting for the compressibility of the local field. The theory will provide accurate estimates of overall parameters such as impedance as well as the actual field in the waveguide.

The Method of Matched Asymptotic Expansions (MAE), in its present implementation, is based on the physical observation that in the vicinity of the height discontinuity, the behaviour of the fluid is essentially incompressible. This is described by a locally valid set of equations whose solution is then integrated into the complete field description. The solution proceeds by considering different sub-problems, each of which is associated with a refinement of a basic approximate solution. Since these sub-problems are based on an ordering scheme, one is able to estimate the asymptotic error at each stage of approximation. It is also possible, only at the cost of additional algebra, to obtain an approximate solution that is as accurate as one may reasonably desire from a

practical point of view. Thus MAE overcomes all the serious difficulties mentioned above.

The limited scope of the classical methods is due to the fact that they are concerned only with solving a boundary-value problem associated with the wave equation. The advantage of MAE, on the other hand, lies in the fact that it is a phenomenological method. In situations where classical methods fail to provide an exact solution, the MAE approach of identifying component physical mechanisms and systematically integrating them into the picture leads usually to a more accurate theory, and inevitably to a better understanding of the problem. We cite Thompson's work on viscous streaming in waveguides (Thompson, 1984c) as an illustration of how different phenomena can be woven in through MAE. The same attitude prevails in the present work. Our main thrust will be to describe the effects of cutoff cross-modes induced by discontinuities in waveguides. We show that we can greatly improve the accuracy of certain overall estimates of scattering by properly accounting for these effects, and by integrating the cutoff modes into the field description, significantly extend the range of applicability of the low-frequency asymptotic theory.

2.1 Governing Equations; Geometry

The equations governing small-amplitude acoustic wave motion are obtained by linearizing the inviscid Navier-Stokes equations about a uniform rest state. The rest state is characterized by a uniform density ρ_0 and a uniform pressure p_0. Let $\overline{p}$, $\overline{\rho}$, $\overline{u}$ and $\overline{v}$ respectively denote the pressure, density, and the $x-$

and $y-$ particle velocities associated with an acoustic disturbance. These are dimensional quantities; the same symbols without overbars will denote nondimensional counterparts. Let X and Y represent dimensional coordinates and let c_0 be the dimensional isentropic sound speed at the undisturbed state. For harmonic two-dimensional disturbances with a time-dependence of $e^{-i\omega t}$, acoustic motion is governed by

$$\rho_0(\overline{u}_X + \overline{v}_Y) = \frac{i\omega}{c_0^2}\overline{p} \tag{2.1}$$

$$i\omega\rho_0\overline{u} = \frac{\partial\overline{p}}{\partial X} \tag{2.2}$$

$$i\omega\rho_0\overline{v} = \frac{\partial\overline{p}}{\partial Y} \tag{2.3}$$

The fluid is enclosed in a rigid-walled waveguide (fig. 3) whose lower boundary is defined by $Y = 0$ and upper boundary by $Y = H(X)$. On the walls, the no-penetration boundary condition must be satisfied :

$$\overline{v} = \overline{u}\frac{dH}{dX} \quad \text{on} \quad Y = H(X) \tag{2.4}$$

$$\overline{v} = 0 \quad \text{on} \quad Y = 0, \tag{2.5}$$

or, equivalently,

$$\frac{\partial \overline{p}}{\partial Y} = \frac{\partial \overline{p}}{\partial X}\frac{dH}{dX} \quad \text{on } Y = H(X) \tag{2.6}$$

$$\frac{\partial \overline{p}}{\partial Y} = 0 \quad \text{on } Y = 0 \tag{2.7}$$

We now turn to the geometry of the waveguide. Let H_0 be a typical value of height and suppose that the height in the smooth sections undergoes $O(H_0)$ changes over lengths typified by L_0; L_0 is thus a "wall wavelength". Then we can represent the height function $H(X)$ as

$$H(X) = H_0 \overline{h}(X/L_0) \tag{2.8}$$

where $\overline{h}()$ is an O(1) function. The smooth sections of the waveguide are joined by a section of rapid height variation. We shall call this section the discontinuity, and assume that the axial extent of the discontinuity is $O(H_0)$, where $H_0 \ll L_0$.

We consider low-frequency wave propagation in the waveguide. Thus if λ denotes a wavelength scale corresponding to free-space propagation at frequency ω, we have

$$\epsilon = \frac{H_0}{\lambda} \ll 1 \tag{2.9}$$

This is the small parameter of the problem. It appears as a perturbation parameter in the nondimensional equations of the next section. We also assume that λ

and L_0 are of the same order. This is not critical; however, it does serve to focus our attention on the main issue of interest - namely, the interaction of low-frequency excitation with the discontinuity. It is also convenient to recast (2.8) in the equivalent form

$$H(X) = H_0 h(X/\lambda) \tag{2.10}$$

With this, we are ready to derive the nondimensional equations of motion in the smooth and discontinuous sections of the waveguide.

2.2 Scaling; Nondimensional Equations

The basic idea in our MAE analysis is to cast the original problem as two separate sub-problems - an "inner" problem in the vicinity of the discontinuity, and an "outer" problem in the smooth sections of the duct. With reference to fig. 3, these may be precisely defined as follows : the inner region is given by $X = O(H_0)$. and the outer region by $X = O(\lambda) = O(L_0)$. The reason for posing two subproblems is that the behaviour of the fluid is qualitatively different in the inner and outer regions - wavelike behaviour prevails in the outer region, while in the inner region, the flow is essentially incompressible. This becomes apparent when the equations of motion are nondimensionalized. We start with the outer region.

In the outer region, let x,y denote nondimensional coordinates and let p,u and v denote nondimensional pressure and the x- and y- particle velocities respectively. Since $X = O(\lambda)$ and $Y = O(H_0)$ in this region, the appropriate

coordinate scaling is $x = X/\lambda$, $y = Y/H_0$. Let U_0 represent a typical dimensional value of particle velocity. Since we are concerned with frequencies below first cutoff, particle motion in the outer region is mainly in the axial direction. Thus the appropriate velocity scalings are $u = \overline{u}/U_0$, $v = \overline{v}/(\epsilon U_0)$. We scale the pressure as $p = \overline{p}/(\omega\rho_0 U_0 \lambda)$, and denote the nondimensional wavenumber by $k = \lambda\omega/c_0$.

With these definitions, (2.1)-(2.3) are converted to

$$u_x + v_y = ik^2 p \tag{2.11}$$

$$iu = p_x \tag{2.12}$$

$$\epsilon^2 iv = p_y \tag{2.13}$$

Here and for the remainder of this thesis, subscripts involving coordinates indicate differentiation with respect to those coordinates. Using (2.10), we can write the boundary conditions (2.6) and (2.7) as

$$p_y = 0 \quad \text{on} \quad y = 0 \tag{2.14}$$

$$p_y = \epsilon^2 h'(x) p_x \quad \text{on} \quad y = h(x) \tag{2.15}$$

where $h'()$ denotes the derivative of h with respect to its argument. Eliminating u and v between (2.11)-(2.13), we obtain the scaled Helmholtz equation for the outer region :

$$p_{yy} + \epsilon^2 (p_{xx} + k^2 p) = 0 \tag{2.16}$$

This, together with the boundary conditions (2.14) and (2.15), defines the

boundary-value problem for the outer pressure. To guarantee uniqueness, we need to supplement this system by two radiation conditions. We shall assume that the waveguide is excited by a plane wave incident from $x \to -\infty$. The appropriate radiation conditions are that the nonpropagating component of the scattered field should go to zero at $x \to -\infty$ and at $x \to +\infty$.

We now turn to the inner scaling. All quantities in the inner region will be denoted as $(\tilde{\ })$. Since $X = Y = O(H_0)$, the coordinates are scaled according to $(\tilde{x},\tilde{y}) = (X,Y)/H_0$. Thus $\tilde{x} = x/\epsilon$, and $\tilde{y} = y$. The x-velocity scaling is the same as in the outer region. However, we should expect y-velocities to be $O(U_0)$ in order to satisfy the no-penetration condition on the rapidly fluctuating inner walls. Thus the fluid undergoes a transition from essentially one-dimensional motion in the outer region to fully two-dimensional motion in the inner region. With this in mind, we set $(\tilde{u},\tilde{v}) = (\overline{u},\overline{v})/U_0$. The pressure scaling remains unchanged : $\tilde{p} = p$. We find that (2.1)-(2.3) take the form

$$\tilde{u}_{\tilde{x}} + \tilde{v}_{\tilde{y}} = i\epsilon k^2 \tilde{p} \tag{2.17}$$

$$i\epsilon \tilde{u} = \tilde{p}_{\tilde{x}} \tag{2.18}$$

$$i\epsilon \tilde{v} = \tilde{p}_{\tilde{y}} \tag{2.19}$$

Eliminating $\tilde{u}$ and $\tilde{v}$ leads to the scaled Helmholtz equation governing pressure in the inner region :

$$\tilde{p}_{\tilde{x}\tilde{x}} + \tilde{p}_{\tilde{y}\tilde{y}} + \epsilon^2 k^2 \tilde{p} = 0 \tag{2.20}$$

To leading order, (2.20) is simply the Laplace equation. The wall boundary

condition requires that the normal component of velocity vanish on the walls. Rather than writing this down for an arbitrary inner region, we state it explicitly in later chapters as specific geometries are considered.

2.3 The Method of Matched Asymptotic Expansions

We conclude this chapter with a brief overview with the Method of Matched Asymptotic Expansions (MAE). Details are provided in Chapters 3 and 4 where the method is applied to specific problems. As we mentioned at the beginning of this chapter, the behaviour of the fluid in the vicinity of the discontinuity is qualitatively different from its behaviour far away from it. This is borne out by the nature of equations (2.16) and (2.20). While the outer equation (2.16) describes essentially one-dimensional low-frequency wave propagation, (2.20) indicates that motion in the inner region is incompressible to leading order. Thus we pose two distinct boundary-value problems in each region; these are defined in Section 2. In mathematical terms, the need for two different sub-problems is reflected in the fact that the solution to any one boundary-value problem is incapable of describing the entire pressure field. This is typical of singular perturbation problems, and is due to the fact that two disparate length scales, λ and H_0, characterize the problem.

Although we have posed a different boundary-value problem in each region, the complete solution of any one problem is dependent on the solution of the other. This is because no conditions have been specified as yet at the "interface" between the two regions. Thus both regions are open-ended, and the

corresponding solutions will generally involve undetermined constants. The constants are determined by asymptotic matching (Van Dyke, pp.77-94; Kevorkian and Cole, pp. 7-16), a procedure that smoothly joins the inner and outer solutions in some overlap region. For purposes of illustration, suppose that the outer and inner solutions may be expressed as asymptotic expansions of the form

$$p(x,y;\epsilon) = \mu_0(\epsilon)p^{(0)}(x,y) + \mu_1(\epsilon)p^{(1)}(x,y) + \mu_2(\epsilon)p^{(2)}(x,y) + o(\mu_2) \quad (2.21)$$

$$\tilde{p}(\tilde{x},\tilde{y};\epsilon) = \nu_0(\epsilon)p^{(0)}(\tilde{x},\tilde{y}) + \nu_1(\epsilon)p^{(1)}(\tilde{x},\tilde{y}) + \nu_2(\epsilon)p^{(2)}(\tilde{x},\tilde{y}) + o(\nu_2) \quad (2.22)$$

where $\mu_0 \gg \mu_1 \gg \mu_2, \cdots$ and $\nu_0 \gg \nu_1 \gg \nu_2, \cdots$ as $\epsilon \to 0$. The outer series (2.21) is valid in region III (fig. 4), where the outer coordinate x is $O(1)$, and the inner series (2.22) is valid where the inner coordinate $\tilde{x} = x/\epsilon$ is $O(1)$. The two series are usually matched by taking the inner limit of the outer expansion and requiring that the result be asymptotic to the outer limit of the inner expansion. Thus we let $x \to 0$ in the outer expansion, that is, find its limiting form as we approach Region I from Region III (fig. 4), and let $\tilde{x} \to \infty$ in the inner expansion, which gives its limiting behaviour as we approach Region III from Region I. Symbolically, this may be stated as

$$(\tilde{x} \text{ fixed}, \epsilon \to 0) \lim p(\epsilon\tilde{x},\tilde{y};\epsilon) \sim (x \text{ fixed}, \epsilon \to 0) \lim \tilde{p}(x/\epsilon,y;\epsilon) \quad (2.23)$$

where $\tilde{x} = x/\epsilon$ and $\tilde{y} = y$ in this example.

The success of this procedure rests on the existence of an overlap or intermediate region (region II in fig. 4), where both expansions are valid and may therefore be required to have asymptotically equivalent representations. The overlap region is in some sense "between" the inner and outer regions, and the

form of each expansion in this zone is obtained by taking the limits $x \to 0$ and $\tilde{x} \to \infty$ slower than that required by (2.23). With this perspective, it is seen that (2.23) is a "strong" matching condition, sufficient, but not necessary. The fundamental requirement is asymptotic equivalence in the intermediate region. Let us define an intermediate coordinate $\overline{x} = x/\eta(\epsilon)$, $1 \gg \eta(\epsilon) \gg \epsilon$ as $\epsilon \to 0$. Keeping in mind that $\tilde{y} = y$ in the present case, the intermediate matching rule may be written as

$$(\overline{x} \text{ fixed}, \epsilon \to 0) \lim p(\eta\overline{x}, y; \epsilon) \sim (\overline{x} \text{ fixed}, \epsilon \to 0) \lim p(\eta\overline{x}/\epsilon, y; \epsilon) \qquad (2.24)$$

The two rules (2.23) and (2.24) may lead to different results, as pointed out by Van Dyke (p.220, Note 4). This becomes apparent in Chapter 3 of the present work, where we find that the restrictive nature of (2.23) precludes the matching of certain physically important terms.

We also point out that the foregoing matching rules are based on applying asymptotic limit processes to Poincaré expansions - that is, asymptotic series of the form of (2.21) and (2.22) in which the gauge functions and spatial functions are separable. While this is not an issue in most applications, failure to heed this condition may lead to significant errors (Van Dyke, p.224). This is precisely the situation we encounter in the next chapter, where certain important terms turn out to be in non-Poincaré form. This makes it necessary to derive an extended matching principle, in which a transformation is employed to convert the inner and outer expansions to Poincaré form. The rule (2.24) is then applied in the transform domain. The method is developed and applied in the next chapter, where details may be found.

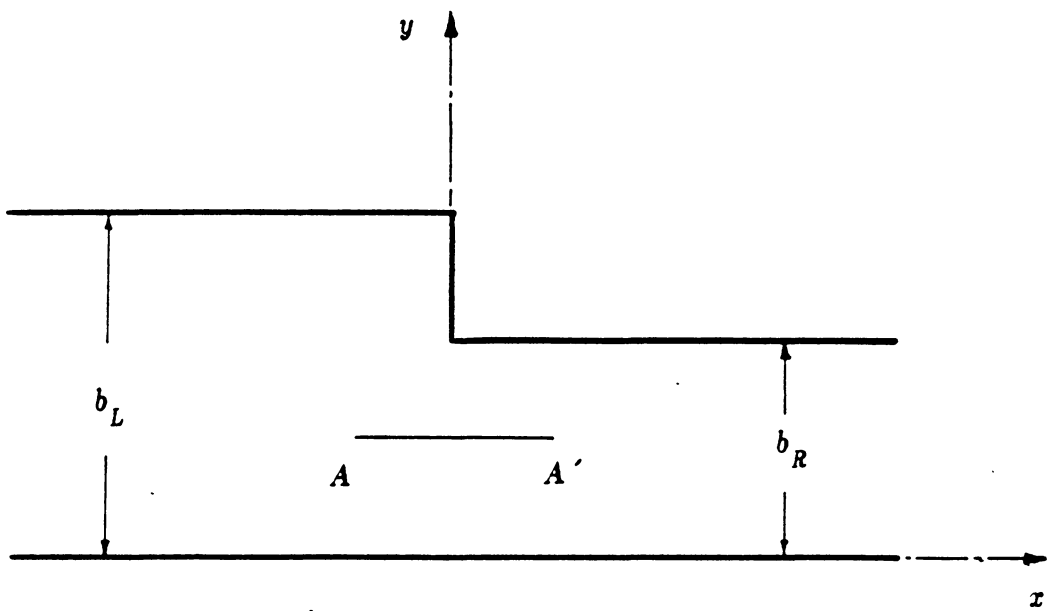

Fig. 1 : Square stepped duct geometry

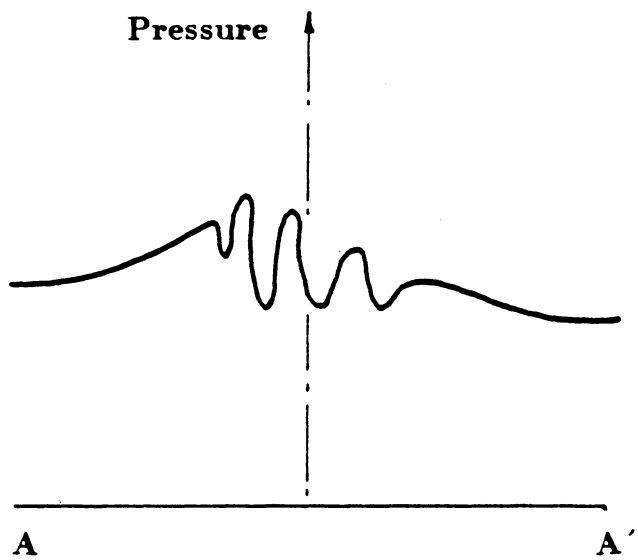

Fig. 2: Typical pressure variation along axial cut AA´ in fig. 1

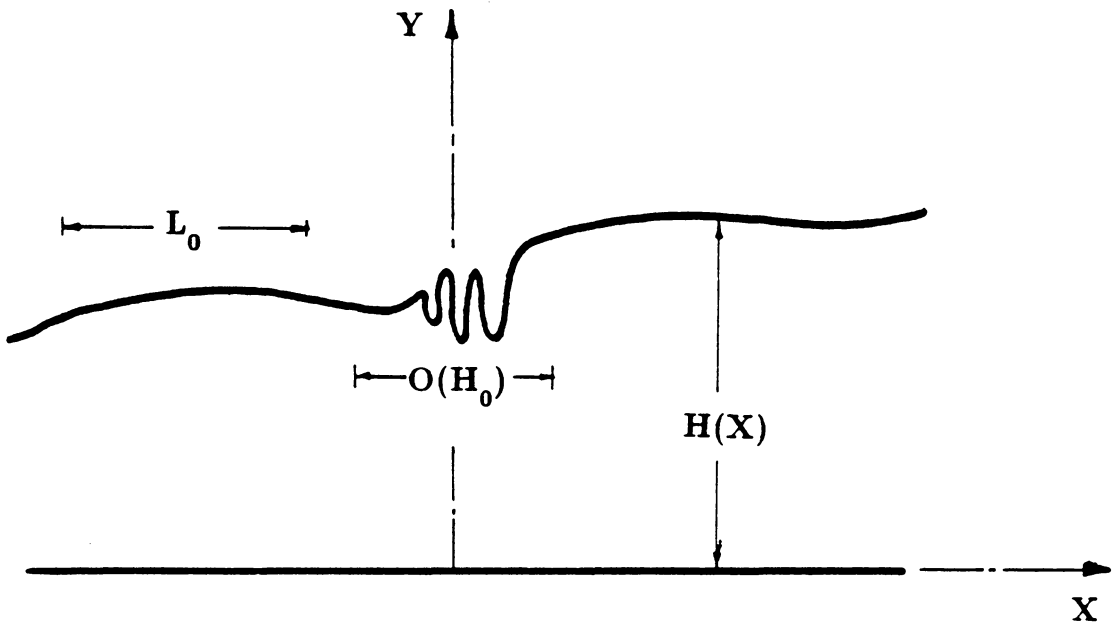

Fig. 3: Waveguide geometry and length scales

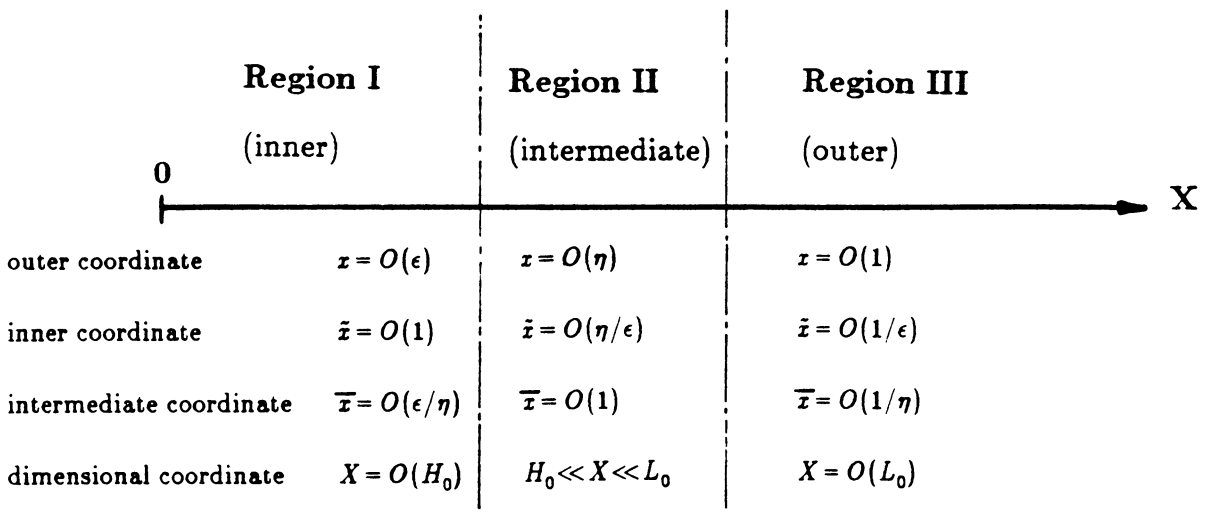

Fig. 4: Schematic of asymptotic regions and coordinate scaling

CHAPTER 3. SCATTERING BY A DISCONTINUITY JOINING TWO UNIFORM WAVEGUIDES

We begin our analysis by considering propagation in two semi-infinite waveguides coupled by a height discontinuity of finite extent (fig. 5). This is a special case of the geometry described in Chapter 2 in that we allow no height variations in the smooth outer sections. This assumption, however, is neither necessary nor restrictive in any sense. It merely allows for a clear exposition of some of the main ideas of this thesis. The main issue in going from the current case to the general one concerns the mathematical description of the outer pressure. Our main focus in this chapter is on the nature of the interaction between the wave and incompressible solutions. In order not to detract from the present goals, which are to establish the basic physical picture and develop the extended matching principle, the treatment of slowly varying outer regions will be postponed until Chapter 5.

We will assume that the duct is subject to plane wave excitation from $x \to -\infty$ at a frequency that is below the first cutoff frequency of the wider section. Thus only the fundamental mode propagates unattenuated. Higher modes excited by the discontinuity decay exponentially in space, and are discernible only in its near vicinity. The usual approach in this situation (Lesser and Lewis, 1972; Thompson, 1984a,b) is to completely ignore the attenuated cross-modes. We shall show, however, that these modes play a significant role in the interaction between the inner and outer pressures. Our main purpose in this chapter is to explain their effects and to show how they may be integrated into the global

solution. In doing so, we shall develop an extension of MAE theory based on some new ideas on asymptotic matching. Although they are evanescent, the cross-modes are responsible for a crucial modification of the inner solution. Since we deal with an arbitrarily shaped inner region in this chapter, this will only be discussed symbolically. Explicit results for a square stepped duct are given in Chapter 4, where we also compare our results with those of previous investigators.

The organization of this chapter is as follows. In Section 1, we construct the inner and outer expansions. In Section 2, we present the idea of matching Laplace transforms of these expansions and derive intermediate expansions in the transform domain. The details of matching in the transform domain are given in Section 3, where we also construct a composite expansion that is uniformly valid throughout the duct.

3.1 Outer and Inner Expansions

We start with the outer boundary-value problem, given by equations (2.14)-(2.16) with $h'(x) = 0$:

$$p_{yy} + \epsilon^2(p_{xx} + k^2 p) = 0 \tag{3.1}$$

$$p_y = 0 \text{ on } y = 0, b_L \text{ for } x<0 \tag{3.2a}$$

$$p_y = 0 \text{ on } y = 0, b_R \text{ for } x>0 \tag{3.2b}$$

Here b_L and b_R are the nondimensional heights of the left and right sections

respectively. Rather than seek a term-by-term perturbation expansion for p, we shall work with the exact solution of (3.1)-(3.2). This is simply a weighted sum of eigenfunctions, given by

$$x<0 \;:\; p = e^{ikx} + R(\epsilon)e^{-ikx} + \sum_{n=1}^{\infty} S_{Ln}\cos(\frac{y}{l_n})e^{x/(\epsilon l_n)\sqrt{1-(\epsilon k l_n)^2}} \tag{3.3}$$

$$x>0 \;:\; p = T(\epsilon)e^{ikx} + \sum_{n=1}^{\infty} S_{Rn}\cos(\frac{y}{r_n})e^{-x/(\epsilon r_n)\sqrt{1-(\epsilon k r_n)^2}} \tag{3.4}$$

where $l_n = b_L/(n\pi)$ and $r_n = b_R/(n\pi)$, and the subscripts L and R refer to quantities in the left ($x<0$) and right ($x>0$) regions respectively. In (3.3), the first term represents the incident wave. The quantities R and T are reflection and transmission coefficients respectively, being associated with the propagating fundamental mode. The S_n are the amplitudes of the cutoff cross-modes, which decay with increasing $|x|$. We note that in equation (3.1), a usual term-wise expansion of p in powers of ϵ would completely fail to generate the cross-mode terms, since they are not in Poincaré form.

We now turn to the inner boundary-value problem for the pressure, defined by equation (2.20) and the rigid wall boundary condition. If we consider the geometry of the discontinuity in inner coordinates (fig. 6), we see that outside a finite region in which $|\tilde{x}| = O(1)$, the height of the duct smoothly approaches its outer asymptotes at $\tilde{x}\to\pm\infty$. This, in fact, follows from the way the inner and outer regions were defined. We will impose the additional requirement that the

height reaches its full asymptotic values for finite $\tilde{x}$; for example, at $\tilde{x} = \tilde{x}_L$ and at $\tilde{x} = \tilde{x}_R$ (fig. 6). This assumption is not crucial; it only helps to keep the algebra simple. In general, the duct height in $\tilde{x} < \tilde{x}_L$ and $\tilde{x} > \tilde{x}_R$ would vary only on the slow outer scale $(\epsilon\tilde{x})$, causing no important changes whatsoever in the basic theory. This is demonstrated in Chapter 5. With this in mind, we note that as far as matching is concerned, it is not necessary to know the inner solution everywhere. It is sufficient to determine the functional form of the inner pressure for $\tilde{x} > \tilde{x}_R$ and $\tilde{x} < \tilde{x}_L$. This will involve certain constants. The relations between these constants must be determined numerically for an arbitrarily shaped discontinuity.

Since the regions beyond $\tilde{x} < \tilde{x}_L$ and $\tilde{x} > \tilde{x}_R$ are uniform, we may use eigenfunction expansions to represent the pressure in these regions. The governing equation for pressure is (2.20) :

$$\tilde{p}_{\tilde{x}\tilde{x}} + \tilde{p}_{yy} + \epsilon^2 k^2 \tilde{p} = 0 \tag{3.5}$$

where we have used the fact that $\tilde{y} = y$. We seek a regular perturbation expansion of (3.5) in the form

$$\tilde{p}(\tilde{x},y) = \tilde{p}^{(0)}(\tilde{x},y) + \epsilon\tilde{p}^{(1)}(\tilde{x},y) + \epsilon^2\tilde{p}^{(2)}(\tilde{x},y) - \epsilon^3\tilde{p}^{(3)}(\tilde{x},y) + \cdots \tag{3.6}$$

Substituting (3.6) into (3.5), we obtain the following problems at different orders of ϵ :

$$O(1) : \tilde{p}^{(0)}_{\tilde{x}\tilde{x}} + \tilde{p}^{(0)}_{yy} = 0 \tag{3.7}$$

$$O(\epsilon) : \tilde{p}^{(1)}_{\tilde{x}\tilde{x}} + \tilde{p}^{(1)}_{yy} = 0 \tag{3.8}$$

$$O(\epsilon^2) : \tilde{p}^{(2)}_{\tilde{x}\tilde{x}} + \tilde{p}^{(2)}_{yy} = -k^2\tilde{p}^{(0)} \tag{3.9}$$

$$O(\epsilon^3) : \tilde{p}^{(3)}_{\tilde{x}\tilde{x}} + \tilde{p}^{(3)}_{yy} = -k^2\tilde{p}^{(1)} \tag{3.10}$$

and so on. Since we are operating in the regions $\tilde{x}<\tilde{x}_L$ and $\tilde{x}>\tilde{x}_R$, the boundary condition at each order is that the y-derivative of each $\tilde{p}^{(i)}$ must vanish on $y = b_L, b_R$.

First consider the O(1) problem. To avoid extra bookkeeping, we anticipate results from matching and set

$$\tilde{p}^{(0)} = B_L^{(0)} = B_R^{(0)} = B^{(0)} \text{ (constant)} \tag{3.11}$$

This result is also intuitively evident; it represents the classical continuity of pressure condition, which is always valid at leading order. At $O(\epsilon)$, we represent the pressure in each region as an expansion in eigenfunctions of the Laplace equation :

$$\tilde{x}<\tilde{x}_L : \tilde{p}^{(1)} = A_L^{(1)}\tilde{x} + B_L^{(1)} + \sum_{n=1}^{\infty} \beta_{Ln}^{(1)} \cos\left(\frac{y}{r_n}\right) e^{\tilde{x}/l_n} \tag{3.12}$$

$$\tilde{x}>\tilde{x}_R : \tilde{p}^{(1)} = A_R^{(1)}\tilde{x} + B_R^{(1)} + \sum_{n=1}^{\infty} \beta_{Rn}^{(1)} \cos\left(\frac{y}{r_n}\right) e^{-\tilde{x}/r_n} \tag{3.13}$$

Here $A_L^{(1)}\tilde{x}$ and $A_R^{(1)}\tilde{x}$ represent volume velocity sources. From conservation of mass, we have $A_L^{(1)}b_L = A_R^{(1)}b_R = Q^{(1)}$, the first-order volume flux. The $\beta_{Ln}^{(1)}$

and $\beta_{Rn}^{(1)}$ are amplitudes of the reflected static (incompressible) modes, and are completely determined by the flux. The constants $B_L^{(1)}$ and $B_R^{(1)}$ are also fixed by $Q^{(1)}$ in the sense that the flux uniquely determines their difference $(B_L^{(1)} - B_R^{(1)})$. The individual values of the constants cannot be fixed at this stage since the solution to a homogeneous Neumann problem may only be determined up to an arbitrary additive constant. We note that (3.12) and (3.13) are not the most general solutions of Laplace's equation for the given boundary conditions; we have omitted static modes that grow exponentially with $|\tilde{x}|$. Here, once again, our choice has been dictated by intuition and some foresight - this is fully corroborated when we do the match in Section 3.

At $O(\epsilon^2)$, the pressure satisfies the Poisson equation (3.9), with $\tilde{p}^{(0)}$ given by (3.11). In the regions of interest, the particular component of $\tilde{p}^{(2)}$ is simply $-\frac{1}{2}k^2\tilde{x}^2\tilde{p}^{(0)}$, while the homogeneous solution has the same form as $\tilde{p}^{(1)}$. Thus for

$\tilde{x}<\tilde{x}_L$,

$$\tilde{p}^{(2)} = A_L^{(2)}\tilde{x} + B_L^{(2)} + \sum_{n=1}^{\infty} \beta_{Ln}^{(2)} \cos(\frac{y}{r_n}) e^{\tilde{x}/r_n} - \frac{1}{2}k^2\tilde{x}^2 B^{(0)} \qquad (3.14)$$

while for $\tilde{x}>\tilde{x}_R$,

$$\tilde{p}^{(2)} = A_R^{(2)}\tilde{x} + B_R^{(2)} + \sum_{n=1}^{\infty} \beta_{Rn}^{(2)} \cos(\frac{y}{r_n}) e^{-\tilde{x}/r_n} - \frac{1}{2}k^2\tilde{x}^2 B^{(0)} \qquad (3.15)$$

The pressure at $O(\epsilon^3)$ is determined similarly, with extra terms appearing due to the more complicated nature of the forcing function $-k^2\tilde{p}^{(1)}$. We get

$$\tilde{x}<\tilde{x}_L : \tilde{p}^{(3)} = A_L^{(3)}\tilde{x} + B_L^{(3)} + \sum_{n=1}^{\infty}\beta_{Ln}^{(3)}\cos(\frac{y}{l_n})e^{\tilde{x}/l_n}$$

$$-\frac{1}{2}k^2\tilde{x}^2B_L^{(1)} - \frac{1}{6}k^2\tilde{x}^3A_L^{(1)} - \frac{1}{2}k^2\tilde{x}\sum_{n=1}^{\infty}l_n\beta_{Ln}^{(1)}\cos(\frac{y}{l_n})e^{\tilde{x}/l_n} \qquad (3.16)$$

$$\tilde{x}>\tilde{x}_R : \tilde{p}^{(3)} = A_R^{(3)}\tilde{x} + B_R^{(3)} + \sum_{n=1}^{\infty}\beta_{Rn}^{(3)}\cos(\frac{y}{r_n})e^{-\tilde{x}/r_n}$$

$$-\frac{1}{2}k^2\tilde{x}^2B_R^{(1)} - \frac{1}{6}k^2\tilde{x}^3A_R^{(1)} + \frac{1}{2}k^2\tilde{x}\sum_{n=1}^{\infty}r_n\beta_{Rn}^{(1)}\cos(\frac{y}{r_n})e^{-\tilde{x}/r_n} \qquad (3.16)$$

It is important to note at this point that unlike the homogeneous problem at $O(\epsilon)$, mass conservation at orders ϵ^2 and ϵ^3 does not yield a simple relation between the corresponding A_L and A_R. This is due to the forcing terms in (3.9) and (3.10). A further consequence is that the simple relations that connect the volume flux Q, the constant terms B_L,B_R and the modal amplitudes β_n of the homogeneous problem do not hold any longer. While the flux uniquely determines the rest of the homogeneous solution for Laplace's equation, the situation is different for Poisson's equation. Even the homogeneous component of the

solution is affected by the forcing - that is , the relation between the homogeneous solution in $\tilde{x}<\tilde{x}_L$ and that in $\tilde{x}>\tilde{x}_R$ is modified. This is a direct result of compressibility at higher orders. Thus when we evaluate B_L, B_R and β_n at these orders, we must be careful to include the effects of the forcing terms.

We will show that this modification of the inner solution is absolutely crucial to the accuracy of the low-frequency theory. The modification is due to compressibility in the inner region at higher orders, a feature that becomes more prominent as the frequency is increased. Thus if this effect is ignored, it is natural to expect that the resulting theory will be limited to very low frequencies. The static modal amplitudes β_n, which appear as forcing terms for higher-order problems, are directly related to the amplitudes of the cutoff dynamic (wave) modes. Thus the cutoff modes have a source-like role in the inner problem. Due to reasons mentioned above, these sources represent an important facet of the interaction between the static and dynamic fields. It is only by properly accounting for them that we can hope to reproduce the accuracy of Schwinger's Static Equivalence solution (Appendix A) while not being constrained by geometrical considerations as in that method.

We close this section by mentioning that Lesser and Lewis (1972), in developing their inner solution, observe that the homogeneous components of $\tilde{p}^{(1)}$ and $\tilde{p}^{(2)}$ are simply related by

$$\tilde{p}^{(2)}_{homog.} = \frac{Q^{(2)}}{Q^{(1)}}\,\tilde{p}^{(1)}_{homog.} \tag{3.18}$$

where $Q^{(2)}$ is the second-order flux. For an arbitrary inner region, this is precisely what would result if one were to ignore the effects of the forcing terms. Fortunately, for the square step considered by Lesser and Lewis, (3.18) remains true at $O(\epsilon^2)$. At higher orders, however, such simple relations do not exist even for the square step (Chapter 4), whereas for arbitrary inner geometries, (3.18) is invalid even at $O(\epsilon^2)$.

3.2 Intermediate Expansions through Laplace Transforms

Having established the role of the cutoff cross-modes, the next question we must deal with is that of including them in an MAE scheme. That this issue deserves special attention becomes apparent when we consider the functional structure of the inner and outer cross-modes in (3.3)-(3.4) and (3.12)-(3.17). The quantity of interest is the cross-mode axial phase factor, $e^{-x/(\epsilon r_n)\sqrt{1-(\epsilon k r_n)^2}}$ $(x>0)$ for the dynamic field and $e^{-\tilde{x}/r_n}$ $(\tilde{x}>\tilde{x}_R)$ for the static field. We note that the usual matching scheme, as described by (2.23), fails to accommodate the phase factors. The outer limit of the inner phase factor is $e^{-x/(\epsilon r_n)}$ - this is clearly subdominant, in some sense, as $\epsilon \to 0$ $(x>0)$. On the other hand, the inner limit of the outer phase factor, given by $e^{-\tilde{x}/r_n\sqrt{1-\epsilon^2 k^2 r_n^2}}$, remains O(1) in the limit. This leads to a contradiction since the orthogonality properties of the transverse eigenfunctions $\cos(y/r_n)$ clearly dictate that there must be a one-to-one correspondence between the inner and outer cross-modes.

The reason behind this paradox is that (2.23) is a "strong" matching rule, as we discussed in Chapter 2, and is too restrictive for our purposes. To match

the inner and outer expansions, it is sufficient to require the existence of an intermediate region in which the two are asymptotically equivalent. In the present context, this means that the limits $x \to 0^+$ and $\tilde{x} \to +\infty$ may be approached at a slower rate than in (2.23), which prescribes the fastest rate possible. This is the idea behind equation (2.24), the intermediate matching rule. Thus if we define the intermediate coordinate $\overline{x} = x/\eta(\epsilon) = \epsilon\tilde{x}/\eta(\epsilon)$, where $\epsilon \ll \eta(\epsilon) \ll 1$ as $\epsilon \to 0$, the intermediate limit is approached by letting $x \to 0^+$, $\overline{x}$ fixed, and $\tilde{x} \to \infty$, $\overline{x}$ fixed. These limits are slower than $x \to 0^+$, $\tilde{x}$ fixed, and $\tilde{x} \to \infty$, x fixed. The region where $\overline{x} = O(1)$ is called the overlap or intermediate region (fig.4). If we now apply the intermediate limit process to the exponential phase factors, we see that both outer and inner phase factors are proportional to $e^{-\eta\overline{x}/(\epsilon r_*)}$. Thus there is indeed an overlap region where both inner and outer cross-modes are of comparable magnitude, and it is conceivable that they may be matched to each other in this region. This resolves the dilemma we faced with rule (2.23). It is clear that (2.23) fails in this case because the actual overlap region is smaller than that prescribed by that rule.

Having verified the existence of an overlap zone, we are still faced with the problem of including the exponential phase factors in a matching scheme. As they stand, the exponentials are subdominant in some sense, since in the limit $\epsilon \to 0$, $e^{-(\eta\overline{x})/(\epsilon r_*)}$ appears to vanish faster than any algebraic power of ϵ. Thus it seems that the cross-modes will always drop out when we do the match, unless one adopts an *ad hoc* scheme such as matching like terms of the form $\epsilon^i e^{-(\eta\overline{x})/(\epsilon r_*)}$ without regard for their magnitude relative to ordinary gauge functions.

Our contention is that one cannot make any precise statements about the order of such terms since they are not in Poincaré form. Fraenkel (1969a,b,c), in his proof of the asymptotic matching principle, points out that it is necessary for the inner and outer expansions to be in Poincaré form - that is, the gauge functions and the spatial functions must be separable. Van Dyke (p. 224) also discusses several examples in which violation of this condition leads to erroneous results. Thus it seems that the separability requirement is fundamental to the theory of asymptotic matching.

What is needed, then, is a device that will convert the exponentials into Poincaré form while at the same time leaving terms that are already in Poincaré form in the xy-plane unchanged in that respect. We propose a Laplace transformation, defined by

$$\overline{x}<0: \quad F^{(-)}(s,\epsilon) = \int_{-\infty}^{0} f(\overline{x},\epsilon)\, e^{s\overline{x}}\, d\overline{x} \tag{3.19}$$

$$\overline{x}>0: \quad F^{(-)}(s,\epsilon) = \int_{0}^{\infty} f(\overline{x},\epsilon)\, e^{-s\overline{x}}\, d\overline{x} \tag{3.20}$$

This idea is similar to that of Sheer (1971), who used logarithms to convert the inner expansion for flow around a sharp-edged airfoil to Poincaré form. We will see in the next section that in the plane of the transform variable s, the cross-mode exponentials have a simple algebraic form, while terms that are already

algebraic in the xy-plane remain so. Thus our procedure will consist of transforming the intermediate expansions of the inner and outer pressure using (3.19)-(3.20), and then matching the resulting expansions in the transform domain. For $x>0$, for example, this reads

$$\lim_{\epsilon\to 0}\int_0^\infty p(\overline{x},\epsilon)e^{s\overline{x}}d\overline{x} \sim \lim_{\epsilon\to 0}\int_0^\infty \tilde{p}(\overline{x},\epsilon)e^{s\overline{x}}d\overline{x} \tag{3.21}$$

Since the limit processes in (3.21) do not affect the integration variable $\overline{x}$, it is highly plausible that there is an underlying Abelian theorem (Bender and Orszag, p.126) that rigorously justifies the transformation. Abelian theorems are concerned with the formal integration of asymptotic relations. To our knowledge, there are no such theorems that deal with asymptotic series in non-Poincaré form. Rather than pursuing a mathematical proof, however, we shall cite our final results as evidence that Laplace domain matching may be put on a more rigorous footing.

As far as ordering is concerned, the transformations (3.19) and (3.20) accomplish a major goal. In the s-plane, there is no ambiguity regarding the magnitude of the exponential phase factors. In the next section, we show that if one properly restricts the size of the overlap region so as to avoid a switchback-like phenomenon, the transformed phase factors in the s-plane behave somewhat like logarithmic gauge functions, in the sense that they "fill in the gaps" between successive integral powers of ϵ. Armed with this knowledge, it is even possible to go back to the xy-plane and treat terms like $\epsilon^i e^{-(\eta\overline{x})/(\epsilon r_*)}$ accordingly, provided

one is careful about relative orders. This procedure is followed in Chapter 5. In this chapter, our goal is to develop the theory of Laplace domain matching, and thus we shall do the $s-$plane matching in full detail. This is accomplished in the next section.

We close this section by presenting the Laplace domain intermediate expansions of the inner and outer pressures. Expressing (3.3) and (3.4) in terms of the intermediate variable $\overline{x}$ and using (3.19) and (3.20) in the appropriate regions, we obtain the following expansions for the outer pressure. Note that the limit $\eta \to 0$ is applied to the transformed expressions.

$$\overline{x}<0: \quad P = \left(\frac{1}{s} - \frac{ik\eta}{s^2} - \frac{k^2\eta^2}{s^3} + \frac{ik^3\eta^3}{s^4} + \frac{k^4\eta^4}{s^5} - \cdots \right)$$

$$+ \left(R^{(0)} + \epsilon R^{(1)} + \epsilon^2 R^{(2)} + \cdots \right) \left(\frac{1}{s} + \frac{ik\eta}{s^2} - \frac{k^2\eta^2}{s^3} - \cdots \right)$$

$$+ \sum_{n=1}^{\infty} \cos\left(\frac{y}{\tau_n}\right) \left(S_{Ln}^{(0)} + \epsilon S_{Ln}^{(1)} + \epsilon^2 S_{Ln}^{(2)} + \epsilon^3 S_{Ln}^{(3)} + \cdots \right)$$

$$\times \left[\frac{\epsilon}{\eta} l_n \left(1 + \frac{1}{2}\epsilon^2 k^2 l_n^{\,2} + \frac{3}{8}\epsilon^4 k^4 l_n^{\,4} + \cdots \right) \right.$$

$$- \frac{\epsilon^2}{\eta^2} s l_n^2 \left(1 + \epsilon^2 k^2 l_n^2 + \epsilon^4 k^4 l_n^4 + \cdots \right)$$

$$+ \frac{\epsilon^3}{\eta^3} s^2 l_n^3 \left(1 + \frac{3}{2}\epsilon^2 k^2 l_n^2 + \frac{15}{8}\epsilon^4 k^4 l_n^4 + \cdots \right) + \cdots \Bigg] \qquad (3.22)$$

$$\overline{x}>0 : \; P = \left(T^{(0)} + \epsilon T^{(1)} + \epsilon^2 T^{(2)} + \cdots \right) \left(\frac{1}{s} + \frac{ik\eta}{s^2} - \frac{k^2\eta^2}{s^3} - \cdots \right)$$

$$+ \sum_{n=1}^{\infty} \cos\left(\frac{y}{r_n}\right) \left(S_{Rn}^{(0)} + \epsilon S_{Rn}^{(1)} + \epsilon^2 S_{Rn}^{(2)} + \epsilon^3 S_{Rn}^{(3)} + \cdots \right)$$

$$\times \Bigg[\frac{\epsilon}{\eta} r_n \left(1 + \frac{1}{2}\epsilon^2 k^2 r_n^2 + \frac{3}{8}\epsilon^4 k^4 r_n^4 + \cdots \right)$$

$$- \frac{\epsilon^2}{\eta^2} s r_n^2 \left(1 + \epsilon^2 k^2 r_n^2 + \epsilon^4 k^4 r_n^4 + \cdots \right)$$

$$+ \frac{\epsilon^3}{\eta^3} s^2 r_n^3 \left(1 + \frac{3}{2}\epsilon^2 k^2 r_n^2 + \frac{15}{8}\epsilon^4 k^4 r_n^4 + \cdots \right) + \cdots \Bigg] \qquad (3.23)$$

Here $P = P(s,\epsilon)$ denotes the Laplace transform of the outer pressure $p(\eta\overline{x},y;\epsilon)$. We have also expanded the reflection and transmission coefficients R, T and the cross-mode amplitudes S_{Rn}, S_{Ln} in powers of ϵ. The intermediate expansion of the inner pressure in the Laplace domain is obtained similarly. We set $\tilde{x} = \eta\overline{x}/\epsilon$ in (3.11)-(3.17) and transform according to (3.19) and (3.20). Letting $\tilde{P}$ stand for the transformed pressure, we obtain

$$\overline{x}<0: \quad \tilde{P} = \frac{B^{(0)}}{s} - \eta\frac{A_L^{(1)}}{s^2} + \epsilon\frac{B_L^{(1)}}{s} - \epsilon\eta\frac{A_L^{(2)}}{s^2} + \epsilon^2\frac{B_L^{(2)}}{s}$$

$$- \eta^2\frac{B^{(0)}k^2}{s^3} - \epsilon^2\eta\frac{A_L^{(3)}}{s^2} + \epsilon^3\frac{B_L^{(3)}}{s} + \eta^3\frac{k^2A_L^{(1)}}{s^4} - \epsilon\eta^2\frac{k^2B_L^{(1)}}{s^3}$$

$$+ \sum_{n=1}^{\infty}\cos(\frac{y}{\gamma_n})(\beta_{Ln}^{(1)} + \epsilon\beta_{Ln}^{(2)} + \epsilon^2\beta_{Ln}^{(3)} - \cdots)\left(\frac{\epsilon^2}{\eta}l_n - \frac{\epsilon^3}{\eta^2}sl_n^2 + \frac{\epsilon^4}{\eta^3}s^2l_n^3 - \cdots\right)$$

$$+ \frac{1}{2}k^2\sum_{n=1}^{\infty}\cos(\frac{y}{\gamma_n})\beta_{Ln}^{(1)}\left(\frac{\epsilon^4}{\eta}l_n^3 - 2\frac{\epsilon^5}{\eta^2}sl_n^4 + 3\frac{\epsilon^6}{\eta^3}s^2l_n^5 - \ldots\right) - \cdots \qquad (3.24)$$

$$\overline{x}>0 : \tilde{P} = \frac{B^{(0)}}{s} + \eta\frac{A_R^{(1)}}{s^2} + \epsilon\frac{B_R^{(1)}}{s} + \epsilon\eta\frac{A_R^{(2)}}{s^2} + \epsilon^2\frac{B_R^{(2)}}{s}$$

$$- \eta^2\frac{B^{(0)}k^2}{s^3} + \epsilon^2\eta\frac{A_R^{(3)}}{s^2} + \epsilon^3\frac{B_R^{(3)}}{s} - \eta^3\frac{k^2A_R^{(1)}}{s^4} - \epsilon\eta^2\frac{k^2B_R^{(1)}}{s^3}$$

$$+ \sum_{n=1}^{\infty}\cos(\frac{y}{r_n})(\beta_{Rn}^{(1)} + \epsilon\beta_{Rn}^{(2)} + \epsilon^2\beta_{Rn}^{(3)} + \cdots)\left(\frac{\epsilon^2}{\eta}r_n - \frac{\epsilon^3}{\eta^2}sr_n^2 + \frac{\epsilon^4}{\eta^3}s^2r_n^3 - \cdots\right)$$

$$+ \frac{1}{2}k^2\sum_{n=1}^{\infty}\cos(\frac{y}{r_n})\beta_{Rn}^{(1)}\left(\frac{\epsilon^4}{\eta}r_n^3 - 2\frac{\epsilon^5}{\eta^2}sr_n^4 + 3\frac{\epsilon^6}{\eta^3}s^2r_n^5 - \cdots\right) + \cdots \quad (3.25)$$

3.3 Matching in the Transform Domain

Our next task is to match the intermediate expansions of the last section using the matching rule (3.21). Matching rules are typically applied at successive orders, *i.e.*, the difference between the left- and right-hand sides of (3.21) is made progressively smaller as $\epsilon \to 0$ by matching more and more terms of the inner and outer expansions. Alternatively, one might match a block of ordered terms in one expansion to a corresponding block in the other expansion in one single step; this is known as block matching (Lesser and Crighton, pp.86-88). Block matching is usually done to avoid the "switchback" phenomenon (Lesser and Crighton, p.80). This is said to occur when one finds, while matching at a certain order, that terms of lower order must be inserted to make the inner and outer expansions consistent. We shall find it necessary to use block matching in this section.

The main issue we have to deal with during the match is the order of the yet unspecified gauge function $\eta(\epsilon)$. Typically, in an intermediate matching scheme, one finds that the extent of the overlap region is successively restricted as one proceeds with the matching (Kevorkian and Cole, pp. 7-16). This is equivalent to restricting the range of $\eta(\epsilon)$, which is initially $1 \ll \eta(\epsilon) \ll \epsilon$ by definition. There are no general guidelines on how η is to be restricted. In the present problem, we find that if we start with an *ad hoc* assumption such as $\epsilon^m \gg \eta(\epsilon) \gg \epsilon^n$, where $0<m<n<1$, we soon encounter a phenomenon akin to switchback. Thus while matching terms corresponding to a certain $\tilde{p}^{(i)}$, we find that our assumption on η forces us to go on to $\tilde{p}^{(i+1)}$ before exhausting the

complete series of $O(\frac{\epsilon^{i+n}}{\eta^n})$, $n = 1,2,3, \cdots$ that correspond to the cross-modes

of $\tilde{p}^{(i)}$ itself. The portion of the series that is left out typically reappears while matching terms from a higher-order $\tilde{p}^{(i)}$. On the other hand, if we start out with $\eta(\epsilon) \ll \epsilon^m$, $0<m<1$, we find that we can delay the switchback-like phenomenon further and further as the value of m is increased. This suggests that if η is always restricted from above, we can completely eliminate switchback; as is indeed the case. Thus we stipulate that

$$\epsilon \ll \eta(\epsilon) \ll \epsilon^m \,, \quad \text{for all } m \text{ such that } 0<m<1 \tag{3.26}$$

making η much like a logarithmic gauge function.

It is interesting to note that this condition is intimately related to the behaviour of the cross-modes. As we saw in Section 3.1, the outer cross-mode phase factors $e^{-x/(\epsilon r_n)\sqrt{1-(\epsilon k r_n)^2}}$ approach unity as $x \to 0$, while the inner phase factors $e^{-\tilde{x}/r_n}$ tend to zero as $\tilde{x} \to \infty$. In the vicinity of the origin, however, the inner phase factors are also O(1); that is, their magnitude is comparable to that of the outer phase factors. Thus to match the inner and outer cross-modes, physical reasoning suggests that the overlap zone should be on the "inner side" of the intermediate region. This is precisely what condition (3.26) enforces. Restricting $\eta(\epsilon)$ from above is equivalent to pushing the overlap region away from the outer region towards the inner region. Thus the limit $x \to 0$ is approached just slightly slower than if we had held $\tilde{x}$ fixed, whereas the limit $\tilde{x} \to \infty$ is approached slower than any algebraic rate given by $(\epsilon^m \tilde{x})$ fixed, $0<m \leqslant 1$. This illustrates the

fact that mathematical inconsistencies such as switchback can often be linked to the underlying physical situation.

Given the condition (3.26), we can now order the gauge functions that appear in (3.22)-(3.25). We see that there are two groups of functions; Group I, in which they have the form $\epsilon^m \eta^p$, $m = 0,1,2, \cdots$; $p = 0,1,2, \cdots$, and Group II, with members ϵ^m / η^p, $m \geq p$, $m = 1,2,3, \cdots$; $p = 1,2,3, \cdots$. The Group I functions correspond to the propagating part of the acoustic pressure, while the Group II functions correspond to the cutoff modes. The two groups are shown in matrix form below, with the small numbers in parentheses denoting a characteristic index i. The index for each group is defined as follows : for Group I, $i_1 = m + p$, and for Group II, $i_2 = m - p$.

$$\underline{\textit{Group I} - \text{index } i_1} \tag{3.27}$$

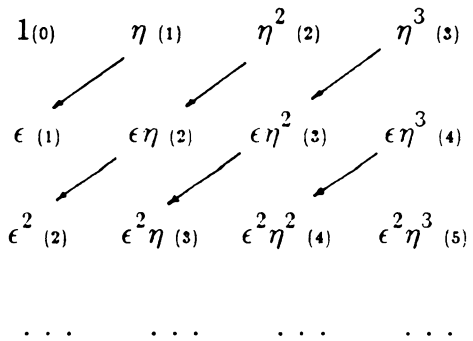

Group II – index i_2 (3.28)

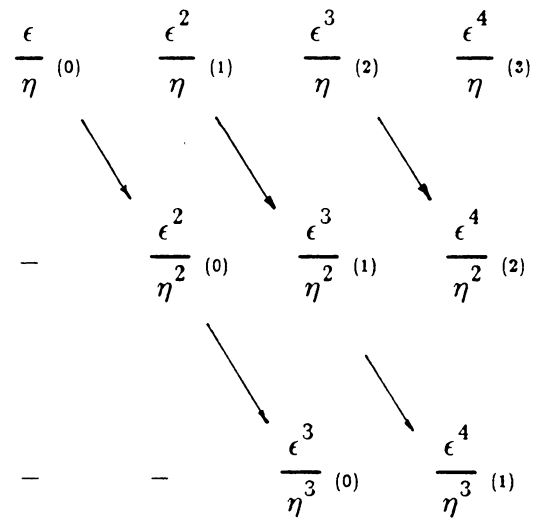

. . . .

The significance of the indices is that within each group, a gauge function with a lower index is larger than one with a higher index. When two Group I functions have the same index, the function with the higher power of η is larger, whereas for two Group II functions with the same index, the function with the lower power of η is larger. Between Group I and Group II, the function with the smaller index is always larger. When $i_1 = i_2$, the Group I function is always larger. These conclusions follow immediately from (3.26), and may be easily verified. The ordering is indicated graphically in (3.27) and (3.28). To match successively higher orders, we start with $i_1 = 0$, proceed to $i_1 = 1$ and follow the arrows, then move to $i_2 = 1$ in Group II and follow the arrows there, come back to Group I and complete the $i_1 = 2$ functions, and so on. Because of the upper triangular structure of (3.28), equal-index sets in Group II are infinite. Each

such set corresponds to cross-modes from a particular order. For example, $i_2 = 1$ comes from the cross-modes in $\tilde{p}^{(1)}$, and so on. We have to match an entire set of functions with $i_2 =$ constant in a block before we can move on to the next Group I functions. Thus our block matching scheme ensures that all cross-modes from a certain $\tilde{p}^{(i)}$ are matched before we start matching terms from $\tilde{p}^{(i+1)}$ and so on. This is similar to matching logarithmic gauge functions in a block (Lesser and Crighton, pp.86-88). It is directly related to the fact that we have avoided switchback by restricting the intermediate gauge function $\eta(\epsilon)$ from above.

With (3.27) and (3.28) in front of us, it is a simple matter to do the match. We match (3.22) with (3.24), and (3.23) with (3.25). The results, to $O(\eta^4)$, are given below.

$$1 - R^{(0)} = T^{(0)} \tag{3.29}$$

$$S_{Ln}^{(0)} = S_{Rn}^{(0)} = 0 \tag{3.30}$$

$$A_L^{(1)} = ik(1 - R^{(0)}), \quad A_R^{(1)} = ikT^{(0)} \tag{3.31}$$

$$B_L^{(1)} = R^{(1)}, \quad B_R^{(1)} = T^{(1)} \tag{3.32}$$

$$S_{Ln}^{(1)} = \beta_{Ln}^{(1)}, \quad S_{Rn}^{(1)} = \beta_{Rn}^{(1)} \tag{3.33}$$

$$A_L^{(2)} = -ikR^{(1)}, \quad A_R^{(2)} = ikT^{(1)} \tag{3.34}$$

$$B_L^{(2)} = R^{(2)}, \quad B_R^{(2)} = T^{(2)} \tag{3.35}$$

$$\beta_{Ln}^{(2)} = S_{Ln}^{(2)}, \quad \beta_{Rn}^{(2)} = S_{Rn}^{(2)} \tag{3.36}$$

$$A_L^{(3)} = -ikR^{(2)}, \quad A_R^{(3)} = ikT^{(2)} \tag{3.37}$$

$$B_L^{(3)} = R^{(3)}, \quad B_R^{(3)} = T^{(3)} \tag{3.38}$$

$$\beta_{Ln}^{(3)} = S_{Ln}^{(3)}, \quad \beta_{Rn}^{(3)} = S_{Rn}^{(3)} \tag{3.39}$$

It is clear from (3.22)-(3.25) that the pattern of equations (3.29)-(3.39) repeats as we go to progressively higher orders. The volume velocity coefficients A_L, A_R are equal to the gradients of the mean outer pressure at $x = 0$, the constant terms are equal to the mean pressure, and the inner and outer cross-mode coefficients are equal to each other. Additional information is obtained when we solve each inner (static) problem fully. This, together with (3.29)-(3.39), would completely determine the inner and outer expansions. However, to obtain the necessary static relations for an arbitrary inner geometry, one must use a numerical method. In the next chapter, we consider a special geometry where the desired relations may be determined analytically. Complete details for the calculation of the inner and outer fields are presented there.

If we suppose for now that the inner and outer pressures are completely known, we may construct a composite expansion by adding the inner and outer expansions and subtracting their common part in the overlap region. It is important to recall that the function $\tilde{p}$ is not the complete inner solution, but is valid only in the uniform sections $\tilde{x}<\tilde{x}_L$ and $\tilde{x}>\tilde{x}_R$. The complete inner solution, which we denote by $\hat{p}$, must be numerically determined, in general. Only for a few special inner geometries, such as the square step considered in Chapter 4, is it possible to obtain closed-form analytical solutions. This, however, is not a hindrance to the theory, since the numerical solution of Laplace's equation or Poisson's

equation in two dimensions is a standard computational task. As we discussed in Chapter 1, numerical schemes for elliptic equations are far more robust than those for the wave equation, especially in regions with reentrant corners and rapid wave variation. Thus an important role of the asymptotic theory is to extend the applicability of computational methods for arbitrary geometries by identifying the appropriate local problem to be solved.

We suppose that $\hat{p}$ may be expanded as

$$\hat{p}(\tilde{x},y) = \hat{p}^{(0)} + \epsilon\hat{p}^{(1)} + \epsilon^2\hat{p}^{(2)} + \cdots \tag{3.40}$$

The common part of the inner and outer expansions in the intermediate region is given, in the s-plane, by (3.24) and (3.25). Since we have matched all orders up to (but not including) $O(\eta^4)$, the smallest terms retained are $O(\frac{\epsilon^{n+3}}{\eta^n})$, $n = 1,2,3,\cdots$. These are transforms of terms that contain $\epsilon^3 e^{\tilde{x}/l_n}$ and $\epsilon^3 e^{-\tilde{x}/r_n}$ in the inner expansion, whereas in the outer series, they are associated with $S_{Ln}^{(3)}$ or $S_{Rn}^{(3)}$ times the outer phase factor. Thus upon transforming the common part back to the physical domain, we obtain

$$x<0: \; p_{composite} = \left(\hat{p}^{(0)} + \epsilon\hat{p}^{(1)} + \epsilon^2\hat{p}^{(2)} + \epsilon^3\hat{p}^{(3)}\right)$$

$$+e^{ikx} + \left(R^{(0)} + \epsilon R^{(1)} + \epsilon^2 R^{(2)} + \epsilon^3 R^{(3)}\right) e^{-ikx}$$

$$+e^{ikx} + \left(R^{(0)} + \epsilon R^{(1)} + \epsilon^2 R^{(2)} + \epsilon^3 R^{(3)}\right) e^{-ikx}$$

$$+ \sum_{n=1}^{\infty} \cos\left(\frac{y}{T_n}\right)\left(\epsilon S_{Ln}^{(1)} + \epsilon^2 S_{Ln}^{(2)} + \epsilon^3 S_{Ln}^{(3)}\right) e^{x/(\epsilon l_n)\sqrt{1-(\epsilon k l_n)^2}}$$

$$- \Bigg[B^{(0)} + \epsilon(A_L^{(1)}\tilde{x} + B_L^{(1)}) + \epsilon^2(A_L^{(2)}\tilde{x} + B_L^{(2)} - \frac{1}{2}k^2x^2B^{(0)})$$

$$+ \epsilon^3(A_L^{(3)}\tilde{x} + B_L^{(3)} - \frac{1}{2}k^2B_L^{(1)}\tilde{x}^2 - \frac{1}{6}k^2A_L^{(1)}\tilde{x}^3) \qquad (3.41)$$

$$+ \sum_{n=1}^{\infty} \cos(\frac{y}{r_n}) \Big(\epsilon S_{Ln}^{(1)} + \epsilon^2 S_{Ln}^{(2)} + \epsilon^3(S_{Ln}^{(3)} - \frac{1}{2}k^2\tilde{x}l_n S_{Ln}^{(1)}) \Big) e^{\tilde{x}/l_n} \Bigg] + O(\eta^4)$$

$$x>0 : \; p_{composite} = \Big(\hat{p}^{(0)} + \epsilon\hat{p}^{(1)} + \epsilon^2\hat{p}^{(2)} - \epsilon^3\hat{p}^{(3)} \Big)$$

$$- \Big(T^{(0)} - \epsilon T^{(1)} + \epsilon^2 T^{(2)} + \epsilon^3 T^{(3)} \Big) e^{ikx}$$

$$+ \sum_{n=1}^{\infty} \cos(\frac{y}{r_n}) \Big(\epsilon S_{Rn}^{(1)} + \epsilon^2 S_{Rn}^{(2)} + \epsilon^3 S_{Rn}^{(3)} \Big) e^{-x/(\epsilon r_n)\sqrt{1-(\epsilon k r_n)^2}}$$

$$- \Bigg[B^{(0)} + \epsilon(A_R^{(1)}\tilde{x} + B_R^{(1)}) + \epsilon^2(A_R^{(2)}\tilde{x} + B_R^{(2)} - \frac{1}{2}k^2x^2B^{(0)})$$

$$+ \epsilon^3 (A_R^{(3)} \tilde{x} + B_R^{(3)} - \frac{1}{2} k^2 B_R^{(1)} \tilde{x}^2 - \frac{1}{6} k^2 A_R^{(1)} \tilde{x}^3) \qquad (3.42)$$

$$+ \sum_{n=1}^{\infty} \cos(\frac{y}{r_n}) \left(\epsilon S_{Rn}^{(1)} + \epsilon^2 S_{Rn}^{(2)} + \epsilon^3 (S_{Rn}^{(3)} + \frac{1}{2} k^2 \tilde{x} r_n S_{Rn}^{(1)}) \right) e^{-\tilde{x}/r_n} \Bigg] + O(\eta^4)$$

Equations (3.41) and (3.42) are valid, in their respective domains, throughout the inner and outer regions. They represent the MAE solution for pressure with the cross-modes included. It is true that the cross-modes decay exponentially as we move away from the discontinuity, and at first sight, appear to do no more than contribute to the fine structure of the field near the discontinuity. But as we noted earlier, the cross-modes contribute in a subtle manner, through their interaction with the inner field. This plays a vital role in determining the dynamic range over which low-frequency theory may be applied. Considering a specific geometry, we show in the next chapter that using (3.41) and (3.42), with the cross-mode source effects properly accounted for, we can extend the range of accuracy of scattering estimates such as junction impedance all the way up to the first cutoff frequency.

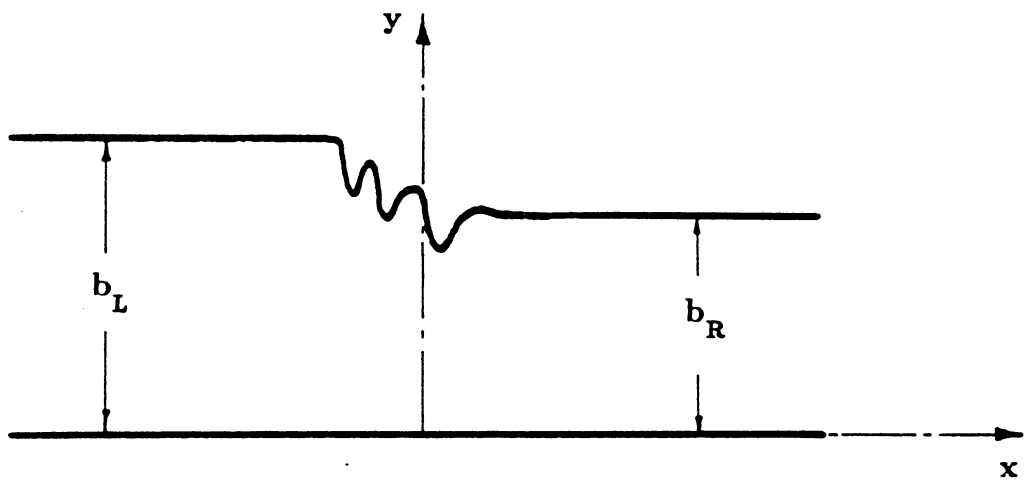

Fig. 5: Waveguide geometry for chap. 3 in outer coordinates

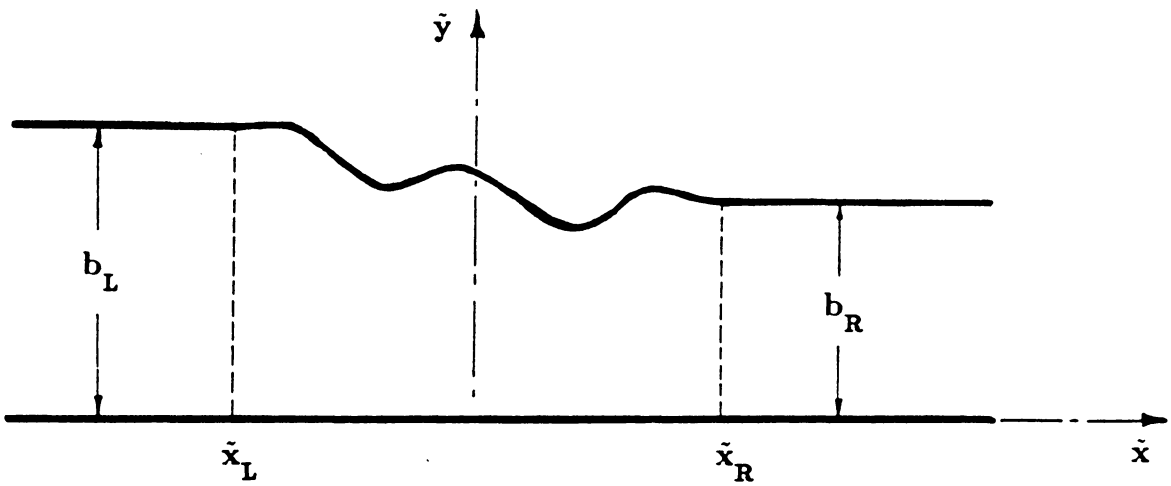

Fig. 6: Waveguide geometry for chap. 3 in inner coordinates

CHAPTER 4 : APPLICATION TO THE SQUARE STEPPED DUCT

Our objective in this chapter is to apply the theory developed in Chapter 3 to scattering by a square step discontinuity connecting two uniform waveguides of unequal height. The geometry is depicted in fig. 7. We will obtain explicit formulae for the junction impedance, the reflection and transmission coefficients, and the composite pressure field. Results will be compared to those of Schwinger (Appendix A) and Lesser and Lewis (1972). It will be shown that the cutoff modes of the outer pressure act as sources at infinity in the inner boundary-value problem. The effect of these sources is to modify the mean pressure in the vicinity of the step, and thereby the junction impedance. This is an effect of the compressibility of the local flow near the step. Although the step has no thickness, its region of influence is finite. The fluid in this region moves back and forth like a rigid mass in the lowest order approximation, the effects of compressibility coming in as higher order corrections. However, as the frequency is increased, these effects become more pronounced. Of particular importance is the modification of the relation between the static volume velocity and the static mean pressure. In the present geometry, this effect is entirely due to the cross-modes. Unless the modal contributions are properly accounted for, no higher-order corrections are obtained for the impedance, and the result obtained is simply proportional to the frequency. This is just the zero-frequency asymptote of the impedance. It illustrates the fact that the cutoff cross-modes play an important role in extending the range of validity of the theory.

Our main task in this chapter is the explicit solution of the inner problems at each order. We seek to obtain relations between the static coefficients that appear in (3.12)-(3.17). These relations depend only on the inner geometry, and may be determined, once and for all, irrespective of the outer field. Once this is done, the results obtained from matching may be used to construct the entire pressure field. The layout of this chapter is as follows. In Section 1, we derive certain reciprocity relations that follow from applying Green's theorem to the inner region. These show that not all static parameters are independent, and that simple relations exist between certain pairs of them. The reciprocity relations are useful checks when we actually solve for the static parameters. They also keep the labour of computing the coefficients down to a minimum. In Section 2, conformal mapping is used to solve the homogeneous Laplace equation. This yields static coefficients for the $O(1)$ and $O(\epsilon)$ inner problems. For higher-order problems, we must solve Poisson's equation. This is done in Section 3, where we show that the cross-mode forcing is equivalent to static sources at infinity. Finally, in Section 4, we derive the junction impedance and the reflection and transmission coefficients. Results are compared with those of previous investigators, and the composite expansion is written out explicitly.

4.1 Static Reciprocity Relations

Before we set out to calculate the static coefficients, it is useful to investigate the relations that exist between them on account of geometry. These are obtained by applying Green's first and second theorems along the contour shown

in fig. 7. First, let us introduce the terminology and define the static parameters we are interested in. We seek solutions of Laplace's equation in the stepped duct of fig. 7. The uniform sections are infinitely long in inner coordinates since we are interested in the entire inner domain $-\infty<\tilde{x}<\infty$. As we noted in Chapter 3, the solution of Laplace's equation in each uniform section may be written as a weighted sum of eigenfunctions appropriate for that region. Let ϕ be a solution of Laplace's equation in the stepped duct. Then for $\tilde{x}<0$,

$$\phi = A_L\tilde{x} + B_L + \sum_{n=1}^{\infty}\beta_{Ln}\cos(y/l_n)e^{\tilde{x}/l_n} + \sum_{n=1}^{\infty}\alpha_{Ln}\cos(y/l_n)e^{-\tilde{x}/l_n} \qquad (4.1a)$$

while for $\tilde{x}>0$,

$$\phi = A_R\tilde{x} + B_R + \sum_{n=1}^{\infty}\beta_{Rn}\cos(y/r_n)e^{-\tilde{x}/r_n} + \sum_{n=1}^{\infty}\alpha_{Rn}\cos(y/r_n)e^{\tilde{x}/r_n} \qquad (4.1b)$$

where $l_n = b_L/n\pi$ and $r_n = b_R/n\pi$ as before, and the subscripts L and R refer to the left ($\tilde{x}<0$) and right ($\tilde{x}>0$) regions respectively. In (4.1) and (4.2), we have allowed static modes with amplitudes α_{Ln}, α_{Rn} that are incident from $-\infty$ and ∞ respectively. Although they are not physically present in the inner field, these modes are helpful in finding solutions of Poisson's equation.

Of the static parameters introduced in (4.1) and (4.2), the volume velocity terms $A_L\tilde{x}$, $A_R\tilde{x}$ and the incident modes associated with α_{Ln} and α_{Rn} play the role of driving functions. Mathematically, this is a consequence of the fact that these terms are associated with boundary conditions at infinity. Thus by the

principle of superposition, we may write

$$\beta_{Ln} = S_{Ln}Q + \sum_{m=1}^{\infty} R^{(L)}_{m\to n}\alpha_{Lm} + \sum_{m=1}^{\infty} T^{(R\to L)}_{m\to n}\alpha_{Rm} \tag{4.3}$$

$$\beta_{Rn} = S_{Rn}Q + \sum_{m=1}^{\infty} R^{(R)}_{m\to n}\alpha_{Rm} + \sum_{m=1}^{\infty} T^{(L\to R)}_{m\to n}\alpha_{Lm} \tag{4.4}$$

where Q is the volume flux, given by

$$Q = A_L b_L = A_R b_R \tag{4.5}$$

The static coefficients in (4.3) and (4.4) have obvious physical meanings. For example, $R^{(L)}_{m\to n}$ is a static reflection coefficient that represents the amount of *nth* mode that would be induced in $\tilde{x}<0$ if only an *mth* mode of unit amplitude were to be incident from the left. Similarly, $T^{(R\to L)}_{m\to n}$ is a static transmission coefficient that represents the the amplitude of an *nth* transmitted mode in $\tilde{x}<0$ that would be caused by a unit *mth* mode incident from the right. The constant terms in ϕ are also a superposition of the volume flux and incident modes. We may write

$$B_L - B_R = a_0 Q + \sum_{n=1}^{\infty} a_{Rn}\alpha_{Rn} + \sum_{n=1}^{\infty} a_{Ln}\alpha_{Ln} \tag{4.6}$$

where a_0, a_{Rn} and a_{Ln} are volume flux and incident mode influence coefficients for the difference of the constant terms. We note that the influence coefficients

only determine the difference $(B_L - B_R)$ uniquely. It is impossible, by purely static considerations, to fix the individual values of B_L and B_R. This is because solutions of the Neumann problem for Laplace's equation are unique only up to an arbitrary additive constant. Thus we may add the same arbitrary constant to B_L and B_R without disturbing the governing equation, the boundary conditions, or continuity conditions across the aperture. This will not change the difference $(B_L - B_R)$, which is uniquely determined by the flux and the incident modes according to (4.6).

Our goal is to determine the static coefficients S_{Ln}, S_{Rn}, $R_{m\to n}$, $T_{M\to n}$, a_0, a_{Rn}, and a_{Ln}. Not all of these coefficients are independent, as we show next by applying Green's theorem. As a consequence of the simple geometry, reciprocity relations exist between certain pairs of them. These considerably simplify our task when we actually calculate the coefficients. Green's first theorem, which in the present context expresses the law of conservation of mass, simply results in equation (4.5). This follows from integrating the normal derivatives of ϕ along the circuit shown in fig. 7. Green's second theorem, applied to two solutions ϕ_a and ϕ_b of Laplace's equation, may be written as

$$\int_0^{b_L} (\phi_a \frac{\partial \phi_b}{\partial \tilde{x}} - \phi_b \frac{\partial \phi_a}{\partial \tilde{x}}) dy = \int_0^{b_R} (\phi_a \frac{\partial \phi_b}{\partial \tilde{x}} - \phi_b \frac{\partial \phi_a}{\partial \tilde{x}}) dy \qquad (4.7)$$

The integral on the left is evaluated on S_1 (fig. 7), the integral on the right on S_2, and we have used the fact that the normal derivatives of ϕ_a and ϕ_b vanish on the rigid walls. Let us choose ϕ_a to be a solution that corresponds to a unit

volume flux with no higher modes incident. Let ϕ_b be a solution corresponding to a single (say *mth*) mode incident from $\tilde{x}\to-\infty$. Then in $\tilde{x}<0$,

$$\phi_a = \tilde{x}/b_L + a_0^{(L)} + \sum_{n=1}^{\infty} S_{Ln}\cos(y/l_n)e^{\tilde{x}/l_n} \tag{4.8}$$

$$\phi_b = \cos(\frac{y}{l_m})e^{-\tilde{x}/l_m} + a_{Lm}^{(L)} + \sum_{n=1}^{\infty} R_{m\to n}^{(L)}\cos(y/l_n)e^{\tilde{x}/l_n} \tag{4.9}$$

and in $\tilde{x}>0$,

$$\phi_a = \tilde{x}/b_R + a_0^{(R)} + \sum_{n=1}^{\infty} S_{Rn}\cos(y/r_n)e^{-\tilde{x}/r_n} \tag{4.10}$$

$$\phi_b = a_{Lm}^{(R)} - \sum_{n=1}^{\infty} T_{m\to n}^{(L\to R)}\cos(y/r_n)e^{-\tilde{x}/r_n} \tag{4.11}$$

Here

$$a_0^{(L)} - a_0^{(R)} = a_0 \tag{4.12}$$

and

$$a_{Lm}^{(L)} - a_{Lm}^{(R)} = a_{Lm} \tag{4.13}$$

the right-hand sides being the influence coefficients defined in (4.6). Substituting (4.8)-(4.11) into (4.7) and using orthogonality relations between the cosines, we find in a straightforward manner that

$$a_{Lm} = -m\pi S_{Lm} \tag{4.14}$$

Similarly, by letting ϕ_b correspond to a unit mode incident from $\tilde{x}\to\infty$ and keeping ϕ_a the same as before, we obtain

$$a_{Rm} = -m\pi S_{Rm} \tag{4.15}$$

Finally, by considering pairs of potentials ϕ_a and ϕ_b that correspond one to an *nth* mode incident from the left and the other to an *mth* mode incident from the right and so on, we obtain reciprocity relations between the static reflection and transmission coefficients. The calculations are analogous to the previous one, and we shall omit the details here. We find that

$$mR^{(L)}_{n\to m} = nR^{(L)}_{m\to n} \tag{4.16}$$

$$mR^{(R)}_{n\to m} = nR^{(R)}_{m\to n} \tag{4.17}$$

$$mT^{(L\to R)}_{n\to m} = nT^{(R\to L)}_{m\to n} \tag{4.18}$$

We mention that identical results hold for inner regions of the general shape considered in Chapter 3 (fig. 6). The mathematical procedure is identical, as long as the surfaces S_1 and S_2 are chosen to be in $\tilde{x}<\tilde{x}_L$ and $\tilde{x}>\tilde{x}_R$ respectively. For inner profiles that require a numerical solution of Laplace's equation, the reciprocity relations (4.14)-(4.18) serve as a useful check on computational

accuracy.

4.2 Conformal Mapping of the Inner Region

We shall now evaluate, by conformal mapping, the static parameters in terms of which our results are expressed. Our analysis up to this point holds for general inner profiles of the class defined in Chapter 3. In this section, we specialize to the square step shown in fig. 3.

In view of the non-separable geometry, the best way to solve Laplace's equation is through the Schwartz-Christoffel transformation (Marsden, p.279). Let $z = \tilde{x} + iy$ represent the physical plane of the duct, and let the complex variable t be associated with a transformed plane. The Schwartz-Christoffel transformation $t(z)$, defined implicitly by

$$\frac{dz}{dt} = \frac{C}{t}\left(\frac{t-\gamma^2}{t-1}\right)^{1/2} \tag{4.19}$$

maps the interior of the duct in the z-plane to the upper half of the t-plane, with boundary points on the duct corresponding to points on the real t-axis. Here $\gamma = b_R/b_R$, and we have chosen the vertices $(0,b_L)$, $(0,b_R)$ and $(\infty,0)$ of the duct to correspond to $t = 1$, $t = \gamma^2$ and $t = 0$ respectively (fig. 8). The constant C and the additional constant that arises from integrating (4.19) govern the scale, rotation and translation associated with the mapping. If we introduce the new variable μ, defined by

$$\mu^2 = \frac{t - \gamma^2}{t - 1}, \quad t = \frac{\mu^2 - \gamma^2}{\mu^2 - 1} \tag{4.20}$$

(4.19) may be integrated directly. By requiring that z changes by (ib_R) as t passes through zero in the direction of increasing t and that z changes by (ib_L) as t passes from $-\infty$ to ∞, we may evaluate the abovementioned constants. The result is (Schwinger and Saxon, p.115)

$$z = \frac{b_L}{\pi}\log\left(\frac{1 - \mu}{1 + \mu}\right) - \frac{b_R}{\pi}\log\left(\frac{\mu - \gamma}{\mu + \gamma}\right) \tag{4.21}$$

Next, we map the interior of a plane parallel duct of unit height in the $\varsigma = \xi + i\eta$ plane on to the upper half of the t-plane, as indicated in fig. 8 . The Schwartz-Christoffel transformation for this mapping is simply

$$t = -e^{-\pi\varsigma} \tag{4.22}$$

Thus by combining (4.20)-(4.22), we may obtain a transformation between the stepped duct in the z-plane and the uniform duct in the ς-plane. By the conformal mapping theorem, any complex function that is analytic in the mapped ς-domain and has zero normal derivative on the boundary of this domain is automatically a solution of the homogeneous Neumann problem for Laplace's equation in the physical z-domain. Thus if $W(\varsigma)$ be such a function, then

$$\phi(x,y) = \mathrm{Re}\Big[\, W(z(\varsigma))\Big] \tag{4.23}$$

and

$$\psi(x,y) = \mathrm{Im}\Big[\, W(z(\varsigma))\Big] \tag{4.24}$$

are harmonic in the interior of the stepped duct, with $\partial\phi/\partial n$ and $i\partial\psi/\partial n$ zero on the walls.

Let us examine the complex potential

$$W(\varsigma) = \varsigma \tag{4.25}$$

In the ς-plane, this represents a uniform streaming flow in the positive ξ-direction. In order to find the potential ϕ, it is necessary to know the inverse mapping $z = z(\varsigma)$. Due to the complicated structure of (4.21), though, it is not possible to obtain this relation explicitly. However, we may obtain expansions of W in $\tilde{x}<0$ and $\tilde{x}>0$ by the implicit function theorem of Lagrange (Whittaker and Watson, pp.132-133). Let $f(\mu)$ be an analytic function of μ at the point $\mu = \gamma$ and in some neighbourhood of it. Given the relation

$$\mu = \gamma - \lambda f(\mu), \tag{4.26}$$

any function $g(\mu)$ analytic about γ may be expanded in a power series about γ by the formula

$$g(\mu) = g(\gamma) + \sum_{n=1}^{\infty} \frac{\lambda^n}{n!} \frac{d^{n-1}}{d\mu^{n-1}} \left(\frac{dg}{d\mu}(\mu) \Big[f(\mu) \Big]^n \right)_{\mu = \gamma} \tag{4.27}$$

We shall use this theorem to expand W in $\tilde{x}<0$ and $\tilde{x}>0$ in terms of static modes

appropriate for each region. Consider the region $\tilde{x}>0$. We can write (4.21) as

$$\mu = \gamma + e^{-\pi z/b_R}\left(\frac{1-\mu}{1+\mu}\right)^{1/\gamma}(\mu+\gamma) \tag{4.28}$$

and use (4.27) to expand $W(\mu)$, which, from (4.25),(4.22) and (4.20), may be written as

$$W = -\frac{1}{\pi}\log\left(\frac{\mu^2-\gamma^2}{1-\mu^2}\right) \tag{4.29}$$

On comparing (4.27) and (4.28), we see that $e^{-\pi z/b_R}$ may be identified with λ. Since $\tilde{x}>0$, $|e^{-\pi z/b_R}| < 1$, and thus the convergence of the series in (4.27) is not upset. Besides, as $|z| \to 0$ in $\tilde{x}>0$, $t \to 0$ and $|\mu| \to \gamma$, so that (4.27) may be properly employed to find an expansion of $W(\mu)$ in the neighbourhood of $\mu = \gamma$. Substituting (4.28) into (4.29), we get

$$W = \frac{z}{b_R} - \frac{1}{\pi}\log\left(\frac{1-\mu}{1+\mu}\right)^{1/\gamma}\frac{(\mu+\gamma)^2}{1-\mu^2}$$

Applying Lagrange's theorem to the second term, we obtain

$$W = \frac{z}{b_R} + \frac{1}{\pi}\log\left(\frac{1+\gamma}{1-\gamma}\right)^{1/\gamma}\left(\frac{1-\gamma^2}{4\gamma^2}\right)$$

$$+ \sum_{n=1}^{\infty} \frac{e^{-n\pi z/b_R}}{n!} \frac{d^{n-1}}{d\mu^{n-1}} \left(\frac{dg}{d\mu}(\mu) \left[f(\mu) \right]^n \right)_{\mu = \gamma} \tag{4.30}$$

where

$$g(\mu) = -\frac{1}{\pi} \log \left(\frac{1-\mu}{1+\mu} \right)^{1/\gamma} \frac{(\mu+\gamma)^2}{1-\mu^2} \tag{4.31}$$

and

$$f(\mu) = \log \left(\frac{1-\mu}{1+\mu} \right)^{1/\gamma} (\mu - \gamma) \tag{4.32}$$

It is clear, from the form of (4.30), that we have found a solution in the z-plane that corresponds to excitation by a unit volume flux in the positive $\tilde{x}$-direction. The pressure or potential is simply the real part of W. From the definitions (4.3)-(4.6), we immediately find

$$a_0^{(R)} = \frac{1}{\pi} \log \left(\frac{1+\gamma}{1-\gamma} \right)^{1/\gamma} \frac{(1-\gamma^2)}{4\gamma^2} \tag{4.33}$$

$$S_{R1} = \frac{2}{\pi} \log \left(\frac{1-\gamma}{1+\gamma} \right)^{1/\gamma} \tag{4.34}$$

$$S_{R2} = -\frac{1}{\pi}\left(\frac{5-\gamma^2}{1-\gamma^2}\right)\left(\frac{1-\gamma}{1+\gamma}\right)^{2/\gamma} \tag{4.35}$$

and so on, with

$$S_{Rn} = \frac{2}{\pi}\left(\frac{1-\gamma^2}{\gamma}\right)\frac{1}{n!}\frac{d^{n-1}}{d\mu^{n-1}}\left(\frac{\mu}{1-\mu^2}(\mu+\gamma)^{n-1}\left(\frac{1-\mu}{1-\mu}\right)^{n/\gamma}\right)_{\mu=\gamma} \tag{4.36}$$

in general.

We can carry out an analogous expansion in $\tilde{x}<0$. Rewriting (4.21) in the form

$$\mu = 1 - e^{\pi z/b_L}\left(\frac{\mu-\gamma}{\mu-\gamma}\right)^{\gamma}(1-\mu)\,, \tag{4.37}$$

substituting into (4.29) and using the Lagrange theorem, we obtain

$$W = \frac{z}{b_L} + a_0^{(L)} + \sum_{n=1}^{\infty} S_{Ln} e^{n\pi z/b_L} \tag{4.38}$$

where

$$a_0^{(L)} = -\frac{1}{\pi}\log\left(\frac{1-\gamma^2}{4\gamma}\right)\left(\frac{1+\gamma}{1-\gamma}\right)^{\gamma} \tag{4.39}$$

so that

$$a_0 = a_0^{(L)} - a_0^{(R)} = -\frac{2}{\pi}\log\left(\frac{1-\gamma^2}{4\gamma}\right)\left(\frac{1+\gamma}{1-\gamma}\right)^{1/2(\gamma+1/\gamma)} \tag{4.40}$$

and

$$S_{L1} = \frac{2}{\pi}\left(\frac{1-\gamma}{1+\gamma}\right)^{\gamma} \tag{4.41}$$

$$S_{L2} = -\frac{1}{\pi}\left(\frac{5\gamma^2-1}{1-\gamma^2}\right)\left(\frac{1-\gamma}{1-\gamma}\right)^{2\gamma} \tag{4.42}$$

$$S_{Ln} = (-1)^{n+1}\frac{2}{\pi}\left(\frac{1-\gamma^2}{n!}\right)\frac{d^{n-1}}{d\mu^{n-1}}\left(\frac{\mu}{\mu^2-\gamma^2}(\mu-1)^{n-1}\left(\frac{\mu-\gamma}{\mu+\gamma}\right)^{n\gamma}\right)_{\mu=1} \tag{4.43}$$

Equations (4.33)-(4.36) and (4.39)-(4.43) are our first set of explicit formulas for the static parameters. In light of the reciprocity relations (4.14) and (4.15), we see that the influence coefficients a_{Rn} and a_{Ln} are also known at this stage.

Next, we turn to the determination of the static reflection and transmission coefficients. Since these are mode-to-mode conversion factors, we need to form a

potential that corresponds to only one static mode incident from the left or right in the physical z-plane. Suppose we consider a *pth* mode incident from $\xi \to -\infty$ in the ς-plane, with complex potential

$$W^{(p)}(\varsigma) = e^{-p\pi(\varsigma - a_0^{(L)})} \tag{4.44}$$

From the previous calculation, we know that for z in $\tilde{x}<0$,

$$\varsigma = z/b_L + a_0^{(L)} + \sum_{n=1}^{\infty} S_{Ln} e^{n\pi z/b_L} \tag{4.45}$$

and that for z in $\tilde{x}<0$,

$$\varsigma = z/b_R - a_0^{(R)} + \sum_{n=1}^{\infty} S_{Rn} e^{-n\pi z/b_R} \tag{4.46}$$

where $a_0^{(L)} - a_0^{(R)} = a_0$. Thus in $\tilde{x}<0$, equation (4.44) becomes

$$W^{(p)} = \exp\left(-p\pi(z/b_L + \sum_{n=1}^{\infty} S_{Ln} e^{n\pi z/b_L}) \right) \tag{4.47}$$

Expanding the exponential in a Taylor series, we obtain

$$W^{(p)}(z) = e^{-p\pi z/b_L}\left(1 - p\pi S_{Li} e^{i\pi z/b_L} + \frac{1}{2} p^2\pi^2 S_{Li} S_{Lj} e^{(i+j)\pi z/b_L} \right.$$

$$- p^3\pi^3 S_{Li} S_{Lj} S_{Lk} e^{(i+j+k)\pi z/b_L} + \cdots \Big) \tag{4.48}$$

where $i,j,k \in 1,2,3, \cdots, \infty$ and we have used the Einstein summation convention on the indices. Similarly, using (4.46), we find that for z in $\tilde{x}>0$,

$$W^{(p)}(z) = e^{p\pi a_0} e^{-p\pi z/b_R} \Big(1 - p\pi S_{ri} e^{-i\pi z/b_R}$$

$$+ \frac{1}{2} p^2\pi^2 e^{-(i+j)\pi z/b_R} + \cdots \Big) \tag{4.49}$$

From (4.48) and (4.49), it is evident that the potential $W^{(p)}$ gives rise to modes incident only from the left in the z-plane, with induced decaying modes present both in $\tilde{x}<0$ and in $\tilde{x}>0$. Thus from (4.49), we see that the the duct is excited from the left by

$$W^{(p)} = \Phi^{(p)} - \Big(p\pi S_{L1} \Phi^{(p-1)} + p\pi S_{L2} \Phi^{(p-2)} + \cdots \Big)$$

$$+ 1/2 p^2\pi^2 \Big(S_{L1}^2 \Phi^{(p-2)} + 2 S_{L1} S_{L2} \Phi^{(p-3)} + \cdots \Big) - \cdots \tag{4.50}$$

Here $\Phi^{(p)}$ is the complex potential that would exist if the duct were to be excited by a unit *pth* mode incident from the left in the z-plane. Thus by superposition, it is clear that in order to obtain pure *pth* mode excitation in the z-plane, we must choose the potential

$$\tilde{W}^{(p)} = \Phi^{(p)} + (p\pi S_{L1})\Phi^{(p-1)}$$

$$+ (p\pi S_{L2} - 1/2p^2\pi^2 S_{L1}^2)\Phi^{(p-2)} + \cdots \tag{4.51}$$

We are now in a position to evaluate the coefficients. $R_{m\to n}^{(L)}$ and $T_{m\to n}^{(L\to R)}$. Setting p = 1,2, etc. in (4.51) and using (4.48) and (4.49) to find the potential in $\tilde{x}<0$ and $\tilde{x}>0$ respectively, we obtain

$$R_{1\to 1}^{(L)} = -\pi S_{L2} + \frac{1}{2}\pi^2 S_{L1}^2 \tag{4.52a}$$

$$R_{1\to 2}^{(L)} = -\pi S_{L3} + \pi^2 S_{L1} S_{L2} - \frac{1}{6}\pi^3 S_{L1}^3 \tag{4.52b}$$

$$R_{2\to 1}^{(L)} = -2\pi S_{L3} + 2\pi^2 S_{L1} S_{L2} - \frac{1}{3}\pi^3 S_{L1}^3 \tag{4.52c}$$

$$T_{1\to 1}^{(L\to R)} = e^{\pi a_0} \tag{4.53a}$$

$$T_{1\to 2}^{(L\to R)} = -\pi S_{R1} e^{-\pi a_0} \tag{4.53b}$$

$$T_{2\to 1}^{(L\to R)} = 2\pi S_{L1} e^{\pi a_0} \tag{4.53c}$$

$$T_{2\to 2}^{(L\to R)} = e^{2\pi a_0} - 2\pi^2 S_{L1} S_{R1} e^{\pi a_0} \tag{4.53d}$$

It is easy to verify that reciprocity relation (4.16) is satisfied. We also find that

$$a_{L1} = -\pi S_{L1}$$

$$a_{L2} = -2\pi S_{L2}$$

which confirms reciprocity relation (4.14).

By an analogous calculation, we can find the coefficients $R^{(R)}_{m\to n}$ and $T^{(R\to L)}_{m\to n}$. The details are similar and shall not be reproduced here. Substituting for a_0 and the S_{Ln} and the S_{Rn}, we finally obtain

$$R^{(L)}_{1\to 1} = \frac{1+3\gamma^2}{1-\gamma^2}\left(\frac{1-\gamma}{1+\gamma}\right)^{2\gamma} \tag{4.54a}$$

$$R^{(L)}_{1\to 2} = -\frac{32}{3}\frac{\gamma^4}{(1-\gamma^2)^2}\left(\frac{1-\gamma}{1+\gamma}\right)^{3\gamma} \tag{4.54b}$$

$$T^{(L\to R)}_{1\to 1} = \frac{16\gamma^2}{(1-\gamma^2)^2}\left(\frac{1-\gamma}{1+\gamma}\right)^{\gamma+1/\gamma} \tag{4.54c}$$

$$T^{(L\to R)}_{1\to 2} \quad \frac{-32\gamma^2}{(1-\gamma^2)^2}\left(\frac{1-\gamma}{1+\gamma}\right)^{\gamma+2/\gamma} \tag{4.54d}$$

$$R^{(R)}_{1\to 1} = -\frac{3+\gamma^2}{1-\gamma^2}\left(\frac{1-\gamma}{1+\gamma}\right)^{2/\gamma} \tag{4.55a}$$

$$R_{1\to 2}^{(R)} = \frac{32}{3}\frac{1}{(1-\gamma^2)^2}\left(\frac{1-\gamma}{1+\gamma}\right)^{3/\gamma} \tag{4.55b}$$

and so on.

4.3 Equivalent Source Solution of Poisson's Equation

In Chapter 3, we saw that at $O(\epsilon^2)$ and higher orders, the inner pressure satisfies Poisson's equation. The main feature of interest at these orders is the modification of the homogeneous part of the solution by the forcing terms. For the square step, this effect is entirely due to cross-mode terms from lower orders. This is because of the fact that the step lies in a transverse plane between two uniform regions. If the region of discontinuity were to have finite thickness, the relation between pressure and velocity on the left edge of the right region and those on the right edge of the left region would be complicated by the finite mass and compressibility of the enclosed fluid. For the square step, however, these relations are simple - the pressure and velocity are continuous across the junction plane. Now for non-modal forcing, particular solutions in each region are just proportional to $\tilde{x}^2$, $\tilde{x}^3$, and so on. On the junction plane, these contribute nothing to the pressure or the axial velocity. Thus the homogeneous fields, which already satisfy continuity conditions across the junction plane, need not be, and indeed, are not disturbed. However, any modal forcing upsets this balance by inducing nonzero pressures and velocities on the junction plane. The

homogeneous solution is thus forced to adjust to the new field distributions on the junction plane. This is manifested, for example, in the fact that the constant $(B_L - B_R)$ is no longer a simple function of the volume flux Q, but depends on the modal forcing as well.

Mathematically, the cross-mode forcing can be replaced by equivalent static sources at infinity. This idea is similar to the Method of Static Equivalence (MSE) (Appendix A), in which the difference between the static and dynamic fields is simulated in this fashion. The main difference is that in MSE, the source amplitudes have to be determined as part of the solution, whereas in the present case, they are known from matching at lower orders. At any rate, once we cast the forcing terms as sources, all the results of the previous section may be applied. Thus in effect, we shall construct solutions to Poisson's equation by combining certain solutions of Laplace's equation. It should be mentioned that this procedure is effective only for certain special geometries, a restriction that extends to MSE as well. For arbitrary inner profiles, a numerical method is the only resort.

Let us consider the model Poisson equations

$$\nabla^2\phi = -k^2\overline{A}_L\tilde{x} - k^2\overline{B}_L - k^2\sum_{n=1}^{\infty}\overline{\beta}_{Ln}\cos(y/l_n)e^{\tilde{x}/l_n} \tag{4.56}$$

in $\tilde{x}<0$, and

$$\nabla^2\phi = -k^2\overline{A}_R\tilde{x} - k^2\overline{B}_R - k^2\sum_{n=1}^{\infty}\overline{\beta}_{Rn}\cos(y/r_n)e^{-\tilde{x}/r_n} \tag{4.57}$$

These include the equations that both $\tilde{p}^{(2)}$ and $\tilde{p}^{(3)}$ satisfy, $\tilde{p}^{(2)}$ being the solution for $\overline{A}_L = \overline{a}_R = \overline{\beta}_{Ln} = \overline{\beta}_{Rn} = 0$. The solutions to (4.56) and (4.57), subject to the no-penetration wall boundary condition, may be directly written down as

$$\phi = A_L\tilde{x} + B_L + \sum_{n=1}^{\infty}\beta_{Ln}\cos(y/l_n)e^{\tilde{x}/l_n} - \frac{1}{6}k^2\overline{A}_L\tilde{x}^3$$

$$- \frac{1}{2}k^2\overline{B}_L\tilde{x}^2 - 1\_2k^2\tilde{x}\sum_{n=1}^{\infty} l_n\overline{\beta}_{Ln}\cos(y/l_n)e^{\tilde{x}/l_n} \quad , \tilde{x}<0 \qquad (4.58)$$

$$\phi = A_R\tilde{x} + B_R + \sum_{n=1}^{\infty}\beta_{Rn}\cos(y/r_n)e^{-\tilde{x}/r_n} - \frac{1}{6}k^2\overline{A}_R\tilde{x}^3$$

$$- \frac{1}{2}k^2\overline{B}_R\tilde{x}^2 - \frac{1}{2}k^2\tilde{x}\sum_{n=1}^{\infty} r_n\overline{\beta}_{Rn}\cos(y/r_n)e^{-\tilde{x}/r_n} \quad , \tilde{x}>0 \qquad (4.59)$$

From these, we can calculate the axial velocity $(\partial\phi/\partial\tilde{x})$ induced on the junction plane :

$$\frac{\partial\phi}{\partial\tilde{x}}(\tilde{x}\to 0^-) = A_L + \sum_{n=1}^{\infty}\frac{1}{\tau_n}\beta_{Ln}\cos(y/l_n)$$

$$- \frac{1}{2}k^2 \sum_{n=1}^{\infty} l_n \overline{\beta}_{Ln} \cos(y/l_n) \tag{4.60}$$

$$\frac{\partial \phi}{\partial \tilde{x}}(\tilde{x} \to 0^+) = A_R - \sum_{n=1}^{\infty} \frac{1}{r_n} \beta_{Rn} \cos(y/r_n)$$

$$+ \frac{1}{2}k^2 \sum_{n=1}^{\infty} r_n \overline{\beta}_{Rn} \cos(y/r_n) \tag{4.61}$$

The axial velocity is continuous across the aperture, and we may set

$$\frac{\partial \phi}{\partial \tilde{x}}(\tilde{x} \to 0^-) = \frac{\partial \phi}{\partial \tilde{x}}(\tilde{x} \to 0^+) = u(y) \tag{4.62}$$

Now from the Fourier expansion theorem, we see that the coefficients in (4.60) and (4.61) are simply modal amplitudes of $u(y)$. Thus

$$A_L = \frac{1}{b_L} \int_0^{b_R} u(y)\, dy \tag{4.63}$$

$$A_R = \frac{1}{b_R} \int_0^{b_R} u(y)\, dy \tag{4.64}$$

$$\beta_{Ln} = \frac{2}{n\pi}\int_0^{b_R} u(y)\cos(y/l_n)\,dy + 1/2k^2 {l_n}^2 \overline{\beta}_{Ln} \tag{4.65}$$

$$\beta_{Rn} = -\frac{2}{n\pi}\int_0^{b_R} u(y)\cos(y/r_n)\,dy + 1/2k^2 {r_n}^2 \overline{\beta}_{Rn} \tag{4.66}$$

In (4.63)-(4.66), we have implicitly used the boundary condition $u(y) = 0$ for $b_R < y < b_L$. By further requiring that ϕ be continuous across the aperture, we obtain the integral equation of the problem :

$$B_L + \sum_{n=1}^{\infty} \beta_{Ln}\cos(y/l_n) = B_R + \sum_{n=1}^{\infty} \beta_{Rn}\cos(y/r_n)\ ,\ y \text{ in aperture} \tag{4.67}$$

On substituting (4.65) and (4.66), this becomes

$$(B_L - B_R) + \sum_{n=1}^{\infty} \cos(y/l_n)\left(\frac{2}{n\pi}\int_0^{b_R} u(z)\cos(\frac{z}{l_n})dz + \frac{1}{2}k^2 {l_n}^2 \overline{\beta}_{Ln} \right)$$

$$= \sum_{n=1}^{\infty} \cos(y/r_n)\left(-\frac{2}{n\pi}\int_0^{b_R} u(z)\cos(\frac{z}{r_n})dz + \frac{1}{2}k^2 {r_n}^2 \overline{\beta}_{Rn} \right) \tag{4.68}$$

This is an integral equation for the axial velocity in the aperture. Once we solve this equation for $u(y)$, we may use (4.65)-(4.68) to directly calculate the difference $(B_L - B_R)$ and the reflected mode amplitudes β_{Ln}, β_{Rn} in terms of the forcing amplitudes $\overline{\beta}_{Ln}$, $\overline{\beta}_{Rn}$, which are assumed to be known from a lower-order problem. Our objective is to solve (4.68) indirectly, by appealing to solutions of Laplace's equation. Specifically, we show that (4.68) may be formally reproduced by considering a static problem with sources at infinity. Let us suppose, then, that we solve a homogeneous problem with higher modes incident from infinity on both sides. The potential in this case is given by

$$\phi = \tilde{A}_L \tilde{x} + \tilde{B}_L + \sum_{n=1}^{\infty} \alpha_{Ln} \cos(y/l_n) e^{-\tilde{x}/l_n} + \sum_{n=1}^{\infty} \gamma_{Ln} \cos(y/l_n) e^{\tilde{x}/l_n} \qquad (4.69)$$

in $\tilde{x}<0$, and in $\tilde{x}>0$, by

$$\phi = \tilde{A}_R \tilde{x} + \tilde{B}_R + \sum_{n=1}^{\infty} \alpha_{Rn} \cos(y/l_n) e^{\tilde{x}/r_n} + \sum_{n=1}^{\infty} \gamma_{Rn} \cos(y/r_n) e^{-\tilde{x}/r_n} \qquad (4.70)$$

Here the α_n represent incident mode amplitudes, and the γ_n are the reflected mode amplitudes. As in the previous calculation, we may express the coefficients in (4.69) and (4.70) as Fourier amplitudes of the axial velocity field $u(y)$ on the junction plane :

$$\tilde{A}_L = \frac{1}{b_L} \int_0^{b_R} u(y) dy \qquad (4.71)$$

$$\tilde{A}_R = \frac{1}{b_R}\int_0^{b_R} u(y)dy \tag{4.72}$$

$$\gamma_{Ln} = \frac{2}{n\pi}\int_0^{b_R} u(y)\cos(y/l_n)dy + \alpha_{Ln} \tag{4.73}$$

$$\gamma_{Rn} = -\frac{2}{n\pi}\int_0^{b_R} u(y)\cos(y/r_n)dy + \alpha_{Rn} \tag{4.74}$$

By requiring ϕ to be continuous across the aperture and using (4.73) and (4.74) to replace the reflected amplitudes, we obtain the integral equation of the homogeneous problem :

$$(\tilde{B}_L - \tilde{B}_R) + \sum_{n=1}^{\infty}\cos(y/l_n)\left(\frac{2}{n\pi}\int_0^{b_R} u(z)\cos(\frac{z}{l_n})dz - 2\alpha_{Ln}\right)$$

$$= \sum_{n=1}^{\infty}\cos(y/r_n)\left(-\frac{2}{n\pi}\int_0^{b_R} u(z)\cos(\frac{z}{r_n})dz + 2\alpha_{Rn}\right) \tag{4.75}$$

But now, on comparing this to (4.68), we see that the two become formally identical if we require that

$$\alpha_{Ln} = \frac{1}{4} k^2 l_n^{\,2} \overline{\beta}_{Ln} \tag{4.76}$$

$$\alpha_{Rn} = \frac{1}{4} k^2 r_n^{\,2} \overline{\beta}_{Rn} \tag{4.76}$$

$$(\tilde{B}_L - \tilde{B}_R) = (B_L - B_R) \tag{4.78}$$

The significance of this observation is that for the homogeneous problem, the effects of the volume flux and cross-mode sources are completely known from our work in Section 2. That is, the difference $(B_L - B_R)$ and the reflected amplitudes γ_{Ln}, γ_{Rn} may be explicitly determined for a given volume flux and given incident mode amplitudes. Since the equivalence of (4.75) and (4.68) implies that the axial velocity on the junction plane is the same in both problems, the volume flux through the aperture is also the same. This, in turn, means that

$$\tilde{A}_L = A_L \tag{4.79}$$

$$\tilde{A}_R = A_R \tag{4.80}$$

Thus if we pose the Laplace problem with the same aperture flux Q as the Poisson problem and with sources prescribed according to (4.76) and (4.77), we can evaluate the γ_{Ln}, γ_{Rn}, and the difference $(\tilde{B}_L - \tilde{B}_R)$ using the static relations of the previous section. But from (4.65)-(4.66) and (4.73)-(4.74), we see that

$\beta_{Ln} = \gamma_{Ln}$, $\beta_{Rn} = \gamma_{Rn}$; while from (4.78), $(B_L - B_R) = (\tilde{B}_L - \tilde{B}_R)$. Thus the coefficients in the homogeneous components of (4.58) and (4.59) are completely determined. Using the static transfer coefficients defined earlier, and the equivalence relations (4.76)-(4.78), we obtain

$$\beta_{Ln} = \gamma_{Ln} = S_{Ln} Q + k^2/4 \sum_{m=1}^{\infty} l_m^2 \overline{\beta}_{Lm} R_{m \to n}^{(L)}$$

$$+ k^2/4 \sum_{m=1}^{\infty} r_m^2 \overline{\beta}_{Rm} T_{m \to n}^{(R \to L)} \tag{4.81}$$

$$\beta_{Rn} = \gamma_{Rn} = S_{Rn} Q + k^2/4 \sum_{m=1}^{\infty} r_m^2 \overline{\beta}_{Rm} R_{m \to n}^{(R)}$$

$$+ k^2/4 \sum_{m=1}^{\infty} l_m^2 \overline{\beta}_{Lm} T_{m \to n}^{(L \to R)} \tag{4.82}$$

$$B_L - B_R = \tilde{B}_L - \tilde{B}_R = a_0 Q + k^2/4 \sum_{n=1}^{\infty} l_n^2 \overline{\beta}_{Ln} a_{Ln}$$

$$+ k^2/4 \sum_{n=1}^{\infty} r_n^2 \overline{\beta}_{Rn} a_{Rn} \tag{4.83}$$

where $Q = A_L b_L = A_R b_R$. Equations (4.81)-(4.83) show the effects of the cross-mode forcing explicitly. Had $\overline{\beta}_{Ln}$ and $\overline{\beta}_{Rn}$ been zero, the equations would reduce down to relations appropriate for a homogeneous problem without incident modes. This is the case for $\tilde{p}^{(2)}$, for example, which satisfies a Poisson equation with non-modal forcing. Thus the cross-mode forcing is the sole agency that causes a shift in the balance between the homogeneous components of pressure on either side of the junction plane. As we discussed earlier, only those forcing terms that induce a nonzero velocity on the junction plane cause this effect.

The forcing amplitudes $\overline{\beta}_{Ln}$ and $\overline{\beta}_{Rn}$ at any order are related to the amplitudes of the cutoff outer cross-modes through matching. Thus the summations in (4.81)-(4.83) represent dynamic effects on the inner solution, which, as we just mentioned, retains an essentially static (incompressible) character unless these effects are taken into account. This is the principal role of the cutoff cross-modes. We show in the next section that if the summations are dropped, the accuracy of the theory becomes limited to very low frequencies. In particular, the formula we would obtain for the junction impedance is just the zero-frequency asymptote, with no subsequent corrections appearing at higher orders of ϵ. On the other hand, even a third-order impedance estimate that includes just two terms from each summation is remarkably accurate through the entire low-frequency range all the way up to the first cutoff.

4.4 Overall Scattering Estimates; Composite Solution

We are now in a position to calculate overall estimates of scattering such as the reflection and transmission coefficients $R(\epsilon)$ and $T(\epsilon)$ and the junction impedance $Z(\epsilon)$. These follow from the matching relations (3.29)-(3.39) and the static relations derived in the last two sections. All the coefficients that appear in the inner and outer expansions will be explicitly determined in the process. Using these, we shall write down the composite expansion for pressure at the end of the section.

We start with the reflection and transmission coefficients. From (3.29), we have $1 + R^{(0)} = T^{(0)}$. Combining this with the first-order mass conservation relation ${A_L}^{(1)} b_L = {A_R}^{(1)} b_R$ and (3.3), we obtain

$$R^{(0)} = \frac{1 - \gamma}{1 + \gamma} \tag{4.84a}$$

$$T^{(0)} = \frac{2}{1 + \gamma} \tag{4.84b}$$

$$Q^{(1)} = {A_L}^{(1)} b_L = {A_R}^{(1)} b_R = \frac{2ikb_R}{1 - \gamma} \tag{4.85}$$

where $\gamma = b_R / b_L$ as before. The first-order flux $Q^{(1)}$ fixes the reflected mode amplitudes and the difference $({B_L}^{(1)} - {B_R}^{(1)})$:

$$\beta_{Ln}^{(1)} = S_{Ln} Q^{(1)} \tag{4.86a}$$

$$\beta_{Rn}^{(1)} = S_{Rn} Q^{(1)} \tag{4.86b}$$

$$B_L^{(1)} - B_R^{(1)} = a_0 Q^{(1)} \tag{4.87}$$

where a_0 is given by (4.40), and the S_{Rn}, S_{Ln} by (4.36) and (4.43). On the other hand, $A_L^{(2)} b_L = A_R^{(2)} b_R$ by mass conservation across the junction at second order, and from (3.32) and (3.34), we have

$$B_L^{(1)} = -\gamma B_R^{(1)} \tag{4.88}$$

Solving, we obtain

$$R^{(1)} = B_L^{(1)} = \frac{Q^{(1)} a_0 \gamma}{1 + \gamma} \tag{4.89a}$$

$$T^{(1)} = B_R^{(1)} = \frac{-Q^{(1)} a_0}{1 + \gamma} \tag{4.89b}$$

where $Q^{(1)}$ is given by (4.85). From (3.34) now,

$$Q^{(2)} = A_L^{(2)} b_L = A_R^{(2)} b_R = -ikb_L \frac{Q^{(1)} a_0 \gamma}{1 + \gamma} \tag{4.90}$$

To find $R^{(2)}$ and $T^{(2)}$, we note that from (3.35) and (3.37),

$$B_L^{(2)} = -\gamma B_R^{(2)}$$

on account of mass conservation across the junction at $O(\epsilon^3)$. However, from

(4.83),

$$B_L^{(2)} - B_R^{(2)} = Q^{(2)} a_0 ,$$

since there is no cross-mode forcing in the $O(\epsilon^2)$ inner equations. Solving, we get

$$R^{(2)} = B_L^{(2)} = \frac{Q^{(2)} a_0 \gamma}{1 + \gamma} \tag{4.91a}$$

$$T^{(2)} = B_R^{(2)} = \frac{-Q^{(2)} a_0}{1 + \gamma} \tag{4.91b}$$

Using (3.37), we also obtain

$$Q^{(3)} = A_L^{(3)} b_L = A_R^{(3)} b_R = -ikb_R \frac{Q^{(2)} a_0}{1 + \gamma} \tag{4.92}$$

Next, from (3.38) and the $O(\epsilon^4)$ analog of (3.37), we get

$$B_L^{(3)} = -\gamma B_R^{(3)}$$

by using mass conservation across the junction. On the other hand, from (4.83),

$$B_L^{(3)} - B_R^{(3)} = Q^{(3)} a_0 + \frac{1}{4} \sum_{n=1}^{\infty} l_n^{\,2} \beta_{Ln}^{(1)} a_{Ln} + \frac{1}{4} \sum_{n=1}^{\infty} r_n^{\,2} \beta_{Rn}^{(1)} a_{Rn} \tag{4.93}$$

From (3.33) and (4.81)-(4.82),

$$\beta_{Ln}^{(1)} = S_{Ln} Q^{(1)} \tag{4.94a}$$

$$\beta_{Rn}^{(1)} = S_{Rn} Q^{(1)} \tag{4.94b}$$

Substituting into (4.93) and using (4.14)-(4.15), we obtain

$$B_L^{(3)} - B_R^{(3)} = Q^{(3)} a_0 - \pi k^2 Q^{(1)}/4 \sum_{n=1}^{\infty} n l_n^{\,2} S_{Ln}^2$$

$$- \pi k^2 Q^{(1)}/4 \sum_{n=1}^{\infty} n r_n^{\,2} S_{Rn}^2 \tag{4.95}$$

Solving for $R^{(3)}$ and $T^{(3)}$, we obtain

$$R^{(3)} = B_L^{(3)} = \frac{\gamma a_0 Q^{(3)}}{1+\gamma} + \frac{\pi k^2 Q^{(1)}}{1+\gamma} \sum_{n=1}^{\infty} n (r_n^{\,2} S_{Rn}^2 + l_n^{\,2} S_{Ln}^2) \tag{4.96a}$$

$$T^{(3)} = B_R^{(3)} = -R^{(3)}/\gamma \tag{4.96b}$$

This completely determines the reflection and transmission coefficients up to third order. To complete our evaluation of all the coefficients that appear in the inner and outer pressures up to third order, we need to calculate the second- and third-order reflected mode amplitudes. The second-order amplitudes are simply

$$\beta_{Ln}^{(2)} = S_{Ln} Q^{(2)} \tag{4.97a}$$

$$\beta_{Rn}^{(2)} = S_{Rn} Q^{(2)} \tag{4.97b}$$

The third-order amplitudes are found from (4.81) and (4.82) :

$$\beta_{Ln}^{(3)} = S_{Ln} Q^{(3)} + k^2/4 \sum_{m=1}^{\infty} l_m^2 \beta_{Lm}^{(1)} R_{m\to n}^{(L)}$$

$$+ k^2/4 \sum_{m=1}^{\infty} r_m^2 \beta_{Rm}^{(1)} T_{m\to n}^{(R\to L)} \tag{4.98a}$$

$$\beta_{Rn}^{(3)} = S_{Rn} Q^{(3)} + k^2/4 \sum_{m=1}^{\infty} r_m^2 \beta_{Rm}^{(1)} R_{m\to n}^{(R)}$$

$$+ k^2/4 \sum_{m=1}^{\infty} l_m^2 \beta_{Lm}^{(1)} T_{m\to n}^{(L\to R)} \tag{4.98b}$$

Next, we calculate the junction impedance. In dimensional form, this is given by

$$\overline{Z} = \Delta \overline{P}_m / \overline{Q}$$

where $\Delta \overline{P}_m$ is the dimensional mean pressure drop across the aperture, and $\overline{Q}$ the dimensional volume velocity through the aperture. If we define the

nondimensional impedance by

$$Z = \overline{Z} \frac{b_L H_0}{\rho_0 c_0} \tag{4.99}$$

then in terms of nondimensional quantities,

$$Z = ik \left(\frac{\Delta p_m}{(\partial p / \partial x)^0_m} \right) \tag{4.100}$$

where Δp_m is the mean nondimensional pressure drop across the aperture, and $(\frac{\partial p}{\partial x})^0_m$ the mean value of $\frac{\partial p}{\partial x}$ as $x \to 0^-$. If we substitute the outer series into this, it reads

$$Z = \left(\frac{T - 1 - R}{1 - R} \right) \tag{4.101}$$

Substituting equations (4.97) and collecting terms with like powers of ϵ, we find that

$$Z = \epsilon Z^{(1)} + \epsilon^2 Z^{(2)} + \epsilon^3 Z^{(3)} + \cdots \tag{4.102}$$

where

$$Z^{(1)} = ikb_L \frac{2}{\pi} \log\left(\frac{1-\gamma^2}{4\gamma} \right) \left(\frac{1+\gamma}{1-\gamma} \right)^{1/2(\gamma + 1/\gamma)} \tag{4.103a}$$

$$Z^{(2)} = 0 \tag{4.103b}$$

$$Z^{(3)} = ik^3 b_L^3 \frac{\pi}{4} \sum_{n=1}^{\infty} \frac{1}{n\pi^2} \left(S_{Ln}^2 + \gamma^2 S_{Rn}^2 \right) \tag{4.103c}$$

In fig. 9, we have plotted the impedance to $O(\epsilon^3)$ for a square step with $b_L = 1$ and $b_R = 0.5$. The top curve is Schwinger's variational-MSE estimate, and may be regarded as the correct value since it can be shown that the maximum error is about 1% (Appendix A). The middle curve is our MAE estimate, with just one cross-mode correction included after first order, and the curve on the bottom is that from Lesser and Lewis' theory with no dynamic corrections. We see that the MAE estimate is accurate to within 2-3% at $\epsilon = 0.25$, which corresponds to half the first cutoff frequency of the wider duct. Even at $\epsilon = 0.4$, which corresponds to 80% of the first cutoff frequency, the error is about 12-13%, a significant improvement over the bottom curve. Lesser and Lewis' result, on the other hand, is reliable only up to about 15% of the first cutoff frequency. Even though our result contains just one dynamic correction term, the improvement is already significant. This can be further improved by adding more terms in the series for Z.

In figs. 10 and 11, the isobars of the composite pressure field are plotted to $O(\epsilon)$. The solid lines are pressure contours with cross-modes included, and the dotted lines are contours without cross-modes. We see that the two sets of curves differ in the vicinity of the discontinuity, as expected, and that the difference increases as the frequency is increased. In the narrower duct, the far field is reached earlier than in the wider duct. In fig. 10, this is seen from the fact that the outer pressure contours are vertical lines - this means that the higher modes have died out. Thus the offset between the solid and dotted lines in this region is not a local effect. It is due to the fact that the cross-modes change the traveling mode amplitudes as well, a feature that is one of the important conclusions of this thesis. In the wider duct, on the other hand, the curvature of the solid isobars indicates that the outer field contains some of the higher modes. Thus the difference between the two sets of contours in this region is due to local features as well, especially in fig. 11, where the frequency is higher. Turning to the inner region - that is, the region near the step, we note that the spatial gradients of the pressure field are much higher than in the outer regions. This was mentioned earlier as one of the main difficulties in using a purely numerical method for the entire problem. When used in conjunction with MAE, however, the numerics is considerably simplified since we would then solve an elliptic equation near the step instead of the wave equation. This would be the approach for an arbitrary inner geometry. In the present case, the inner solution may be determined analytically, as we showed in sections 2 and 3.

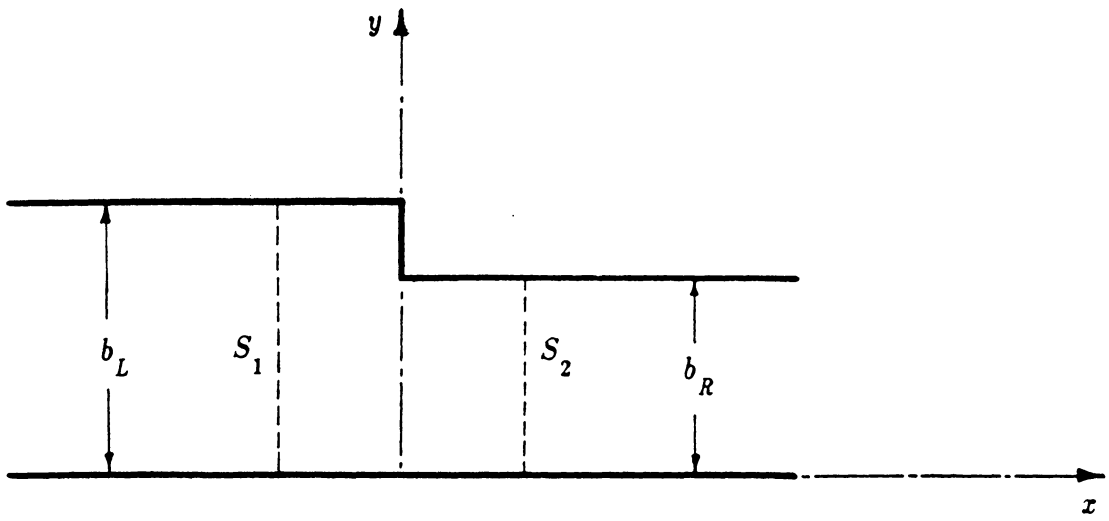

Fig. 7: Waveguide geometry for chap.4

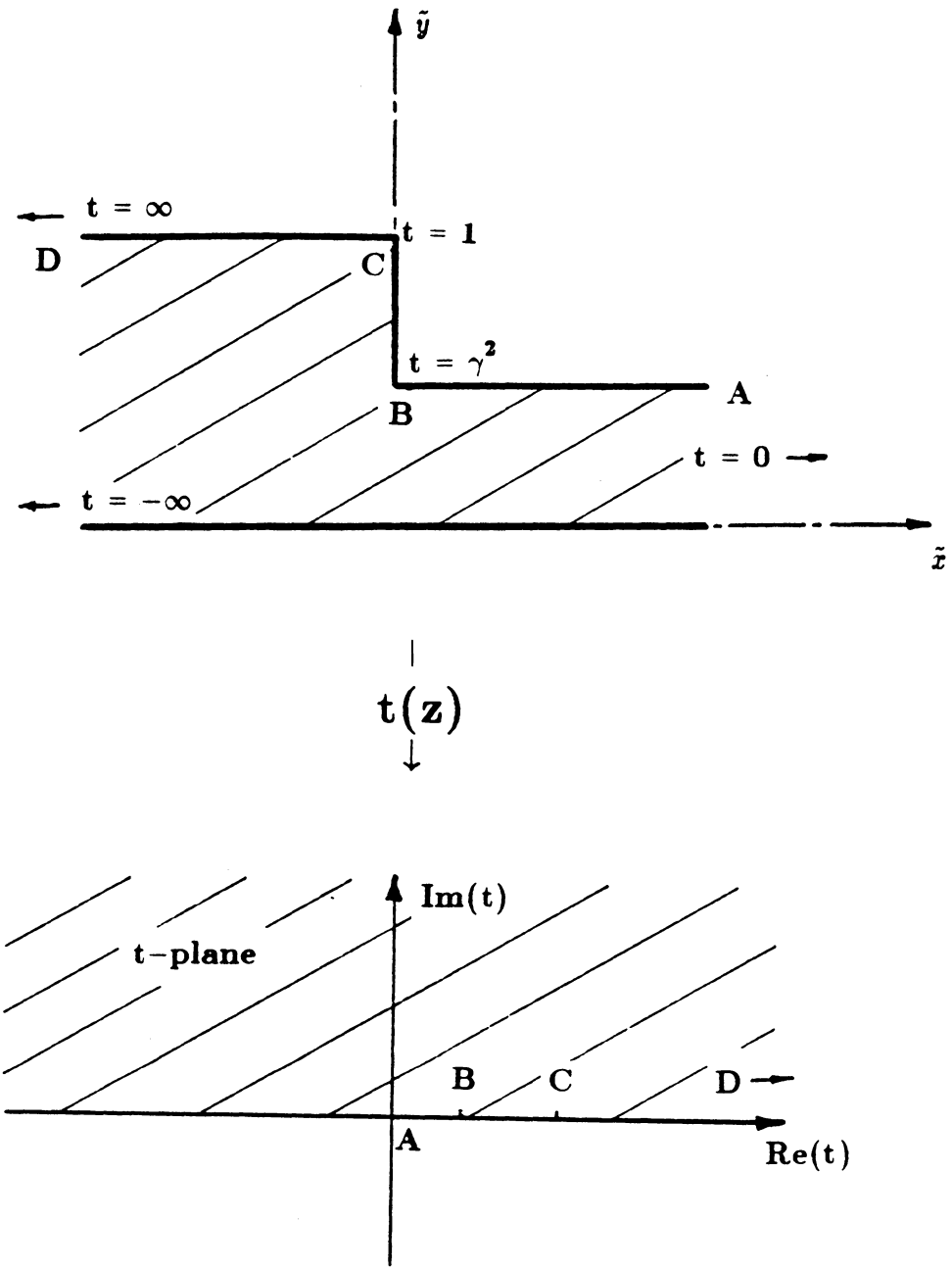

Fig. 8: Conformal mapping of the square stepped duct

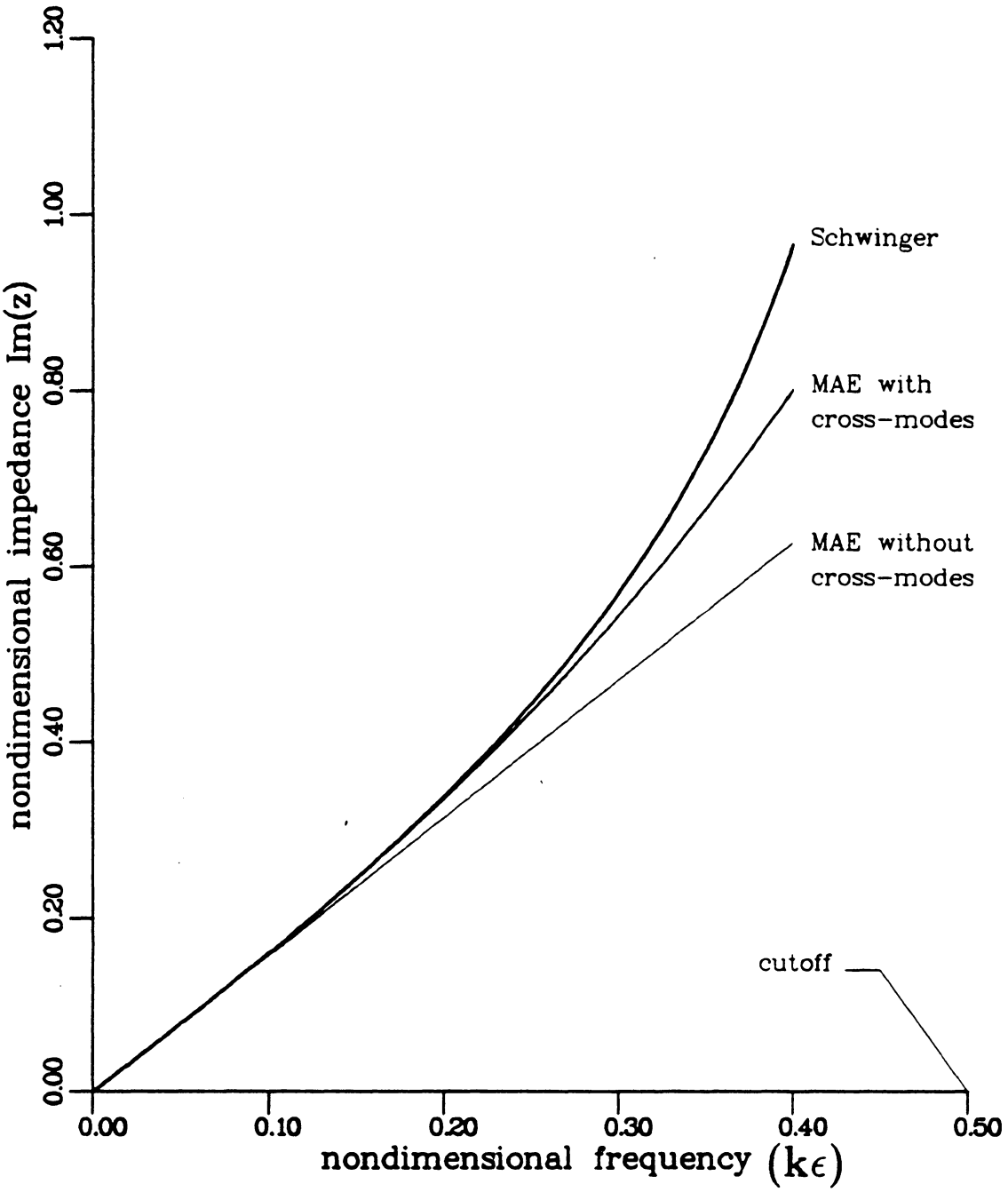

Fig. 9: Junction impedance of square stepped duct; b_L = 1.0, b_R = 0.5

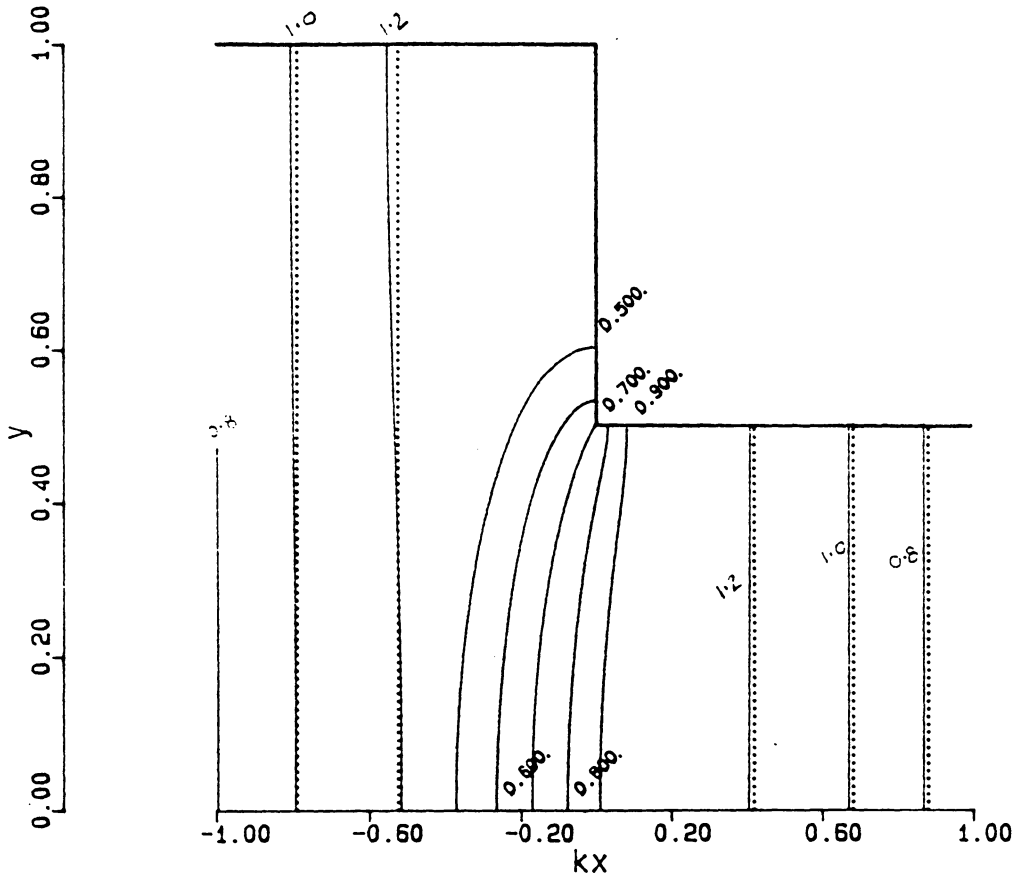

Fig. 10: Isobars of composite pressure at 40% cutoff

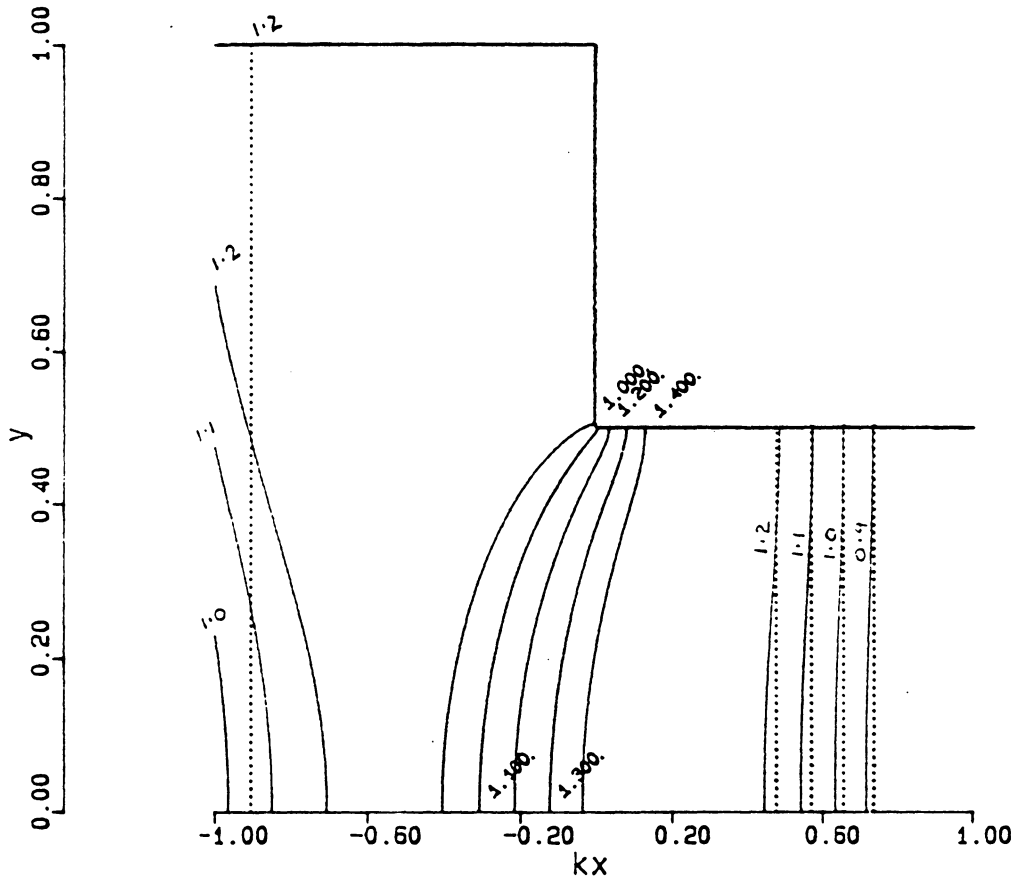

Fig. 11: Isobars of composite pressure at 80% cutoff

CHAPTER 5: EXTENSION TO SLOWLY VARYING OUTER REGIONS

In this chapter, we develop the theory of low-frequency wave propagation in slowly varying waveguides coupled by a step discontinuity. This is precisely the problem considered by Lesser and Lewis (1972). However, to incorporate the ideas presented in the previous chapters, our theory will depart significantly from that of Lesser and Lewis. The main differences lie in the mathematical formulation of propagation in the slowly varying outer regions. Lesser and Lewis and Thompson (1984a) use a regular perturbation series to describe the pressure field in the slowly varying sections. This is the standard approach in low-frequency duct acoustics, and away from the region in which the outer field interacts with the field near the discontinuity, it is sufficient. We have shown in Chapters 3 and 4, however, that reflected cross-modes, although localized near the discontinuity, have a profound effect on the junction impedance as well as on the scattered field itself. Once we admit these cross-modes, the scaled Helmholtz equation in the outer region is seen to possess a singular nature. Thus in order to include the cross-modes in the description of the outer pressure, it is necessary to carry out a singular perturbation analysis of the outer regions. It will be evident that our perturbation series, so constructed, contains the series of Lesser and Lewis. The extra terms in the present theory account for the cross-modes which Lesser and Lewis neglect, and reflect the singularity of the expansion.

Once the outer field is constructed, the analysis follows the lines of Chapter 3. We recognize that the important function of the cross-modes is their appearance as sources in the inner region. This affects the mean pressure level in the vicinity of the junction, and consequently, the impedance of the junction.

To evaluate these effects, the inner problem must be solved numerically. This is discussed in Chapter 3. In this chapter, we shall use only the general form of the inner solution in the matching region. The text is organized as follows. We first develop a WKB analysis of the outer region in Section 1. In Section 2, we construct the inner expansion in the matching region, this being somewhat different from its counterpart in Chapter 3 due to nonzero wall slopes. Finally, in Section 3, we use the matching scheme developed in Chapter 3 and construct a composite expansion.

5.1 WKB Analysis of Outer Region

The reason for abandoning a standard regular perturbation series for the outer pressure (Lesser and Lewis,1972; Thompson,1984a) is that it fails to generate any cross-modes. This is not surprising since this method can only produce a Poincaré sequence - that is, one in which the gauge functions and the spatial functions are in separated form. In Chapter 3, however, we saw that the cross-mode terms cannot be expressed in Poincaré form in the physical xy-plane. The reason for neglecting these terms, implicit in the works of Lesser and Lewis and Thompson, is that the cross-mode phase factors $e^{\pm n\pi x/\epsilon}$ are presumed to be subdominant as $\epsilon \to 0$. However, the very fact that they are non-Poincaré prevents us

from making this assertion since the usual rules of asymptotic ordering, used in matching expansions, are not applicable to such terms, as we discussed in Chapter 3. It is natural to expect a similar functional structure for the slowly varying waveguide. The rapid phase variations of cross-modes in the uniform duct suggests the use of a WKB expansion in the present case. Examining the uniform duct phase factor $e^{x/\epsilon\sqrt{n^2\pi^2/b^2 - k^2\epsilon^2}}$, we note that the fast component of the phase is associated with the transverse wavenumbers $n\pi/b$, while the fundamental wavenumber k contributes to a slow axial modulation. In the scaled Helmholtz equation

$$p_{yy} + \epsilon^2 p_{xx} + \epsilon^2 k^2 p = 0 ,$$

it is the first two terms that cause the fast phase variations. This is so because for a cross-mode, p_{yy} is essentially $(-n^2\pi^2/b^2)p$, thus making it a high-frequency term compared to the others. This totally changes the nature of the equation from one which admits a regular perturbation expansion to one in which singular behaviour can now be expected. With this perspective, it is easier to appreciate the need for a high-frequency formalism like the WKB method in this low-frequency problem.

We start with the boundary-value problem for pressure in the outer region :

$$p_{yy} + \epsilon^2 (p_{xx} + k^2 p) = 0 \qquad (5.1)$$

with

$$p_y = 0 \text{ on } y = 0 \qquad (5.2)$$

and

$$p_y = \epsilon^2 h'(x) p_x \quad \text{on } y = h(x) \tag{5.3}$$

In view of the comments in the last paragraph, we set

$$p(x,y;\epsilon) = f(x,y;\epsilon) e^{i\Omega(x)/\epsilon} \ , \tag{5.4}$$

the WKB approximation. Here f is a slowly varying amplitude which we shall represent as

$$f(x,y;\epsilon) = f^{(0)}(x,y) + \epsilon f^{(1)}(x,y) + \epsilon^2 f^{(2)}(x,y) + O(\epsilon^3) \tag{5.5}$$

Substituting (5.4) into (5.1)-(5.3), we obtain

$$f_{yy} - \Omega'^2 f + \epsilon(2i\Omega' f_x - i\Omega'' f) + \epsilon^2(f_{xx} - k^2 f) = 0 \tag{5.6}$$

with

$$f_y = 0 \quad \text{on } y = 0 \tag{5.7}$$

and

$$f_y = i\epsilon h'(x)\Omega' f + \epsilon^2 h'(x) f_x \quad \text{on } y = h(x) \tag{5.8}$$

Substituting the expansion (5.5) into (5.6)-(5.8), we obtain the following problem at $O(1)$

$$f^{(0)}_{yy} - \Omega'^2 f^{(0)} = 0 \tag{5.9}$$

$$\text{with } f^{(0)}_y = 0 \text{ on } y = 0 \text{ and on } y = h(x) \tag{5.10}$$

The eigenvalues of Ω' are given by

$$\Omega_n' = \pm\frac{in\pi}{h(x)}, \quad n = 0,1,2,\cdots \tag{5.11}$$

with corresponding eigenfunctions $S_n^{(0)}(x)\cos(n\pi y/h(x))$. The positive and negative signs in (5.11) correspond to the $x>0$ and $x<0$ regions respectively. This ensures decay of the phase factor

$$e^{i\Omega/\epsilon} = e^{\pm\frac{n\pi}{\epsilon}\int_0^x \frac{ds}{h(s)}} \tag{5.12}$$

in the appropriate directions.

The amplitudes $S_n^{(0)}(x)$ are unknown at this point, and their form is typically dictated by the solvability of a higher-order problem. However, we can avoid much labor by taking a cue from Chapter 3 and anticipating that in order to match the leading-order constant inner solution, we must have

$$S_n^{(0)}(x) = 0, \quad n > 0 \tag{5.13}$$

Likewise, for $n = 0$, we expect that the solution to

$$f_{0yy}^{(0)} = 0 \tag{5.14}$$

with $f_{0y}^{(0)} = 0$ on $y = 0,h(x)$ is a solution $w(x)$ of the Webster horn equation

$$h(x)w''(x) + h'(x)w'(x) + k^2h(x)w(x) = 0 \tag{5.15}$$

This can be shown rigorously by considering the solvability of higher-order

problems associated with (5.6)-(5.8). In fact, choosing any other solution of (5.14) leads to a contradiction at $O(\epsilon^2)$, as we shall see. For now, we just mention that since $f_0^{(0)}$ is the $y-$independent $O(1)$ solution of (5.1), it may be inferred from the work of Lesser and Lewis (1972) and Thompson (1984a) that $f_0^{(0)}$ is indeed a Webster horn function. We shall denote this by

$$f_0^{(0)} = w^{(0)}(x) , \tag{5.16}$$

where $w^{(0)}$ satisfies (5.15).

At $O(\epsilon)$, we have to solve the problem

$$f_{nyy}^{(1)} - \Omega_n{}'^2 f_n^{(1)} = -2i\Omega_n{}' f_{nx}^{(0)} - i\Omega_n{}'' f_n^{(0)} \tag{5.17}$$

with

$$f_{ny}^{(1)} = 0 \text{ on } y = 0 \tag{5.18}$$

and

$$f_{ny}^{(1)} = ih'(x)\Omega_n{}' f_n^{(0)} \text{ on } y = h(x) \tag{5.19}$$

For $n = 0$, $\Omega_n \equiv 0$ and we obtain

$$f_{0yy}^{(1)} = 0$$

with homogeneous boundary conditions. As in the $O(1)$ problem, the solution to this is a Webster horn function :

$$f_0^{(1)} = w^{(1)}(x) \tag{5.20}$$

For $n>0$, we have to solve the homogeneous version of (5.17) with homogeneous boundary conditions, since $f_n^{(0)} \equiv 0$ for $n>0$. Thus

$$f_n^{(1)} = S_n^{(1)}(x)\cos\left(\frac{n\pi y}{h(x)}\right) \tag{5.21}$$

where the amplitudes $S_n^{(1)}(x)$ have to be determined at higher order.

Now consider the $O(\epsilon^2)$ problem, given by

$$f_{nyy}^{(2)} - \Omega_n'^2 f_n^{(2)} = -2i\Omega_n' f_{nx}^{(1)} - i\Omega_n'' f_n^{(1)} - f_{nxx}^{(0)} - k^2 f_n^{(0)} \tag{5.22}$$

with

$$f_{ny}^{(2)} = 0 \text{ on } y = 0 \tag{5.23}$$

and

$$f_{ny}^{(2)} = ih'(x)\Omega_n' f_n^{(1)} - h'(x) f_{nx}^{(0)} \text{ on } y = h(x) \tag{5.24}$$

For $n = 0$, we get

$$f_{0yy}^{(2)} = -w_{xx}^{(0)} - k^2 w^{(0)} \tag{5.25}$$

$$f_{0y}^{(2)} = 0 \text{ on } y = 0 \tag{5.26}$$

$$f_{0y}^{(2)} = h'(x) w_x^{(0)}(x) \text{ on } y = h(x) \tag{5.27}$$

However, since $w^{(0)}$ satisfies the Webster horn equation (5.15), the right-hand side of (5.25) reduces to $\dfrac{h'(x)w_x^{(0)}}{h(x)}$. Thus

$$f_0^{(2)} = \frac{y^2 h'(x)}{2h(x)} w_x^{(0)} + w^{(2)}(x) , \tag{5.28}$$

because of (5.26), and we see that (5.27) is automatically satisfied. Here $w^{(2)}$ is a Webster horn function and represents the homogeneous component of $f_0^{(2)}$. This corroborates the claim, made earlier, about the form of $f_0^{(0)}$; only the Webster horn solution $w^{(0)}(x)$ ensures compatibility with the second-order problem.

When $n>0$, $f_n^{(0)} \equiv 0$ and (5.22)-(5.24) become

$$f_{nyy}^{(2)} - \Omega_n'^2 f_n^{(2)} = -2i\Omega_n' f_{nx}^{(1)} - i\Omega_n'' f_n^{(1)} \tag{5.29}$$

$$f_{ny}^{(2)} = 0 \text{ on } y = 0 \tag{5.30a}$$

$$f_{ny}^{(2)} = ih'(x)\Omega_n' f_n^{(1)} \text{ on } y = h(x) \tag{5.30b}$$

We have to ensure that the inhomogeneous terms in (5.29)-(5.30) are such that the system is solvable; this will impose certain conditions on the first-order amplitudes $f_n^{(1)}$. The condition of solvability is that the inhomogeneous terms must be orthogonal to the eigensolutions of the associated adjoint homogeneous problem (Stakgold). It is simplest to enforce this by first converting (5.29)-(5.30) to a problem with homogeneous boundary conditions. We now specialize to $x>0$. The subscript R will be used to denote quantities in this region. Define

$$F_n = f_n^{(2)} - \frac{(-1)^{n+1} n\pi h'(x) y^2 S_{Rn}^{(1)}(x)}{2h^2(x)} \tag{5.31}$$

Then (5.29)-(5.30) can be recast as

$$F_{nyy} + \left(\frac{n^2\pi^2}{h^2(x)} \right) F_n = (-1)^{n+1} \frac{n\pi h'(x)}{h^2(x)} S^{(1)}_{Rn}(x) - (-1)^{n+1} y^2 \frac{n^3\pi^3 h'(x)}{2h^4(x)} S^{(1)}_{Rn}(x)$$

$$+ \frac{2n\pi}{h(x)} \left(S^{(1)}_{Rnx} \cos\left(\frac{n\pi y}{h(x)} \right) + \frac{n\pi y}{h^2(x)} S^{(1)}_{Rnx} \sin\left(\frac{n\pi y}{h(x)} \right) \right) \tag{5.32}$$

$$- \frac{n\pi h'(x)}{h^2(x)} S^{(1)}_{Rnx} \cos\left(\frac{n\pi y}{h(x)} \right)$$

$$F_{ny} = 0 \text{ on } y = 0 \text{ and } y = h(x) \tag{5.33}$$

Here we have explicitly used $\Omega_n' = \frac{in\pi}{h(x)}$ for $x>0$. The homogeneous problem is self-adjoint, with eigenfunctions $\cos\left(n\pi y/h(x) \right)$. Thus if $R_n(x,y)$ represents the right-hand side of (5.32), we must ensure that

$$\int_0^{h(x)} R_n(x,y) \cos\left(\frac{n\pi y}{h(x)} \right) dy = 0 \tag{5.34}$$

for each $n>0$. Carrying out the algebra, we find that this leads to

$$S_{Rn}^{(1)} = \textit{constant} \tag{5.35}$$

This result is in keeping with what one would physically expect, in light of the remarks preceding equation (5.1). If we expand the exponent of the cross-mode terms for the uniform waveguide, we see that $x-$dependence on the fundamental wavelength scale starts at $O(\epsilon^2)$. At $O(\epsilon)$, the fast phase factor is unmodulated. Similar results hold for $x<0$.

Combining (5.29)-(5.30) with (5.35), we may write down the general form of $f_n^{(2)}(x,y)$ for $n>0$:

$$f_n^{(2)} = A_n^{(2)}(x)\cos\left(\frac{n\pi y}{h(x)}\right) - \frac{n\pi y^2 h'(x)}{2h^2(x)} S_{Rn}^{(1)}\cos\left(\frac{n\pi y}{h(x)}\right) \tag{5.36}$$

The first term is the homogeneous solution, and the second term is due to the forcing functions in (5.29)-(5.30). For $n = 0$, $f_n^{(2)}$ is given by (5.28).

The form of the homogeneous amplitudes $A_n^{(2)}(x)$ is as yet undetermined. As in the $O(\epsilon)$ problem, we have to ensure solvability at next order to see what conditions the amplitudes must satisfy. Thus consider the $O(\epsilon^3)$ problem :

$$f_{nyy}^3 + \left(\frac{n^2\pi^2}{h^2(x)}\right) f_n^{(3)} = \frac{2n\pi}{h(x)} f_{nx}^{(2)} - \frac{n\pi h'(x)}{h^2(x)} f_n^{(2)} - f_{nxx}^{(1)} - k^2 f_n^{(1)} \tag{5.37}$$

with

$$f_{ny}^{(3)} = 0 \text{ on } y = 0 \tag{5.38}$$

and

$$f_{ny}^{(3)} = -\frac{n\pi h'(x)}{h(x)} f_n^{(2)} + h'(x) f_{nx}^{(1)} \text{ on } y = h(x) \tag{5.39}$$

Once again, we use the device of converting to a problem with homogeneous boundary conditions. The transformation that effects this is given by

$$F_n = f_n^{(3)} - (-1)^n y^2 \frac{n\pi h'(x)}{h^2(x)} \left(\frac{1}{2} n\pi h'(x) S_{Rn}^{(1)} - A_n^{(2)}(x) \right) \tag{5.40}$$

If $R_n(x,y)$ now represents the transformed right-hand side of (5.37), the solvability condition is

$$\int_0^{h(x)} R_n(x,y) \cos\left(\frac{n\pi y}{h(x)} \right) dy = 0 \tag{5.41}$$

It is a straightforward - though tedious - matter to impose this condition, and the details will therefore be omitted. We find that for $n>0$, (5.41) yields

$$A_n^{(2)}(x) = S_{Rn}^{(2)} + \frac{xS_{Rn}^{(1)}}{6n\pi} \left(3k^2 h(x) + n^2\pi^2 h''(x) - \frac{2}{h(x)} n^2\pi^2 h'(x)^2 \right) \tag{5.42}$$

where $S_{Rn}^{(2)}$ is a constant. For $n = 0$, no new conditions are imposed; we merely find that the formula (5.28) is consistent with the boundary-value problem for $f_0^{(3)}$.

It is a useful check to see whether (5.42) agrees with the straight duct solution when we set $h'(x) = h''(x) \equiv 0$. Expanding the radical $\left(1-\epsilon^2 k^2 b^2/n^2\pi^2\right)^{1/2}$, we find that for the straight duct, the fast phase term $e^{\frac{-n\pi x}{\epsilon b}}$ is modulated by the factor

$$\epsilon S_{Rn}^{(1)} + \epsilon^2\left(\frac{1}{2}S_{Rn}^{(1)}\frac{xk^2b}{n\pi} + S_{Rn}^{(2)}\right) + O(\epsilon^3) \tag{5.43}$$

Setting the derivatives of h equal to zero, we see that (5.35) and (5.42) do indeed reduce down to (5.43).

We are now in a position to write down the outer expansion to $O(\epsilon^2 e^{-x/\epsilon})$. Using the subscript R to denote the region to the right of the step ($x>0$), we get

$$p_R = w_R^{(0)}(x) + \epsilon\left[w_R^{(1)}(x) + \sum_{n=1}^{\infty} S_{Rn}^{(1)}\cos\left(\frac{n\pi y}{h(x)}\right) e^{\frac{-n\pi}{\epsilon}\int_0^x \frac{ds}{h(s)}}\right]$$

$$+ \epsilon^2\left[w_R^{(2)}(x) + \frac{1}{2}y^2\frac{h'(x)}{h(x)}w_{Rx}^{(0)}(x) + \sum_{n=1}^{\infty}\cos\left(\frac{n\pi y}{h(x)}\right) e^{\frac{-n\pi}{\epsilon}\int_0^x \frac{ds}{h(s)}}\right. \tag{5.44}$$

$$\left(S_{Rn}^{(2)} - \frac{n\pi h'(x)}{2h^2(x)} y^2 S_{Rn}^{(1)} + \frac{xS_{Rn}^{(1)}}{6n\pi} \left(3k^2 h(x) + n^2\pi^2 h''(x) - \frac{2}{h(x)} n^2\pi^2 h'(x)^2 \right) \right) \right]$$

The corresponding expansion in $x<0$ may be obtained from (5.44) by replacing Ω_n' by its negative. This is tantamount to substituting $(-n)$ for n.

5.2 Inner Region

We will now construct an expansion for the pressure in the vicinity of the step. As in the straight duct, the appropriate coordinates are $\tilde{x} = x/\epsilon$, $\tilde{y} = y$. It is important to note that our analysis will be restricted to the portions of the inner region that are away from the step. This is implicit in our assumption that the height varies slowly on the inner scale, a condition that is violated at the step. A complete description of the inner field may only be obtained numerically. For matching purposes, however, we are only interested in the $\tilde{x}\to\pm\infty$ asymptotes of the inner pressure, and it is the functional form of these asymptotes that we seek below. Since we consider a zero-thickness step, the assumption of slow height variation is valid everywhere except at the step. Thus the series we construct below are valid for all such locations. To actually determine the relations between the coefficients that enter these series, one must resort to a numerical solution of the inner boundary-value problem.

The nondimensional inner equations we must solve are

$$\tilde{p}_{\tilde{x}\tilde{x}} + \tilde{p}_{yy} + \epsilon^2 k^2 \tilde{p} = 0 \qquad (5.45)$$

with

$$\tilde{p}_y = 0 \text{ on } y = 0 \tag{5.46}$$

and

$$\tilde{p}_y = \epsilon h'(\epsilon\tilde{x}) \text{ on } y = h(\epsilon\tilde{x}) \tag{5.47}$$

where $h'()$ denotes the derivative of h with respect to its entire argument. It is necessary to expand (5.47) in order to obtain boundary conditions at different orders of ϵ. To this end, we rewrite (5.47) as

$$\tilde{p}_y(\tilde{x},h(\epsilon\tilde{x})) = \epsilon h'(\epsilon\tilde{x})\tilde{p}_{\tilde{x}}(\tilde{x},h(\epsilon\tilde{x})) \tag{5.48}$$

and substitute the Taylor series of h :

$$h(\epsilon\tilde{x}) = h_0 + \epsilon\tilde{x}h_0' + \frac{1}{2}\epsilon^2\tilde{x}^2h_0'' + O(\epsilon^3) \tag{5.49}$$

Here we have used the notation $h_0 = h(0)$, $h_0' = h'(0)$, etc. We also expand $\tilde{p}$ as

$$\tilde{p} = \tilde{p}^{(0)} + \epsilon\tilde{p}^{(1)} + \epsilon^2\tilde{p}^{(2)} + O(\epsilon^3) \tag{5.50}$$

Equating like powers of ϵ, we obtain the following boundary conditions :

$$O(1) : \tilde{p}_y^{(0)}(\tilde{x},h_0) = 0 \tag{5.51}$$

$$O(\epsilon) : \tilde{p}_y^{(1)}(\tilde{x},h_0) = -\tilde{x}h_0'\tilde{p}_{yy}^{(0)}(\tilde{x},h_0) + h_0'\tilde{p}_{\tilde{x}}^{(0)}(\tilde{x},h_0) \tag{5.52}$$

$$O(\epsilon^2): \quad \tilde{p}_y^{(2)}(\tilde{x},h_0) = -\tilde{x}h_0'\tilde{p}_{yy}^{(1)}(\tilde{x},h_0) - \frac{1}{2}\tilde{x}^2h_0''\tilde{p}_{yy}^{(0)}(\tilde{x},h_0) - \frac{1}{2}\tilde{x}^2h_0'^2\tilde{p}_{yyy}^{(0)}(\tilde{x},h_0)$$

$$+ h_0'\tilde{p}_{\tilde{x}}^{(1)}(\tilde{x},h_0) + \tilde{x}h_0'^2\tilde{p}_{\tilde{x}y}^{(0)}(\tilde{x},h_0) + \tilde{x}h_0''\tilde{p}_{\tilde{x}}^{(0)}(\tilde{x},h_0) \tag{5.53}$$

We are now ready to consider the boundary-value problem for each $\tilde{p}^{(i)}$ in turn. At $O(1)$, we find that $\tilde{p}^{(0)}$ has to satisfy the Laplace equation with zero y-derivatives on $y = 0$ and on $y = h_0$. From our experience with the uniform duct problem, we set

$$\tilde{p}^{(0)} = B_R^{(0)} \text{ (constant)} \tag{5.54}$$

where we specialize now to region R ($x>0$). Since $\tilde{p}^{(0)}$ = constant makes the right-hand side of (5.52) drop out, we obtain an identical problem for $\tilde{p}^{(1)}$. We will, however, allow $\tilde{p}^{(1)}$ to contain higher modes, as in the uniform duct. Thus

$$\tilde{p}^{(1)} = A_R^{(1)}\tilde{x} + B_R^{(1)} + \sum_{n=1}^{\infty}\beta_{Rn}^{(1)}\cos\left(\frac{n\pi y}{h_0}\right)e^{-n\pi\tilde{x}/h_0} \tag{5.55}$$

Using (5.45) and (5.55), we can now explicitly write down the problem for $\tilde{p}^{(2)}$. This is given by

$$\tilde{p}_{\tilde{x}\tilde{x}}^{(2)} + \tilde{p}_{yy}^{(2)} = -k^2B_R^{(0)} \tag{5.56}$$

with

$$\tilde{p}_y^{(2)} = 0 \text{ on} y = 0 \tag{5.57}$$

and

$$\tilde{p}_y^{(2)} = A_R^{(1)} h_0' + \frac{h_0'}{h_0} \sum_{n=1}^{\infty} (-1)^n n\pi(\tilde{x}n\pi/h_0 - 1)\beta_{Rn}^{(1)} e^{-n\pi\tilde{x}/h_0}$$

$$\text{on } y = h_0 \tag{5.58}$$

The right-hand side of (5.58) causes the particular solution of $\tilde{p}^{(2)}$ to differ from the straight duct case. The difference is proportional to the wall slope h_0' at $\tilde{x} = 0$, so that for a square step, the formulas become identical to those in Chapter 3. We find that the appropriate solution of (5.56)-(5.58) is

$$\tilde{p}^{(2)} = A_R^{(2)}\tilde{x} + B_R^{(2)} + \sum_{n=1}^{\infty} \beta_{Rn}^{(2)} \cos\left(\frac{n\pi y}{h_0}\right) e^{-n\pi\tilde{x}/h_0}$$

$$-\frac{1}{2}\tilde{x}^2\left(k^2 B_R^{(0)} + \frac{h_0'}{h_0} A_R^{(1)}\right) + \frac{1}{2} y^2 \frac{h_0'}{h_0} A_R^{(1)} \tag{5.59}$$

$$+ \frac{1}{2}\frac{h_0'}{h_0^2} \sum_{n=1}^{\infty} n\pi\beta_{Rn}^{(1)} \left(2\tilde{x}y \sin\left(\frac{n\pi y}{h_0}\right) + \tilde{x}^2 \cos\left(\frac{n\pi y}{h_0}\right) - y^2 \cos\left(\frac{n\pi y}{h_0}\right)\right) e^{-n\pi\tilde{x}/h_0}$$

Equation (5.59) does not necessarily represent the most general solution of the system (5.56)-(5.58). Our choice, however, has been guided by matching considerations, which enable us to omit terms that would drop out at the matching stage. We are now in a position to perform the match. As in the outer solution, the $\tilde{x}<0$ counterpart of (5.59) can be obtained by simply replacing n by $-n$. Besides, the mechanics of the matching is identical for the left and right regions. Thus we shall present details for $x,\tilde{x} > 0$ only and infer the corresponding results in $x<0$ by analogy.

5.3 Matching, Composite Expansion

Since the key issue in matching the inner and outer expansions is handling the cross-mode phase factors, the matching scheme necessary in the present case is identical to that presented in Chapter 3. However, to simplify our presentation, we will not repeat the Laplace domain matching in detail. We note that the main purpose of matching in the Laplace domain was to transform the exponential phase factors $e^{\pm n\pi x/\epsilon}$ into Poincaré terms, to which then the usual rules of asymptotic matching could be applied. The outcome of this is that terms of the form $\epsilon^i e^{n\pi x/\epsilon}$ can be equated for equal values of i and be treated like Poincaré terms for matching purposes. This is the procedure we follow in this chapter. We shall not deal in detail with the precise ordering of these exponentials with respect to ordinary gauge functions; the reader is referred to Chapter 3 for complete details. For present purposes, it is sufficient to note that the exponentials fill in the gaps between successive powers of ϵ, much like the

functions $(\log\epsilon)^i$ do, and that by properly restricting the overlap region between the inner and outer expansions, one is able to avoid switchback. We therefore proceed heuristically, with the tacit understanding that our handling of the exponentials can be put on a more rigorous footing.

Thus consider the inner expansion of the outer series (5.44) to $O(\epsilon^2 e^{-x/\epsilon})$. This is obtained by substituting $\epsilon\tilde{x}$ for x in that equation and expanding $p_R(\epsilon\tilde{x})$ in a Taylor series. Truncating the resulting expression to $O(\epsilon^2 e^{-x/\epsilon})$ and expressing the result in terms of the outer coordinate x, we get

$$\lim_{(\epsilon\to 0,\ \tilde{x}\ \text{fixed})} p_R(\epsilon\tilde{x},y) = \left\{ w_R^{(0)}(0) + x w_{Rx}^{(0)}(0) + \frac{1}{2}x^2 w_{Rxx}^{(0)}(0) \right\}$$

$$+ \frac{1}{2}x^2 \frac{h_0'}{h_0^2} \sum_{n=1}^{\infty} n\pi S_n^{(1)} \cos\left(\frac{n\pi y}{h_0}\right) e^{-n\pi x/(\epsilon h_0)} + \epsilon\left\{ w_R^{(1)}(0) + x w_{Rx}^{(1)}(0) \right\}$$

$$+ \epsilon \sum_{n=1}^{\infty} e^{-n\pi x/(\epsilon h_0)} S_{Rn}^{(1)} \left\{ \cos\left(\frac{n\pi y}{h_0}\right) + n\pi x y \frac{h_0'}{h_0^2} \sin\left(\frac{n\pi y}{h_0}\right) \right\}$$

$$+ \epsilon^2\left\{ w_R^{(2)}(0) + \frac{1}{2}y^2 \frac{h_0'}{h_0} w_{Rx}^{(0)}(0) \right\}$$

$$+\epsilon^2 \sum_{n=1}^{\infty} e^{-n\pi x/(\epsilon h_0)} \cos\left(\frac{n\pi y}{h_0}\right)\left(S_{Rn}^{(2)} - \frac{1}{2}y^2 n\pi \frac{h_0'}{h_0^2} S_{Rn}^{(1)}\right) + o(\epsilon^2 e^{-x/\epsilon}) \quad (5.60)$$

We now consider the outer expansion of the inner series. Combining (5.54),(5.55) and (5.59) and taking the outer limit

$$(\epsilon \to 0,\ \tilde{x} \text{ fixed}) \lim \tilde{p}_R(x/\epsilon, y) = \lim_{\epsilon \to 0}\left(\tilde{p}^{(0)}(x/\epsilon, y) + \epsilon \tilde{p}^{(1)}(x/\epsilon, y) + \epsilon^2 \tilde{p}^{(2)}(x/\epsilon, y)\right)$$

we obtain

$$\tilde{p}_R = \left\{ B_R^{(0)} + A_R^{(1)} x - \frac{1}{2}x^2\left(k^2 B_R^{(0)} + \frac{h_0'}{h_0} A_R^{(1)}\right)\right\}$$

$$+ \frac{1}{2}x^2 \frac{h_0'}{h_0^2} \sum_{n=1}^{\infty} n\pi \beta_{Rn}^{(1)} \cos\left(\frac{n\pi y}{h_0}\right) e^{-n\pi x/(\epsilon h_0)} + \epsilon\left\{ B_R^{(1)} + A_R^{(2)} x\right\}$$

$$+ \epsilon \sum_{n=1}^{\infty} e^{-n\pi x/(\epsilon h_0)} \beta_{Rn}^{(1)}\left[\cos\left(\frac{n\pi y}{h_0}\right) + \frac{h_0'}{h_0^2} n\pi x y \sin\left(\frac{n\pi y}{h_0}\right)\right]$$

$$+ \epsilon^2\left\{ B_R^{(2)} + \frac{1}{2}y^2 \frac{h_0'}{h_0} A_R^{(1)}\right\}$$

$$+ \epsilon^2 \sum_{n=1}^{\infty} e^{-n\pi x/(\epsilon h_0)} \cos\left(\frac{n\pi y}{h_0} \right) \left(\beta_{Rn}^{(2)} - \frac{1}{2} n\pi y^2 \frac{h_0'}{h_0^2} \beta_{Rn}^{(1)} \right) + o(\epsilon^2 e^{-x/\epsilon}) \quad (5.61)$$

It is now a straightforward matter to do the match. Treating the exponentials as gauge functions as mentioned earlier, we pass to the limit $\epsilon \to 0$ in (5.60) and (5.61) and compare them at each order. The following relations are then obtained :

$$B_R^{(0)} = w_R^{(0)}(0) \quad (5.62)$$

$$A_R^{(1)} = w_{Rx}^{(0)}(0) \quad (5.63)$$

$$B_R^{(1)} = w_R^{(1)}(0) \quad (5.64)$$

$$A_R^{(2)} = w_{Rx}^{(1)}(0) \quad (5.65)$$

$$B_R^{(2)} = w_R^{(2)}(0) \quad (5.66)$$

$$\beta_{Rn}^{(1)} = S_{Rn}^{(1)} \quad (5.67)$$

$$\beta_{Rn}^{(2)} = S_{Rn}^{(2)} \quad (5.68)$$

It is clear that these relations are completely analogous to the results obtained for the uniform duct. Thus the values of the coefficients in the inner and outer series may be determined in a similar manner. However, since the Webster horn functions $w^{(i)}(x)$ must be determined numerically for an arbitrary height variation $h(x)$, we will discuss the evaluation of the coefficients only

symbolically. Firstly, we can derive an analogous set of formulas for the region $x<0$. These are symbolically identical to (5.62)-(5.68), with the subscript R replaced by L. Thus equation (5.62) and its left counterpart yield $w_R^{(0)}(0) = B^{(0)} = w_L^{(0)}(0)$, where $B^{(0)} = B_R^{(0)} = B_L^{(0)}$ follows from the $O(1)$ inner problem. Similarly, from the $O(\epsilon)$ inner problem, conservation of mass leads to $A_R^{(1)} h_0^{+} = A_L^{(1)} h_0^{-}$, where h_0^{+} and h_0^{-} are the heights at the right and left ends of the step, respectively. Thus we have

$$w_R^{(0)} = w_L^{(0)} \tag{5.69}$$

and

$$h_0^{+} w_{Rx}^{(0)}(0) = h_0^{-} w_{Lx}^{(0)}(0) \tag{5.70}$$

Since $w_R^{(0)}$ and $w_L^{(0)}$ are solutions of a second-order ordinary differential equation, we need a total of four conditions to determine them uniquely. Equations (5.69) and (5.70) constitute two conditions; together with the radiation conditions at each end of the waveguide, they completely characterize $w_R^{(0)}$ and $w_L^{(0)}$. Once these are known, equation (5.63) and its left counterpart yield $A_R^{(1)}$ and $A_L^{(1)}$. These represent the volume velocity sources at $O(\epsilon)$, and therefore fix the difference $(B_R^{(1)} - B_L^{(1)})$ and the modal amplitudes $\beta_{Rn}^{(1)}$, $\beta_{Ln}^{(1)}$. The difference $(B_R^{(1)} - B_L^{(1)})$ is nothing but $(w_R^{(1)}(0) - w_L^{(1)}(0))$. Together with the relation between $w_{Rx}^{(1)}(0)$ and $w_{Lx}^{(1)}(0)$ obtained by considering mass conservation at $O(\epsilon^2)$, this completely fixes $w_R^{(1)}$ and $w_L^{(1)}$. The relation between $A_R^{(2)}$ and $A_L^{(2)}$ has to be obtained numerically. Once this is done, $w_R^{(1)}$ and $w_L^{(1)}$ are fixed, and then $A_R^{(2)}$ and $A_L^{(2)}$ themselves may be found. These in turn yield $(B_R^{(2)} - B_L^{(2)})$, $\beta_{Rn}^{(2)}$, $\beta_{Ln}^{(2)}$

and so on.

We will now construct the composite expansion to $O(\epsilon^2 e^{-x/\epsilon})$. The coefficients in the inner and outer expansions will be assumed to be known from the above procedure. We recall that the perturbation series $\tilde{p}_R$ and $\tilde{p}_L$ are not valid at the step. We denote the actual inner solution, which must be determined numerically, by $\hat{p}$, and suppose that it may be expanded as

$$\hat{p} = \hat{p}^{(0)} + \epsilon\hat{p}^{(1)} + \epsilon^2\hat{p}^{(2)} + \cdots \tag{5.71}$$

The composite expansion is obtained by adding $\hat{p}$ to the outer expansion and then subtracting their common value in the overlap region; this is given by either of (5.60) and (5.61). Using (5.44), (5.60) and (5.71), we obtain for $x>0$

$$p_{composite} = \left\{ \hat{p}^{(0)} + w_R^{(0)}(x) - w_R^{(0)}(0) - xw_{Rx}^{(0)}(0) - \frac{1}{2}x^2 w_{Rxx}^{(0)}(0) \right.$$

$$\left. - \frac{1}{2}x^2 \frac{h_0'}{h_0^2} \sum_{n=1}^{\infty} n\pi S_{Rn}^{(1)} \cos\left(\frac{n\pi y}{h_0}\right) e^{-n\pi x/(\epsilon h_0)} \right\}$$

$$+ \epsilon \left\{ \hat{p}^{(1)} + w_R^{(1)}(x) - w_R^{(1)}(0) - xw_{Rx}^{(1)}(0) + \sum_{n=1}^{\infty} S_{Rn}^{(1)} e^{\frac{-n\pi}{\epsilon}\int_0^x \frac{ds}{h(s)}} \right.$$

$$- \sum_{n=1}^{\infty} S_{Rn}^{(1)} e^{-n\pi x/(\epsilon h_0)} \left(\cos\left(\frac{n\pi y}{h_0} \right) + n\pi x y \frac{h_0'}{h_0^2} \sin\left(\frac{n\pi y}{h_0} \right) \right) \Bigg\}$$

$$+ \epsilon^2 \Bigg\{ \hat{p}^{(2)} + w_R^{(2)}(x) + \frac{1}{2} y^2 \frac{h'(x)}{h(x)} w_{Rx}^{(0)}(x) - w_R^{(2)}(0) - \frac{1}{2} y^2 \frac{h_0'}{h_0} w_{Rx}^{(0)}(0)$$

$$+ \sum_{n=1}^{\infty} \cos\left(\frac{n\pi y}{h(x)} \right) e^{\frac{-n\pi}{\epsilon} \int_0^x \frac{ds}{h(s)}} \left(S_{Rn}^{(2)} - \frac{1}{2} n\pi y^2 \frac{h'(x)}{h^2(x)} S_{Rn}^{(1)} + \frac{x S_{Rn}^{(1)}}{6n\pi} (3k^2 h(x) \right.$$

$$\left. + n^2\pi^2 h''(x) - 2n^2\pi^2 \frac{h'^2(x)}{h(x)}) \right)$$

$$- \sum_{n=1}^{\infty} \cos\left(\frac{n\pi y}{h_0} \right) e^{-n\pi x/(\epsilon h_0)} \left(S_{Rn}^{(2)} - \frac{1}{2} y^2 n\pi \frac{h_0'}{h_0^2} S_{Rn}^{(1)} \right) \Bigg\} + o(\epsilon^2 e^{-x/\epsilon}) \quad (5.72)$$

For $x<0$, we merely need to exchange the subscript R for L and replace n by $(-n)$. The coefficients appearing in (5.72) must be determined numerically, as discussed earlier.

CHAPTER 6 : SUMMARY AND CONCLUSIONS

A low-frequency theory of acoustic wave propagation in waveguides with boundary discontinuities has been developed in this thesis. The motivation was to improve the range of validity of prevailing asymptotic theories, which are accurate only at very low frequencies. Previous investigators overlooked the important function of the waveguide cross-modes. We showed that this is the main reason behind the restricted accuracy of their results.

Although the cross-modes are discernible only in the immediate vicinity of a discontinuity, they contain important information about the interaction between the traveling far-field and the evanescent local field near the discontinuity. It is only when we account for the cross-modes that the compressibility of the local flow is correctly modeled. The effects of compressibility become important as the frequency is increased. Thus the cross-mode interaction contains the key to obtaining a theory valid over a wide frequency range.

The cross-modes affect the traveling far-field modes through the local flow. We showed that they may be viewed as sources at infinity that drive the local flow. This causes a modification of the outer asymptotes of the local pressure, and thereby the far-field amplitudes. The new theory, which includes the cross-mode interaction, was tested for a square stepped duct, for which accurate variational estimates are available. Just a few cross-mode terms were seen to result in a marked improvement in the impedance estimate.

The second new feature of this thesis concerns the mathematical description of the cross-mode effects. We found that the method of Matched Asymptotic

Expansions (MAE), in its usual form, is incapable of describing the interaction. The reason was shown to be the exponential non-Poincaré structure of the cross-modes. A naive application of asymptotic limits renders the inner cross-modes subdominant, with the paradoxical result that they cannot then be matched to the outer cross-modes. To resolve this problem, an extended MAE technique was developed. The new technique is based on block matching Laplace transforms of intermediate expansions. The difficulty in using the usual MAE method was shown to be two-fold. Firstly, the Van Dyke matching rule is too restrictive for our purposes, since it implicitly requires an overlap region that is much larger than what exists between the inner and outer cross-modes. Thus it was necessary to appeal to the more fundamental method of intermediate limits. Although this produces results equivalent to the Van Dyke method in most cases, it is of prime importance in the present problem since it helps to establish the existence of an overlap region. The second aspect of the difficulty with MAE is the fact that matching theorems break down when asymptotic limits are applied to expansions that are non-Poincaré. The method of matching in a Laplace transform domain was put forward to resolve this difficulty. In the plane of the transform variable, the expansions become Poincaré series, which makes it possible to match the cross-modes in a rational manner. We also found that the size of the overlap region, which must be established with increasing precision as one matches higher orders, follows naturally from certain block matching arguments. The connection between the resulting ordering relations and the physical nature of the cross-modes was also established.

No attempt was made to obtain a strict mathematical justification of the transform matching technique. However, based on the significant improvement in the scattering theory as well as the physical corroboration of some of the mathematical results, we expect that the technique may be put on a rigorous mathematical footing. From an applied point of view, the technique offers a rational method of dealing with non-Poincaré expansions, and may well have useful applications in problems in which evanescent terms are important.

We conclude with a few remarks on the interesting parallels between the MAE method and classical integral equation approaches to the scattering problem. Integral equation methods are based on continuity conditions imposed on the junction plane. From an MAE point of view, this is equivalent to shrinking the overlap region down to a plane. This is analogous to patching, in contrast to matching, and it explains why the integral equation method fails for non-planar discontinuities. MAE, on the other hand, merges the wave fields on either side of the discontinuity through finite overlap regions. Thus it may be viewed as a generalization of the integral equation method. The analogy is stronger for ducts with uniform smooth sections. In such cases, the outer field in MAE may be obtained directly from an eigenfunction expansion, which is completely equivalent to expressing the field using Green's theorem.

In addition to such structural similarities, however, there is the possibility that the connection between MAE and classical methods runs deeper. This is especially apparent in the light of Schwinger's method of Static Equivalence (MSE). Firstly, Schwinger's formulation of the field on the junction plane as a solution of an equivalent static problem strongly resembles the MAE approach

of posing a separate local problem, which is also static (incompressible) to leading order. At this point, the two methods diverge - in MAE, one is able to construct successively better approximations by forward substitution, whereas MSE calls for the simultaneous solution of an infinite algebraic system. This system is solved approximately using a variational technique. It may be possible to show, however, that the variational solution is related to the asymptotic series that results from MAE. It would be interesting to see, for example, how Padé approximants to the asymptotic series relate to the variational expression. Our remarks are based on two observations. Firstly, Schwinger's result comes out naturally in the form of rational fractions. This suggests the possibility of obtaining a greater radius of convergence of the asymptotic series by recasting it in terms of Padé fractions. And secondly, it has been shown in quantum scattering theory (Baker and Graves-Morris, 1981) that Padé approximants are intimately related to variational principles of the Rayleigh-Ritz type. Thus it is reasonable to expect that a deeper correspondence may be established between the MAE method and Schwinger's MSE-variational solution. It seems likely that the MAE method may have to be recast in terms of energy, rather than primitive field variables, since variational approximations use quadratic forms related to energy. Since energy is not explicitly considered in MAE, the extra constraint of energy conservation might well lead to asymptotic series with larger regions of validity as well as the valuable byproduct of error bracketing that is characteristic of Padé fraction and variational methods.

REFERENCES

G.A. Baker and P.R. Graves-Morris (1981) *Padé Approximants*; Addison-Wesley, Reading, Mass.

C.M. Bender and S.A. Orszag (1978) *Advanced Mathematical Methods for Scientists and Engineers*; McGraw-Hill, New York

Fraenkel, L.E. (1969) On the method of Matched Asymptotic Expansions. Part I: A matching principle; *Proc. Camb. Phil. Soc.* **(65)**, p.209

Y. Kagawa and T. Omote (1976) Finite-element simulation of acoustic filters of arbitrary profile with circular cross section; J. Acoust. Soc. Am. **60**(5), p.1003

J. Kevorkian and J.D. Cole (1981) *Perturbation Methods in Applied Mathematics*; Springer-Verlag, New York

M.B. Lesser and D.G. Crighton (1975) *Physical Acoustics and the Method of Matched Asymptotic Expansions*; in *Physical Acoustics* Vol. XI, W.P. Mason and R.N. Thurston eds., Academic, New York

M.B. Lesser and J.A. Lewis (1972) Application of Matched Asymptotic Expansions to acoustics I : the Webster horn equation and the stepped duct; J. Acoust. Soc. Am. **51**(5), p.1664

J.E. Marsden (1973) *Basic Complex Analysis*; Freeman, San Francisco

J.W. Miles (1946a) The analysis of plane discontinuities in cylindrical tubes, Part I; J. Acous. Soc. Am. **17**, p.259

J.W. Miles (1946b) *loc. cit.* Part II; J. Acous. Soc. Am. **17**, p.272

R. Mittra and S.W. Lee (1971) *Analytical Techniques in the Theory of Guided Waves*; Macmillan, New York

P.M. Morse and K.U. Ingard (1968) *Theoretical Acoustics*; McGraw-Hill, New York

B. Noble (1958) *Methods Based on the Wiener-Hopf Technique for the Solution of Partial Differential Equations*; Pergamon, New York

Lord Rayleigh (1897) *Philos. Mag.* **44**, p.28

J. Schwinger and D.S. Saxon (1968) *Discontinuities in Waveguides*, Notes on lectures by Julian Schwinger; Gordon and Breach, New York

Sheer, A.F. (1971) A uniformly asymptotic solution for incompressible flow past thin sharp-edged aerofoils at zero incidence; *Proc. Camb. Phil. Soc.* **(70)**, p.135

J.C. Slater (1942) *Microwave Transmission*; McGraw-Hill, New York

I. Stakgold (1967) *Boundary Value Problems of Mathematical Physics, Vol. 1*, p.85; Macmillan, New York

C. Thompson (1984a) Linear Inviscid Wave Propagation in a Waveguide Having a Single Boundary Discontinuity: Part I: Theory; J. Acous. Soc. Am. **75**(2), p.346

C. Thompson (1984b) *loc. cit.* Part II: Application; J. Acous. Soc. Am. **75**(2), p.356

C. Thompson (1984c) Acoustic Streaming in a Waveguide with Slowly Varying Height; J. Acous. Soc. Am. **75**(1), p.97

M. Van Dyke (1975) *Perturbation Methods in Fluid Mechanics*; Parabolic Press, Stanford

Whittaker and Watson (1942) *A Course in Modern Analysis*; Cambridge

APPENDIX A: VARIATIONAL PRINCIPLES AND THE METHOD OF STATIC EQUIVALENCE

The method of Matched Asymptotic Expansions is a fairly new technique, originating in the 1950s in the context of fluid mechanics. It was not until the 1960s that the method was formally applied to problems in acoustics, although the concept of nonuniformity of a single expansion may be found in Rayleigh's (1897) work. On the other hand, variational methods, also attributable in part to Rayleigh, have long been used to obtain approximate analytical solutions of physical problems. Applications to waveguide problems are based on minimization principles related to the Rayleigh-Ritz principle. In order to obtain estimates of overall parameters of wave scattering problems, the quantity of interest, say junction impedance, is expressed in terms of integrals of the unknown field variables. Such an expression can usually be derived from the integral equation governing the field. For a wide class of equations encountered in scattering and propagation problems, Morse and Ingard (p. 155) show that in the vicinity of the correct solution, the impedance is stationary with respect to variations in the field. Thus if one uses a trial function that is $O(\delta)$ different from the actual field, the error in the impedance, as determined from the integral equation, will be $o(\delta)$.

There are many versions of this basic idea. As Morse and Ingard point out, the derivation of such variational principles hinges on expressing the quantity of interest in terms of a symmetric quadratic form. Since the integral equation of a scattering problem can be derived using a symmetric Green's function, such

problems lend themselves naturally to the variational approach. Of particular interest in the present context is the variational principle used by Schwinger (pp. 66-68, 103). Schwinger shows that by considering quadratic forms involving different field variables, such as pressure and velocity, it is possible to obtain upper and lower limits of the impedance. Thus one is able to bracket the error introduced by using a trial function for the field. We will show that in addition to this feature, Schwinger's variational expression enjoys the stationarity property discussed above.

From an MAE point of view, however, the most interesting aspect of Schwinger's calculations is the derivation of the trial field by the Method of Static Equivalence (MSE). The success of any variational procedure depends heavily on the choice of the trial field in the aperture. If the trial function is close to the correct function, the variational expression minimizes the error in the impedance; an injudicious choice, however, will only magnify the error. Now in the vicinity of the aperture, the pressure field is incompressible to leading order, as we have seen. Thus a reasonable trial function could be obtained by solving the local potential flow problem (Morse and Ingard, pp. 483-488). This approach, however, ignores dynamic effects on the local static field, thereby limiting the accuracy of the approximation.

In the method of Static Equivalence, on the other hand, the local field is determined by rewriting the reduced wave equation as a Poisson equation :

$$\nabla^2 p = -k^2 p \qquad \text{(A.1)}$$

The forcing term is regarded to be known through the requirement that the

resulting field must be equivalent to the actual dynamic field on the junction plane. Schwinger shows that the forcing term may be replaced by static sources at infinity, their amplitudes being chosen so as to achieve this equivalence. Thus dynamic effects on the static field are embodied in the source amplitudes.

This approach has many parallels with the method of Matched Asymptotic Expansions. The requirement of equivalence of the static and dynamic fields on the junction plane is essentially a patching procedure, the matching region having been shrunk to zero faster than any cross-mode wavelengths. Viewing the dynamic effects as forcing terms is also an attitude characteristic of MAE. As in the MAE theory, the important dynamic effect on the local field is the change in the mean pressure level in the vicinity of the aperture due to the forcing terms. In MSE, it is the equivalent sources at infinity that cause this change. Although the equivalent static problem in MSE is solved approximately, we will see that the inclusion of dynamic effects greatly extends the range of validity of the variational estimate.

The remainder of this appendix is organized as follows. In Section 1, we derive the integral equation and obtain the statement of static equivalence. The variational expression for the impedance and its properties are derived in Section 2. In Section 3, we present explicit results for the junction impedance.

A.1 The Integral Equation and the Statement of Static Equivalence

We start by deriving the integral equation for the dynamic problem. As in Chapter 3, we express the pressure in $x<0$ and $x>0$ as weighted sums of

corresponding eigenfunctions :

$$x<0:\ p = e^{ikx} + Re^{-ikx} + \sum_{n=1}^{\infty} S_{Ln} \cos\frac{n\pi y}{b_L} e^{x[(n\pi/b_L)^2 - k^2]^{1/2}} \tag{A.2}$$

$$x>0:\ p = Te^{ikx} + \sum_{n=1}^{\infty} S_{Rn} \cos\frac{n\pi y}{b_R} e^{-x[(n\pi/b_R)^2 - k^2]^{1/2}} \tag{A.3}$$

Now on the junction plane, the axial velocity may be expressed as

$$\frac{\partial p}{\partial x}(x\to 0^-) = ik(1 - R) + \sum_{n=1}^{\infty} S_{Ln} \cos\frac{n\pi y}{b_L} [(n\pi/b_L)^2 - k^2]^{1/2} \tag{A.4}$$

$$\frac{\partial p}{\partial x}(x\to 0^+) = ikT - \sum_{n=1}^{\infty} S_{Rn} \cos\frac{n\pi y}{b_R} [(n\pi/b_R)^2 - k^2]^{1/2} \tag{A.5}$$

Since $\frac{\partial p}{\partial x}$ must be continuous through the aperture, we set

$$u(y) = \frac{\partial p}{\partial x}(x\to 0^-) = \frac{\partial p}{\partial x}(x\to 0^+)\ ,\ y \text{ in aperture} \tag{A.6}$$

From (A.4) and (A.5), we see that the modal amplitudes are simply Fourier coefficients of the axial velocity on the junction plane. Thus

$$ik(1 - R) = \frac{1}{b_L}\int_0^{b_R} u(y)\,dy \tag{A.7}$$

$$ikT = \frac{1}{b_R}\int_0^{b_R} u(y)\,dy \tag{A.8}$$

$$S_{Ln} = \frac{2}{b_L[(n\pi/b_L)^2 - k^2]^{1/2}}\int_0^{b_R} u(y)\cos\frac{n\pi y}{b_L}\,dy \tag{A.9}$$

$$S_{Rn} = -\frac{2}{b_R[(n\pi/b_R)^2 - k^2]^{1/2}}\int_0^{b_R} u(y)\cos\frac{n\pi y}{b_R}\,dy \tag{A.10}$$

In equations (A.7) - (A.10), we have implicitly used the boundary condition $\frac{\partial p}{\partial x}(x\to 0^-) = 0$ for $b_R < y < b_L$. We also introduce the junction impedance at this point. This is given by

$$Z = \frac{\Delta\overline{P}}{Q} \tag{A.11}$$

where $\Delta\overline{P}$ is the mean pressure drop across the aperture, and Q the volume flux through the aperture. From (A.2) and (A.3), we find that

$$\Delta\overline{P} = T - 1 - R \tag{A.12}$$

The volume flux is given by

$$Q = \frac{1}{i\omega\rho_0}\int_0^{b_R} u(y)\,dy = \frac{kb_L(1-R)}{\omega\rho_0} \tag{A.13}$$

Thus

$$Z = \frac{\omega\rho_0}{kb_L}\left(\frac{T-1-R}{1-R}\right) \tag{A.14}$$

The integral equation of the problem is obtained by requiring continuity of pressure across the aperture. From (A.2) and (A.3), we see that this gives

$$T - 1 - R = \sum_{n=1}^{\infty} S_{Ln}\cos(n\pi y/b_L) - \sum_{n=1}^{\infty} S_{Rn}\cos(n\pi y/b_R)$$

Substituting (A.7) - (A.10) for the Fourier amplitudes and using (A.14), we can write this as

$$\frac{-iZ}{\omega\rho_0}\int_0^{b_R} u(y)\,dy = \frac{2}{\pi}\sum_{n=1}^{\infty}\cos(n\pi y/b_L)\int_0^{b_R}\frac{u(y')\cos(n\pi y'/b_L)\,dy'}{[n^2-(kb_L/\pi)^2]^{1/2}}$$

$$+\frac{2}{\pi}\sum_{n=1}^{\infty}\cos(n\pi y/b_R)\int_0^{b_R}\frac{u(y')\cos(n\pi y'/b_R)\,dy'}{[n^2-(kb_R/\pi)^2]^{1/2}},\quad y \text{ in aperture} \qquad (A.15)$$

This is the integral equation governing the axial velocity distribution over the aperture. If $u(y)$ can be obtained from this equation, the pressure at any point may be calculated using the Fourier expansions (A.2) and (A.3).

We now note that for a static problem ($k = 0$), the square roots in (A.15) reduce to n. Thus we may decompose the kernel into static and dynamic components and rewrite (A.15) as

$$\frac{iZ}{\omega\rho_0}\int_0^{b_R} u(y)dy + \frac{2}{\pi}\sum_{n=1}^{\infty}\cos(n\pi y/b_L)\int_0^{b_R}\frac{1}{n}u(y')\cos(n\pi y'/b_L)dy'$$

$$+\frac{2}{\pi}\sum_{n=1}^{\infty}\cos(n\pi y/b_R)\int_0^{b_R}\frac{1}{n}u(y')\cos(n\pi y'/b_R)dy' \qquad (A.16)$$

$$= -\frac{2}{\pi}\sum_{n=1}^{\infty}\left(\frac{1}{[n^2-(kb_L/\pi)^2]^{1/2}}-\frac{1}{n}\right)\cos(n\pi y/b_L)\int_0^{b_R}u(y')\cos(n\pi y'/b_L)dy'$$

$$-\frac{2}{\pi}\sum_{n=1}^{\infty}\left(\frac{1}{[n^2-(kb_R/\pi)^2]^{1/2}}-\frac{1}{n}\right)\cos(n\pi y/b_R)\int_0^{b_R}u(y')\cos(n\pi y'/b_R)dy'$$

This is completely equivalent to rewriting the Helmholtz equation as the Poisson equation (A.1). The terms on the right-hand side of (A.16) represent dynamic effects, and correspond to the forcing term in (A.1).

The next step in MSE is to show that one can obtain the same axial velocity distribution $u(y)$ on the junction plane in an equivalent static problem. That is, by allowing for static sources at infinity to simulate the forcing terms, we can derive an integral equation that is formally identical to (A.16). Thus consider solutions of Laplace's equation in the stepped duct. As in the dynamic case, the static pressure ϕ in each region may be expressed as an eigenfunction expansion :

$$\phi = A_L x + B_L + \sum_{n=1}^{\infty}\beta_{Ln}\cos(n\pi y/b_L)e^{n\pi x/b_L}$$

$$+\sum_{n=1}^{\infty}\alpha_{Ln}\cos(n\pi y/b_L)e^{-n\pi x/b_L} \qquad \text{(A.17)}$$

for $x<0$, and

$$\phi = A_R x + B_R + \sum_{n=1}^{\infty} \beta_{Rn} \cos(n\pi y/b_R) e^{-n\pi x/b_R}$$

$$+ \sum_{n=1}^{\infty} \alpha_{Rn} \cos(n\pi y/b_R) e^{n\pi x/b_R} \qquad \text{(A.18)}$$

for $x>0$. Here $A_L b_L = A_R b_R$ to satisfy conservation of mass, β_{Ln},β_{Rn} are reflected amplitudes, and α_{Ln},α_{Rn} are incident or source amplitudes. We denote the axial velocity in the aperture by $u(y)$, as before. From (A.17) and (A.18), we find that

$$x \to 0^-: u(y) = A_L + \frac{\pi}{b_L} \sum_{n=1}^{\infty} n\beta_{Ln} \cos(n\pi y/b_L) - \frac{\pi}{b_L} \sum_{n=1}^{\infty} n\alpha_{Ln} \cos(n\pi y/b_L)$$

$$x \to 0^+: u(y) = A_R - \frac{\pi}{b_R} \sum_{n=1}^{\infty} n\beta_{Rn} \cos(n\pi y/b_R) + \frac{\pi}{b_R} \sum_{n=1}^{\infty} n\alpha_{Rn} \cos(n\pi y/b_R)$$

Thus by the Fourier expansion theorem,

$$\beta_{Ln} - \alpha_{Ln} = \frac{2}{n\pi} \int_0^{b_R} u(y') \cos(n\pi y'/b_L) dy' \qquad \text{(A.19)}$$

$$\alpha_{Rn} - \beta_{Rn} = \frac{2}{n\pi}\int_0^{b_R} u(y')\cos(n\pi y'/b_R)dy' \qquad \text{(A.20)}$$

By requiring that ϕ be continuous across the aperture, we obtain the integral equation of the static problem :

$$B_L - B_R + \sum_{n=1}^{\infty}(\beta_{Ln}+\alpha_{Ln})\cos(n\pi y/b_L) - \sum_{n=1}^{\infty}(\beta_{Rn}+\alpha_{Rn})\cos(n\pi y/b_R) = 0$$

In terms of Fourier amplitudes, this reads

$$B_L - B_R + \frac{2}{\pi}\sum_{n=1}^{\infty}\frac{1}{n}\cos(n\pi y/b_L)\int_0^{b_R} u(y')\cos(n\pi y'/b_L)dy'$$

$$+ \frac{2}{\pi}\sum_{n=1}^{\infty}\frac{1}{n}\cos(n\pi y/b_R)\int_0^{b_R} u(y')\cos(n\pi y'/b_R)dy' \qquad \text{(A.21)}$$

$$= -2\sum_{n=1}^{\infty}\alpha_{Ln}\cos(n\pi y/b_L) + 2\sum_{n=1}^{\infty}\alpha_{Rn}\cos(n\pi y/b_R)$$

But now, on comparison with the dynamic integral equation (A.16), we see that

the two become formally identical if we require that

$$B_L - B_R = \frac{iZ}{\omega\rho_0}\int_0^{b_R} u(y)\,dy \tag{A.22}$$

$$\alpha_{Ln} = \frac{1}{\pi}\left(\frac{1}{[n^2 - (kb_L/\pi)^2]^{1/2}} - \frac{1}{n}\right)\int_0^{b_R} u(y)\cos(n\pi y/b_L)\,dy \tag{A.23}$$

$$\alpha_{Rn} = -\frac{1}{\pi}\left(\frac{1}{[n^2 - (kb_R/\pi)^2]^{1/2}} - \frac{1}{n}\right)\int_0^{b_R} u(y)\cos(n\pi y/b_R)\,dy \tag{A.24}$$

Equations (A.22)-(A.24) constitute the statement of static equivalence. We see that it fixes the source amplitudes and the difference of the constants B_L and B_R. Since the solution of a homogeneous Neumann problem for Laplace's equation is arbitrary up to an additive constant, B_L and B_R cannot be fixed individually. However, their difference is determined uniquely by the volume velocity and cross-mode sources and this is now given by the statement of static equivalence.

Although the α_n are given in terms of the yet unknown field amplitudes, we may eliminate the Fourier integrals between equations (A.19), (A.20) and

(A.23), (A.24). This yields

$$\beta_{Ln} = K_{Ln}\alpha_{Ln} = \frac{n + [n^2 - (kb_L/\pi)^2]^{1/2}}{n - [n^2 - (kb_L/\pi)^2]^{1/2}}\ \alpha_{Ln} \tag{A.25}$$

$$\beta_{Rn} = K_{Rn}\alpha_{Rn} = \frac{n + [n^2 - (kb_R/\pi)^2]^{1/2}}{n - [n^2 - (kb_R/\pi)^2]^{1/2}}\ \alpha_{Rn} \tag{A.26}$$

But now, by the principle of superposition, we can express the reflected mode amplitudes as a linear combination of the incident amplitudes α_n and the volume velocity source $Q = A_L b_L = A_R b_R$:

$$\beta_{Ln} = S_{Ln}Q + \sum_{m=1}^{\infty} R^{(L)}_{m\to n}\alpha_{Lm} + \sum_{m=1}^{\infty} T^{R\to L}_{m\to n}\alpha_{Rm} \tag{A.27}$$

$$\beta_{Rn} = S_{Rn}Q + \sum_{m=1}^{\infty} R^{(R)}_{m\to n}\alpha_{Rm} + \sum_{m=1}^{\infty} T^{L\to R}_{m\to n}\alpha_{Lm} \tag{A.28}$$

The same applies to the difference $(B_L - B_R)$. Using (A.22), we may write

$$B_L - B_R = \frac{iZQ}{\omega\rho_0} = a_0 Q + \sum_{n=1}^{\infty} a_{Rn}\alpha_{Rn} + \sum_{n=1}^{\infty} a_{Ln}\alpha_{Ln} \tag{A.29}$$

The parameters R and T in (A.27) and (A.28) denote static reflection and transmission coefficients. Superscripts indicate region (left or right), and subscripts indicate mode numbers. S_{Ln}, S_{Rn} and a_0 are volume velocity influence coefficients, while a_{Rn} (a_{Ln}) stands for the difference $(B_L - B_R)$ that would be induced if only an *nth* mode were incident from the right (left).

These parameters depend only on the geometry of the duct and may therefore be determined, once and for all, independently of the dynamic field. We showed in Chapter 4 how they may be obtained by conformal mapping. Thus we may suppose that these parameters are known. Equations (A.25)-(A.29) now constitute a closed system that may, in principle, be solved. Thus from (A.25)-(A.28), we may find the α_n, proportional to Q. Substituting these into (A.29) should then yield the value of Z in a straightforward manner. We have thus found a formal solution to the problem. Due to the infinite sums involved, however, this approach is quite hopeless from a practical point of view. We therefore use a variational technique that utilizes an approximate solution of (A.25)-(A.29) as a trial field. The variational expression used by Schwinger is developed in the following section. Although an approximation to the true solution, the trial field includes dynamic effects through the statement of static equivalence. This, combined with the stationarity property of the variational expression, greatly extends the dynamic range of validity of the impedance estimate.

A.2 The Variational Principle

In this section, we shall derive the stationarity and bracketing properties of Schwinger's variational formula for the junction impedance. The formula itself is easy to obtain from the integral equation. Thus we write (A.15) in the form

$$\lambda \int u(y)dy = \sum A_n \phi_n(y) \int u(y')\phi_n(y')dy'$$

$$+ \sum B_n \psi_n(y) \int u(y')\psi_n(y')dy' \qquad \text{(A.30)}$$

where $\phi_n(y) = \cos(n\pi y/b_L)$, $\psi_n(y) = \cos(n\pi y/b_L)$, $A_n = 2\left(n^2\pi^2 - k^2 b_L{}^2 \right)^{-1/2}$,

$B_n = 2\left(n^2\pi^2 - k^2 b_R{}^2 \right)^{-1/2}$, $\lambda = -iZ/\omega\rho_0$ and the range of the summations and integrals are understood. Multiplying both sides by $u(y)$ and integrating from 0 to b_R, we immediately obtain

$$\lambda \left(\int u(y)dy \right)^2 = \sum A_n \left(\int \phi_n(y)u(y)dy \right)^2$$

$$+ \sum B_n \left(\int \psi_n(y)u(y)dy \right)^2 \qquad \text{(A.31)}$$

Introducing the shorthand notation

$$u_n = \int \phi_n(y)u(y)dy$$

$$v_n = \int \psi_n(y)u(y)dy$$

$$u_0 = \int u(y)dy \ ,$$

this may be written more compactly as

$$\lambda = \frac{1}{u_0^2}\sum(A_n u_n^2 + B_n v_n^2) \tag{A.32}$$

We note that λ is an eigenvalue of the homogeneous integral equation (A.30); i.e., nontrivial solutions $u \neq 0$ exist only for certain discrete values $\overline{\lambda}$. For values of λ outside this set, the equation as it stands yields no information, both sides being identically equal to zero. However, we may still use (A.32) with a trial function $u(y)$ in order to obtain an estimate λ. We shall denote a true value of λ by $\overline{\lambda}$, and the corresponding eigenfunctions by $\overline{u}(y)$. Then

$$\overline{\lambda} = \frac{1}{\overline{u}_0^2}\sum(A_n \overline{u}_n^2 + B_n \overline{v}_n^2) \tag{A.33}$$

where $\overline{u}_n$, $\overline{v}_n$, and $\overline{u}_0$ are the Fourier coefficients of $\overline{u}$. We now proceed to show that the formula (A.32) will always overestimate the true eigenvalue. Thus consider the inequality

$$\sum A_n\left(\frac{u_n}{u_0} - \frac{\overline{u}_n}{\overline{u}_0}\right)^2 + B_n\left(\frac{v_n}{u_0} - \frac{\overline{v}_n}{\overline{u}_0}\right)^2 \geqslant 0 \ ,$$

which, upon expanding, becomes

$$\sum\left(A_n \frac{u_n^{\,2}}{u_0^{\,2}} + B_n \frac{v_n^{\,2}}{u_0^{\,2}} \right) + \sum\left(A_n \frac{\overline{u}_n^{\,2}}{\overline{u}_0^{\,2}} + B_n \frac{\overline{v}_n^{\,2}}{\overline{u}_0^{\,2}} \right)$$

$$- \frac{2}{u_0 \overline{u}_0} \sum (A_n u_n \overline{u}_n + B_n v_n \overline{v}_n) \geqslant 0$$

Using equations (A.32) and (A.33), we may write this as

$$\lambda + \overline{\lambda} - \frac{2}{u_0 \overline{u}_0} \sum (A_n u_n \overline{u}_n + B_n v_n \overline{v}_n) \geqslant 0 \qquad \text{(A.34)}$$

Now for a correct eigenvalue $\overline{\lambda}$, (A.30) reads

$$\overline{\lambda} \overline{u}_0 = \sum (A_n \phi_n(y) \overline{u}_n - B_n \psi_n(y) \overline{v}_n)$$

Multiplying both sides by the trial function $u(y)$ and integrating, we get

$$\overline{\lambda} = \frac{1}{u_0 \overline{u}_0} \sum (A_n u_n \overline{u}_n + B_n v_n \overline{v}_n)$$

It immediately follows from (A.34) that

$$\lambda - \overline{\lambda} \geqslant 0 \qquad \text{(A.35)}$$

Thus no matter what trial field we use, the impedance obtained from (A.32) will always provide an upper bound for the true value. This conclusion is based on

formulating the integral equation in terms of the axial velocity in the aperture. If one starts instead from the integral equation for the pressure in the aperture, it can be shown that (Schwinger and Saxon, pp. 104-106) a lower bound is obtained for the impedance. Thus one is able to bracket the error resulting from an approximate solution of the equivalent static problem. We shall not reproduce the latter calculation here. However, it shall be referred to when discussing the accuracy of the impedance estimate.

To obtain the stationarity property of the expression (A.32), we rewrite (A.32) as

$$\lambda u_0^{\,2} = \sum (A_n u_n^{\,2} + B_n v_n^{\,2}) \tag{A.36}$$

Now suppose that the trial function $u(y)$ is only slightly different from the true function $\overline{u}(y)$, that is, let

$$u(y) = \overline{u}(y) + \epsilon d(y), \quad \epsilon = o(1) \tag{A.37}$$

Let us also denote the Fourier amplitudes of $d(y)$ as follows :

$$d_0 = \int d(y)\, dy$$

$$d_n = \int \phi_n(y) d(y)\, dy$$

$$e_n = \int \psi_n(y) d(y)\, dy$$

Then (A.36) may be written as

$$\lambda(\overline{u}_0 + \epsilon d_0)^2 = \sum \Big(A_n(\overline{u}_n + \epsilon d_n)^2 + B_n(\overline{v}_n + \epsilon e_n)^2 \Big)$$

which, upon squaring, becomes

$$\lambda(\overline{u}_0^{\,2} + 2\epsilon d_0 \overline{u}_0) = \sum[A_n(\overline{u}_n^{\,2} + 2\epsilon \overline{u}_n d_n) + B_n(\overline{v}_n^{\,2} + 2\epsilon \overline{v}_n e_n)] + O(\epsilon^2) \tag{A.38}$$

Now (A.33) may be written as

$$\overline{\lambda}\overline{u}_0^{\,2} = \sum(A_n \overline{u}_n^{\,2} + B_n \overline{v}_n^{\,2}) \tag{A.39}$$

Subtracting (A.39) from (A.38), we obtain

$$(\lambda - \overline{\lambda})\overline{u}_0^{\,2} + 2\epsilon\lambda d_0 \overline{u}_0 = 2\epsilon\sum(A_n \overline{u}_n d_n + B_n \overline{v}_n e_n) + O(\epsilon^2) \tag{A.40}$$

However, if we multiply (A.30) for a true eigenvalue by $d(y)$ and integrate over y, we obtain

$$\overline{\lambda} d_0 \overline{u}_0 = \sum(A_n d_n \overline{u}_n + B_n e_n \overline{v}_n)$$

Thus (A.40) becomes

$$(\lambda - \overline{\lambda})(\overline{u}_0^{\,2} + 2\epsilon d_0 u_0) = O(\epsilon^2)$$

We immediately conclude that

$$\lambda - \overline{\lambda} = O(\epsilon^2) \tag{A.41}$$

This proves our contention that in the vicinity of the true solution, the eigenvalue is stationary with respect to small changes in the field. Thus if one uses an axial velocity field that reasonably approximates the correct distribution in the

aperture, the impedance obtained from (A.32) will be at least second-order accurate.

A.3 Impedance

We now derive an explicit formula for the junction impedance of a stepped duct using an approximate solution of (A.25)-(A.29) as the trial field. To this end, (A.32) is written as

$$\lambda Q^2 = \frac{2}{\pi} \sum_{n=1}^{\infty} \frac{1}{n} (u_n^{\,2} + v_n^{\,2}) \tag{A.42}$$

$$+ 2 \sum_{n=1}^{\infty} \left[u_n^{\,2} \left(\frac{1}{(n^2\pi^2 - k^2 b_L^{\,2})^{1/2}} - \frac{1}{n\pi} \right) + v_n^{\,2} \left(\frac{1}{(n^2\pi^2 - k^2 b_R^{\,2})^{1/2}} - \frac{1}{n\pi} \right) \right]$$

where $\lambda = -iZ/\omega\rho_0$ as before and we have used

$$Q = \int_0^{b_R} u(y)\, dy \tag{A.43}$$

for the volume velocity. Now if we multiply both sides of the static equation (A.21) by $u(y)$ and integrate, and also use (A.22) and (A.29) to replace $(B_L - B_R)$, we obtain

$$a_0 Q^2 + Q \sum_{n=1}^{\infty} a_{Rn}\alpha_{Rn} + Q \sum_{n=1}^{\infty} a_{Ln}\alpha_{Ln} + \frac{2}{\pi} \sum_{n=1}^{\infty} \frac{1}{n}(u_n^{\,2} + v_n^{\,2})$$

$$= -2 \sum_{n=1}^{\infty} \alpha_{Ln} u_n + 2 \sum_{n=1}^{\infty} \alpha_{Rn} v_n \qquad \text{(A.43)}$$

Combining (A.42) and (A.43), we get

$$\lambda Q^2 = -a_0 Q^2 - Q \sum_{n=1}^{\infty} a_{Rn}\alpha_{Rn} - Q \sum_{n=1}^{\infty} a_{Ln}\alpha_{Ln} - 2 \sum_{n=1}^{\infty} u_n \alpha_{Ln} + 2 \sum_{n=1}^{\infty} v_n \alpha_{Rn}$$

$$+ 2 \sum_{n=1}^{\infty} u_n^{\,2} \left(\frac{1}{(n^2\pi^2 - k^2 b_L^{\,2})^{1/2}} - \frac{1}{n\pi} \right)$$

$$+ 2 \sum_{n=1}^{\infty} v_n^{\,2} \left(\frac{1}{(n^2\pi^2 - k^2 b_R^{\,2})^{1/2}} - \frac{1}{n\pi} \right) \qquad \text{(A.44)}$$

We now use (A.19) and (A.20) to eliminate the Fourier amplitudes u_n and v_n from (A.44). This gives

$$\lambda Q^2 = -a_0 Q^2 - Q \sum_{n=1}^{\infty} a_{Rn}\alpha_{Rn} - Q \sum_{n=1}^{\infty} a_{Ln}\alpha_{Ln}$$

$$- \pi \sum_{n=1}^{\infty} n\alpha_{Ln}(\beta_{Ln} - \alpha_{Ln}) - \pi \sum_{n=1}^{\infty} n\alpha_{Rn}(\beta_{Rn} - \alpha_{Rn}) \qquad \text{(A.45)}$$

$$+ 2 \sum_{n=1}^{\infty} (n\pi/2)^2(\beta_{Ln} - \alpha_{Ln})^2 \left(\frac{1}{(n^2\pi^2 - k^2 b_L^{\,2})^{1/2}} - \frac{1}{n\pi} \right)$$

$$+ 2 \sum_{n=1}^{\infty} (n\pi/2)^2(\beta_{Rn} - \alpha_{Rn})^2 \left(\frac{1}{(n^2\pi^2 - k^2 b_R^{\,2})^{1/2}} - \frac{1}{n\pi} \right)$$

While this expression is capable of yielding an exact value of λ in principle, we seek an approximate variational estimate, for reasons mentioned earlier. Suppose we consider only a finite set of incident modes as follows :

$$\begin{aligned} \alpha_{Ln} &\neq 0 \text{ for } n \leqslant N_1 \\ \alpha_{Ln} &\equiv 0 \text{ for } n > N_1 \\ \alpha_{Rn} &\neq 0 \text{ for } n \leqslant N_2 \\ \alpha_{Rn} &\equiv 0 \text{ for } n > N_2 \end{aligned} \qquad \text{(A.46)}$$

We adopt the following strategy : for $n \leqslant N_1, N_2$ we use the statements of static equivalence, (A.25) and (A.26), to replace the α_n, while for higher values of n, we use the static relations (A.27) and (A.28) to replace the β_n. (A.45) then

becomes

$$\lambda Q^2 = -a_0 Q^2 - Q \sum_{n=1}^{N_1} a_{Ln}\alpha_{Ln} - Q \sum_{n=1}^{N_2} a_{Rn}\alpha_{Rn}$$

$$- \pi \sum_{n=1}^{N_1} n \frac{\beta_{Ln}^2}{K_{Ln}}(1 - 1/K_{Ln}) - \pi \sum_{n=1}^{N_2} n \frac{\beta_{Rn}^2}{K_{Rn}}(1 - 1/K_{Rn}) \qquad \text{(A.47)}$$

$$+ 2 \sum_{n=1}^{N_1} (n\pi/2)^2 \beta_{Ln}^2 (1 - 1/K_{Ln})^2 \left(\frac{1}{(n^2\pi^2 - k^2 b_L^2)^{1/2}} - 1/n\pi \right)$$

$$+ 2 \sum_{n=1}^{N_2} (n\pi/2)^2 \beta_{Rn}^2 (1 - 1/K_{Rn})^2 \left(\frac{1}{(n^2\pi^2 - k^2 b_R^2)^{1/2}} - 1/n\pi \right)$$

$$+ 2 \sum_{n=N_1+1}^{\infty} (n\pi/2)^2 \beta_{Ln}^2 \left(\frac{1}{(n^2\pi^2 - k^2 b_L^2)^{1/2}} - \frac{1}{n\pi} \right)$$

$$+ 2 \sum_{n=N_2+1}^{\infty} (n\pi/2)^2 \beta_{Rn}^2 \left(\frac{1}{(n^2\pi^2 - k^2 b_R^2)^{1/2}} - \frac{1}{n\pi} \right)$$

Using the relations

$$\frac{n\pi}{2}\left(\frac{1}{(n^2\pi^2 - k^2 b_L^{\,2})^{1/2}} - \frac{1}{n\pi} \right) = \frac{1}{K_{Ln} - 1}$$

$$\frac{n\pi}{2}\left(\frac{1}{(n^2\pi^2 - k^2 b_R^{\,2})^{1/2}} - \frac{1}{n\pi} \right) = \frac{1}{K_{Rn} - 1}$$

(A.47) may be simplified to

$$\lambda Q^2 = -a_0 Q^2 - Q \sum_{n=1}^{N_1} \alpha_{Ln} a_{Ln} - Q \sum_{n=1}^{N_2} \alpha_{Rn} a_{Rn}$$

$$+ \sum_{n=N_1+1}^{\infty} \frac{n\pi}{K_{Ln} - 1} \left(S_{Ln} Q + \sum_{m=1}^{N_1} R^{(L)}_{m\to n} \alpha_{Lm} + \sum_{m=1}^{N_2} T^{R\to L}_{m\to n} \alpha_{Rm} \right)^2 \qquad \text{(A.48)}$$

$$+ \sum_{n=N_2+1}^{\infty} \frac{n\pi}{K_{Rn} - 1} \left(S_{Rn} Q + \sum_{m=1}^{N_2} R^{(R)}_{m\to n} \alpha_{Rm} + \sum_{m=1}^{N_1} T^{L\to R}_{m\to n} \alpha_{Lm} \right)^2$$

This expression will be used to calculate the junction impedance. The α_n appearing in (A.48) will be determined by solving the following equations,

obtained by combining (A.25) and (A.26) with (A.27) and (A.28) respectively :

$$K_{Ln}\alpha_{Ln} = S_{Ln}Q + \sum_{m=1}^{N_1} R^{(L)}_{m\to n}\alpha_{Lm} + \sum_{m=1}^{N_2} T^{R\to L}_{m\to n}\alpha_{Rm}\ ,\ n = 1,2,\cdots,N_1 \quad \text{(A.49)}$$

$$K_{Rn}\alpha_{Rn} = S_{Rn}Q + \sum_{m=1}^{N_2} R^{(R)}_{m\to n}\alpha_{Rm} + \sum_{m=1}^{N_1} T^{L\to R}_{m\to n}\alpha_{Lm}\ ,\ n = 1,2,\cdots,N_2 \quad \text{(A.50)}$$

It is evident that the α_n obtained from these equations will be proportional to the yet unknown volume velocity Q. Thus when we substitute into (A.48), the common factor Q^2 will cancel out.

We consider the simplest case, $N_1 = N_2 = 1$. The last-obtained equations yield

$$\frac{\alpha_{L1}}{Q} = \frac{1}{D}\left((K_{R1} - R^{(R)}_{1\to 1})S_{L1} + T^{R\to L}_{1\to 1} S_{R1}\right) \quad \text{(A.51)}$$

$$\frac{\alpha_{R1}}{Q} = \frac{1}{D}\left((K_{L1} - R^{(L)}_{1\to 1})S_{R1} + T^{L\to R}_{1\to 1} S_{L1}\right) \quad \text{(A.52)}$$

where

$$D = (K_{L1} - R^{(L)}_{1\to 1})(K_{R1} - R^{(R)}_{1\to 1}) - T^{L\to R}_{1\to 1}\, T^{R\to L}_{1\to 1}$$

Once again, the infinite sums in (A.48) pose a problem. However, Schwinger and

Saxon (p.123) point out that their main numerical contribution comes from the first term and that the relative error in neglecting them is only about 1/2% even at cutoff. Substituting the values of the static parameters from Chapter 4 and rearranging, we find that the nondimensional impedance from (A.48) is

$$Z = \frac{ikb_L}{\pi}\left[\ln\left(\frac{1-\gamma^2}{4\gamma}\right)\left(\frac{1+\gamma}{1-\gamma}\right)^{1/2(\gamma+\frac{1}{\gamma})} + 2\frac{A + A' - 2C}{AA' - C^2}\right.$$

$$\left. + (kb_L/\pi)^2\left(\frac{1-\gamma}{1+\gamma}\right)^{4\gamma}\left(\frac{5\gamma^2-1}{1-\gamma^2} + \frac{4\gamma^2 C}{3A}\right)^2\right] \qquad \text{(A.53)}$$

where

$$\gamma = \frac{b_R}{b_L}$$

$$A = \left(\frac{1-\gamma}{1+\gamma}\right)^{2\gamma}\frac{1+G_L}{1-G_L} - \frac{1+3\gamma^2}{1-\gamma^2}$$

$$A' = \left(\frac{1-\gamma}{1+\gamma}\right)^{\frac{2}{\gamma}}\frac{1+G_R}{1-G_R} - \frac{3+\gamma^2}{1-\gamma^2}$$

$$C = \left(\frac{4\gamma}{1 - \gamma^2} \right)^2$$

$$G_L = \left(1 - k^2 b_L{}^2 / \pi^2 \right)^{1/2}$$

$$G_R = \left(1 - k^2 b_R{}^2 / \pi^2 \right)^{1/2}$$

As mentioned earlier, Schwinger also obtained a lower bound for the variational estimate of Z by formulating the integral equation in terms of the aperture pressure. Thus with both bounds known, he is able to bracket the maximum error (Schwinger and Saxon, p.122) :

$$\delta = \frac{\Delta Z}{\overline{Z}} = \frac{Z_{upper} - Z_{lower}}{\overline{Z}} \qquad \text{(A.54)}$$

where $\overline{Z}$ represents the exact value of impedance. He shows that even at the cut-off frequency for the first cross-mode, the error inherent in (A.53) is only about 1%.

The vita has been removed from the scanned document